UNIVERZITA KARLOVA

Přírodovědecká fakulta

Studijní program: Analytická chemie

Mgr. Michaela Malečková

A study of non-volatile nitroso compounds in brewing

Studium netěkavých nitrososloučenin v pivovarství

Disertační práce

Školitelka: RNDr. Jana Sobotníková, Ph.D.

Konzultant: RNDr. Tomáš Vrzal, Ph.D.

Praha 2023

Prohlášení autora

Prohlašuji, že jsem tuto závěrečnou práci zpracovala samostatně a že jsem uvedla všechny použité informační zdroje a literaturu. Tato práce ani její podstatná část nebyla předložena k získání jiného nebo stejného akademického titulu.

Jsem si vědoma toho, že případné využití výsledků, získaných v této práci, mimo Univerzitu Karlovu je možné pouze po písemném souhlasu této univerzity.

V Praze dne 11. prosince 2023.

Abstract

Nitroso compounds are beer contaminants related to carcinogenicity and can be naturally formed during brewing. They are generally categorized as volatile and non-volatile. Well-characterized and proven carcinogenic compounds are mostly volatile *N*-nitrosamines, whereas specific non-volatile nitroso compounds are nearly unknown even by structure. This deficiency limits improvements in health-risk assessment and control of beer. The present study focused on these barely known compounds in beer, related to their molecule structures and natural occurrence in beer and malt. Since these compounds form by nitrite reactions with naturally occurring compounds in beer or raw materials, the beer sample was parallelly treated by nitrite and isotopically labelled nitrite-^{15}N at acidic conditions. Due to isotopic labelling, formed nitrite-related reaction products were distinguished by gas chromatography with tandem mass spectrometry. By this approach, up to 22 unknown nitrite-related reaction products (N-products) were found and structurally studied from mass spectrometric fragmentation patterns. Besides previously found *N*-nitrosoproline and *N*-nitrosoproline ethyl ester, newly characterized compounds in beer were 4-cyanophenol, pyruvic acid oxime, 2-methoxy-5-nitrophenol, nitrosoguaiacol, and 4-nitrosophenol. Several N-products coincided with the retention time and mass spectra with nitrite-related reaction products of tyrosine or vanillic acid. Also, nearly all N-products were found in nitrosated malts treated with nitrogen oxides and showed great extractability into the wort. The acquired chromatographic and mass spectrometric data led to the development of a specific method for monitoring N-products in commercial beers and malts (up to 200 samples each). The observation of relative responses and frequency of N-products appearance by multivariate analyses distinguished important N-products that could be interesting for future investigations. For instance, synthesizing standard compounds of sufficient purity would lead to accurate N-products determination in beer and studies of their potential health-effect on consumers.

Abstrakt

Nitrososloučeniny jsou kontaminanty piva s karcinogenními účinky, které se přirozeně tvoří během pivoarského procesu. Obecně jsou děleny na těkavé a netěkavé. Dostatečně charakterizované a prokázané karcinogenní látky jsou těkavé *N*-nitrosaminy, což nelze konstatovat pro strukturně neznámé zástupce netěkavých nitrososloučenin. Tato neznalost limituje vývoj nových analytických metod vedoucí k přesnějšímu zhodnocení a kontrole zdravotních rizik piva. Předložená studie se proto zabývá těmito méně známými sloučeninami, zejména strukturou molekul a jejich přirozeným výskytem v pivu i sladu. Jelikož je jejich vznik spojován s reakcemi dusitanu se sloučeninami piva a jeho surovin, byl vzorek piva paralelně ošetřen dusitanem (standardním a izotopickým-^{15}N) v kyselém prostředí. Díky izotopickému značení byly vzniklé reakční produkty identifikovány plynovou chromatografií s tandemovou hmotnostní spektrometrií. Tímto přístupem bylo nalezeno a strukturně studováno až 22 neznámých reakčních produktů dusitanu (N-produktů) pomocí hmotnostně spektrometrických fragmentací. Kromě dříve nalezeného *N*-nitrosoprolinu a *N*-nitrosoprolin ethyl esteru, byly nově v pivu charakterizovány: 4-kyanofenol, oxim kyseliny pyrohroznové, 2-methoxy-5-nitrofenol, nitrosoguajakol a 4-nitrosofenol. Několik N-produktů bylo chromatograficky i spektrometricky ve shodě s reakčními produkty dusitanu s tyrosinem nebo kyselinou vanilovou. Většina N-produktů byla detekována i v experimentálně nitrosovaném sladu pomocí oxidů dusíku, a vykazovala vysokou extrahovatelnost do mladiny. Získaná chromatografická a hmotnostně spektrometrická data vedla k vývoji specifické metody pro pozorování N-produktů v komerčních pivech a sladech (téměř 200 vzorků). Pozorování relativních odezev a četnosti výskytu N-produktů pomocí vícerozměrných analýz odlišilo důležité N-produkty, jež by mohly být zajímavé pro budoucí výzkum. Například syntéza standardních sloučenin o požadované čistotě by vedla k přesnějšímu stanovení N-produktů v pivu či ke studiu jejich možných zdravotních účincích na spotřebitele.

Acknowledgment

Významné poděkování náleží mému konzultantovi panu RNDr. Tomáši Vrzalovi, Ph.D. z Výzkumného ústavu pivovarského a sladařského za odborné a profesionální vedení. Dále děkuji mé školitelce paní RNDr. Janě Sobotníkové, Ph.D. z Katedry analytické chemie na Přírodovědecké fakultě Univerzity Karlovy za přátelskou spolupráci i vstřícné odborné vedení napříč celým doktorským studiem. Děkuji všem kolegyním i kolegům z Výzkumného ústavu pivovarského a sladařského za spolupráci a velmi přátelské pracovní prostředí.

Dále srdečně děkuji své životní kamarádce Mgr. Lence Honesové za pomoc s grafickou úpravou publikací a disertační práce, ale zejména za dodání inspirace a odvahy během celého vysokoškolského studia i osobního života. A v poslední řadě děkuji svým rodičům, celé své rodině i přátelům, kteří mi též byli po celou dobu nenahraditelnou podporou.

Table of content

List of abbreviations

ATNC	Apparent total *N*-nitroso compounds
BSA	Bis(trimethylsilyl)acetamide
BSTFA	*N,O*-bis(trimethylsilyl)trifluoroacetamide
GC-MS/MS	Gas chromatography with tandem mass spectrometry
GC-NCD	Gas chromatography with nitroso-specific chemiluminescence detection
HPLC	High-performance liquid chromatography
MSA	*N*-methyl-*N*-trimethylsilyl-acetamide
MSTFA	*N*-methyl-*N*-trimethylsilyl-trifluoracetamid
MTBSTFA	*N*-*tert*-butyldimethylsilyl-*N*-methyltrifluoroacetamide
NCD	Nitroso-specific chemiluminescence detector
NDEA	*N*-nitrosodiethylamine
NDMA	*N*-nitrosodimetylamine
NMOR	*N*-nitrosomorpholine
NOCs	Nitroso compounds
NPIC	*N*-nitrosopipecolic acid
NPIP	*N*-nitrosopiperidine
NPRO	*N*-nitrosoproline
N-products	Nitrite-related reaction products
NPYR	*N*-nitrosopyrrolidine
NSAR	*N*-nitrososarcosine
SMILES	Simplified molecular-input line-entry system
SPE	Solid-phase extraction
TEA	Thermal energy analyzer

Objectives of the study

Nitroso compounds (NOCs) are common beer contaminants mainly formed during production. They contain characteristic nitroso groups attached to organic low-to-medium-size molecules. Depending on a feature of the organic moiety, they are divided into volatile and non-volatile. Whereas volatile NOCs, known carcinogenic compounds, are well-studied, the non-volatile NOCs are barely known. The reason is that most non-volatile NOCs have not yet been described by structure. A demand to characterize representatives of non-volatile NOCs in brewing still was not sufficiently achieved and is necessary for the progress towards better quality control of beer and health-safety assessment. Specifically, knowing molecular structures allows us to synthesize standards of sufficient purity, which can be applied to develop novel methods for determination, used for studies about their formation and elimination in beer, and to study their possible health-impact.

The presented investigation was designed to study these unknown non-volatile NOCs occurring in brewing in the following two scopes:

(i) The first aim was to artificially prepare, detect, and structurally characterize unknown nitroso-related compounds in beer. Gas chromatography with tandem mass spectrometry (GC-MS/MS) was chosen since it allows structural elucidation and specific detection of unknown compounds in complex matrices.

(ii) The second aim was to monitor and observe their natural occurrence in commercial beers and malts. For this purpose, a specific GC-MS/MS method was developed based on the first study's acquired spectrometric data of the new compounds.

Achievements of both scopes are summarised in two publications placed in the result and discussion. In addition, a universal computation tool for predicting retention index based on molecule structure was also developed along with the presented investigation. This tool was extensively used in the first study and is attached as a third paper in **Supplementary data – Appendix 1**.

1. Introduction to nitroso compounds

The following section summarises essential differences between volatile and non-volatile NOCs, various toxicological effects, and their distinct formation during brewing. It also discusses possible precursors (and their nitrite-related reaction products) that can be formed in beer or raw materials.

1.1 Nitroso compounds

As the name suggests, NOCs are specific by nitroso group (-N=O). If the nitroso group links to a molecule via a nitrogen atom, they are classified as *N*-nitroso compounds. The same applies to *C*-nitroso, *S*-nitroso, or *O*-nitroso compounds. Due to different physical-chemical properties, NOCs are divided into volatile and non-volatile, and different mechanisms form them. It also implies variable acceptance by the organism, and volatile NOCs, mostly N-nitrosamines, specifically undergo biotransformation that causes mutagenicity or carcinogenicity [1].

1.1.1 Volatile *N*-nitrosamines and NDMA

Volatile *N*-nitrosamines are small molecules of symmetric or asymmetric amine derivatives. Many representatives have carcinogenic and mutagenic properties and are common contaminants in foods and beverages, including beer and malt [2, 3]. The first found *N*-nitrosamine in beer was *N*-nitrosodimethylamine (NDMA) in 1979. Its average concentration reached 2.7 µg/kg; the maximum was up to 68 µg/kg (158 beer samples) [4]. Since then, a comprehensive investigation of NDMA and *N*-nitrosamines in beer has brought technological improvements, minimizing their formation. For instance, between the period 2000 and 2006, only 1 % of tested German beers exceeded the NDMA maximum limit of 0.5 µg/kg (418 beer samples) [5]. Likewise, in the period from 2001 to 2015, a decrease in the percentage (from 11 to 0 %) of beers that exceeded the maximum limit was observed every year (1280 beer samples). The average concentrations of NDMA per

year were below 0.2 µg/kg. During the same period, only 4-14 % of malt samples exceeded the maximum limit of 2.5 µg/kg (4115 malt samples), and every year, the average NDMA concentrations were about 0.8 µg/kg [6].

Other studied *N*-nitrosamines in beer and malt are *N*-nitrosopyrrolidine (NPYR), *N*-nitrosopiperidine (NPIP), *N*-nitrosodiethylamine (NDEA), and *N*-nitrosomorpholine (NMOR), and their structures are shown in **Figure 1**. NPYR and NPIP are occasionally detected, and NDEA with NMOR has not been observed.[a] *N*-nitrosamines are generally well controlled, but various maximum limits exist depending on the region.[b] Rarely detected extreme concentrations usually indicate technological or microbial defects [4, 6, 8, 11].

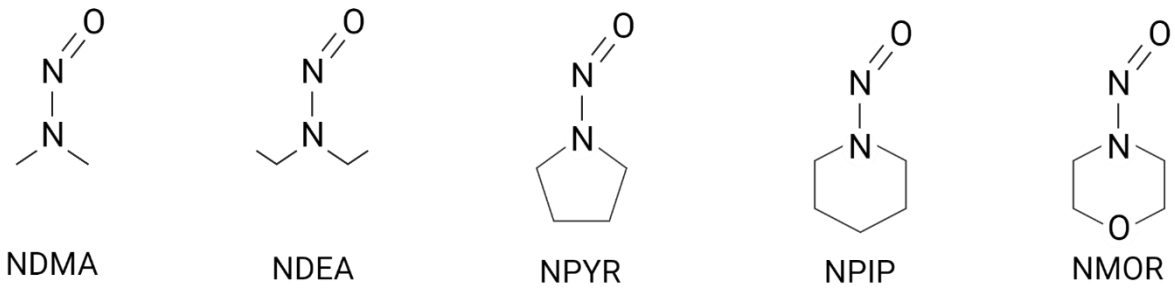

Figure 1. Volatile *N*-nitrosamines monitored in beer and malt.

1.1.2 Non-volatile NOCs

Besides volatile *N*-nitrosamines, beer contains a more complex group of non-volatile NOCs. Their occurrence is so far proved by an Apparent total *N*-nitroso compounds (ATNC) determination. The ATNC determination is based on the chemical cleavage of the nitrosyl group from molecule resin and subsequent detection of generated nitrosyl radicals [1, 12]. For this reason, the ATNC does not provide structural information about the individual compounds; however, it is a unique standardized determination of total NOCs in beer, providing a sum of volatile and non-volatile NOCs together. Determined ATNC

[a] Unpublished observation from an analyst from the Research Institute of Brewing and Malting in the past 9 years.
[b] So far, EU legislation to control *N*-nitrosamines in foods and beverages is not in force [3]. In Germany, the *Bavarian State Office for Health and Food Safety* recommended the maximum level of NDMA to be 2.5 ppb for malt and 0.5 ppb for beers [7]. The *Czech Beer and Malt Association* recommends a stringent level for NDMA in malt to be less than 1.0 ppb. This was found a hard-to-achieve task for some types of malt (e.g. Munich style) [6,8]. On the opposite, the *U.S. Food and Drug Administration* sets relatively high limits, 10 ppb for malt and 5 ppb for beer [9,10].

concentrations in beers can occasionally reach hundreds of µg(NNO)/kg[c], and their formation is potentially associated with microbial contamination [15, 16]. No specific legislation for ATNC exists; however, brewing authorities such as the *Brewers Society* (GB), *Czech Beer and Malt Association* (CZ), and *Technical Benchmark* (DE) are consistent in the recommended maximum level of 20 µg(NNO)/kg [6, 17, 18].

Until now, *N*-nitrosoproline (NPRO), *N*-nitrososarcosine (NSAR), *N*-nitrosopipecolic acid (NPIC), and recently, *N*-nitrosoproline ethyl ester were observed in beer or malt (see the structures in **Figure 2**) [19, 20]. Previously determined concentrations of NSAR in beer and malt did not exceed 20 µg/kg, and NPIC was below the detection limit [21]. Another study determined the average concentration of NPRO as 1.7 µg/kg in beers (ranging from <0.7 to 6.0 µg/kg, 28 samples) and 24.1 µg/kg in malts (ranging from 5.0 up to 113.0 µg/kg, 11 samples) [22]. However, a comparison of ATNC with NDMA and NPRO concentrations did not show any correlation, and these compounds contributed to concentrations of ATNC in beer by less than 1% for NDMA and about 10 % for NPRO [15, 18, 19, 23]. Recent studies indicated that *C*- nitroso compounds can also contribute to ATNC response. Hence, the specificity of ATNC solely for the *N*-nitroso compounds can be questioned [16, 20].

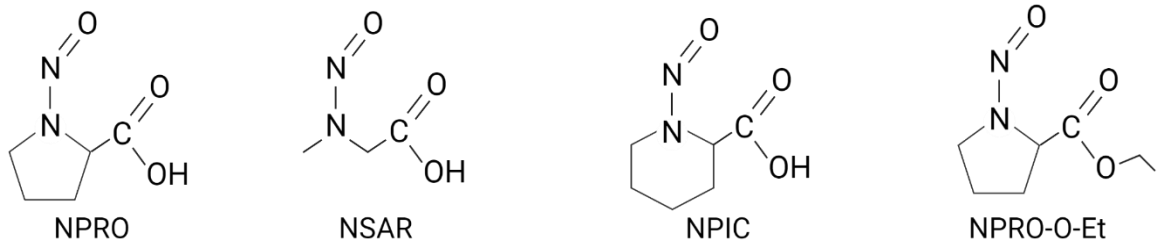

Figure 2. Structures of non-volatile *N*-nitroso compounds studied in beer and malt.

ATNC-positive compounds are structurally unknown, but some features were suggested experimentally. The presence of polar groups, such as carboxyl or hydroxyl, was proved by the high extractability of ATNC from malt to water or other polar solvents and by acidic and alkaline hydrolysis experiments. The extractability of ATNC-positive

[c] Units of ATNC determination are µg(NNO)/kg, which refers to the weight of -N-N=O moiety per kilogram (or eventually liter of beer). The density of beer can be approximated to ~1.0 kg/L [13, 14].

compounds from sweet wort to ethyl acetate ranged from 80 % to 100 % at acidic conditions (pH=1.5) and was <20 % at neutral conditions (pH=7.0) [24]. The presence of polar groups and a higher molar mass imply the lower volatility of NOCs of this specific group [15, 19, 24].

1.2. Health-considerations

1.2.1 Toxicity of *N*-nitrosamines

Hydrophobic compounds undergo structural transformations to become more hydrophilic and to facilitate biodegradation. Such biotransformation can form highly reactive and toxic species. The structure of volatile *N*-nitrosamines follows this theory since they comprise a highly polar but less hydrophobic *N*-nitroso group linked to short alkyl substituents [25]. Their carcinogenic and mutagenic properties were described as follows: *N*-nitrosamines are first activated by the cytochrome P450 family enzymes accompanied by oxygen and NADPH oxidase. These enzymes can exist in various human organs, such as kidneys, liver, lungs, or skin. The activating reaction is α-hydroxylation, leading to aldehyde formation (e.g., NDMA forms formaldehyde) and monoalkyl nitrosamine. The monoalkyl nitrosamine further degrades through intramolecular shifts into carbocations or diazo alkanes (alkyl diazocations). Formed aldehydes, carbocations, and diazo alkanes are highly reactive species, causing genetic damage by alkylation on DNA [26-29].

Enzymatic activation is crucial for the toxicity of *N*-nitrosamines and depends on a molecule's structure, size, and enzyme subfamily. For example, an enzyme subfamily P450 2E1 has a higher affinity to symmetrical *N*-nitrosamines (NDMA, NDEA), and its efficiency decreases with the alkyl chain length. Whereas enzyme subfamily P450 2A6 activated even non-symmetric and bulky alkyl chains of *N*-nitrosamines [28, 30].

1.2.2 Possible risk of non-volatile NOCs

The alkyl and hydroxyl-alkyl substituents and their different positions can affect the toxic properties of NOCs, as was studied by a computational model, Quantitative Structure-

Activity Relationship. It was shown that hydroxyl groups and unsaturated alkyls decrease the compound's mutagenic potency, and saturated alkyl substituents (such as *N*-nitrosamines) have the counterpart effect [31]. This aspect can predict the lower risk of non-volatile NOCs consumed in food or beverages. A potential risk is often attributed to the endogenous formation of toxic compounds intermediated specifically by non-volatile NOCs [32, 33]. For instance, NPRO can undergo trans-nitrosation, forming carcinogenic *N*-nitroso-*N*-methyl urea in the presence of thiourea at acidic stomach conditions [33]. Some residues of thioureas (ethylene thiourea and propylene thiourea) can be present in beer or hops [34].

Another example is the endogenous formation of *N*-nitroso derivatives of indoles, Amadori compounds, and glycosamines. All can be related to beer: indoles are known as off-flavors in beer, and Amadori compounds and glycosamines are Maillard reaction products of malting and brewing processes [35]. The toxicity of *N*-nitroso derivatives of indoles and Amadori compounds was attributed to their direct ability to transnitrosate the nucleophilic parts of purine bases in DNA directly [36, 37]. The toxicity of *N*-nitroso glycosamines varies depending on sugar and amine type, and it was attributed to the formation of arene diazocations (similar to alkyl diazocations in NDMA) [37].

Carcinogenic *N*-nitrosamines can also be formed exogenously during meat or malt treatment, with non-volatile NOCs as intermediates [21]. For example, by decarboxylation at a high temperature, NPRO can form volatile NPYR, and NSAR can form NDMA. These decarboxylation reactions can partly contribute to the total concentration of the corresponding *N*-nitrosamine [38].

1.3. Formation and chemistry of NOCs

The sources of NOCs formation in foods and beverages can be generally classified into three categories. The first is a food treatment (e.g., meat or malt) where drying or smoking gas containing nitrogen oxides is used [39, 40]. Second is the artificial or natural presence

of nitrites/nitrates in foods. Nitrites are additives to meat or cheese to preserve and avoid harmful bacterial growth. Vegetables and hops are also natural sources of nitrates. They do not form NOCs directly but can be reduced to nitrites, as shown later [41-44]. The third source of NOCs is the side effects of bacterial contamination or fermentation, where an enzymatic reduction of nitrates into nitrites can subsequently form NOCs [45-47]. All three mechanisms can contribute to the total NOCs content in beer. However, the latter two are suggested to be the most significant for forming non-volatile NOCs and ATNC-positive compounds [15, 17, 39].

1.3.1. Nitrosation in brewing

During the malting and brewing processes, the raw beer material or brewed beer can come into contact with the sources of potential nitrosation reagents (**Figure 3: steps 1-8)**. The quantity of nitrosation reagent naturally depends on the exposure type, amount, and length. For instance, freshly harvested barley is sometimes dried by air (**Figure 3: step 1**) to reach the desired moisture level for storage [48]. Since this treatment is not always necessary, the contribution of this resource was hypothetically estimated to be very low. A more significant impact was proved for nitrogen oxides in the drying air used in malt kilns (**Figure 3: step 4**). In the past, they were primarily responsible for volatile *N*-nitrosamine formation in malt. The chemistry of *N*-nitrosamine formation has already been well explained in several publications. Their formation was the most efficiently eliminated by replacing direct burners that contain relatively high amounts of NO_x with indirect burners with low NO_x content [39, 40, 49].

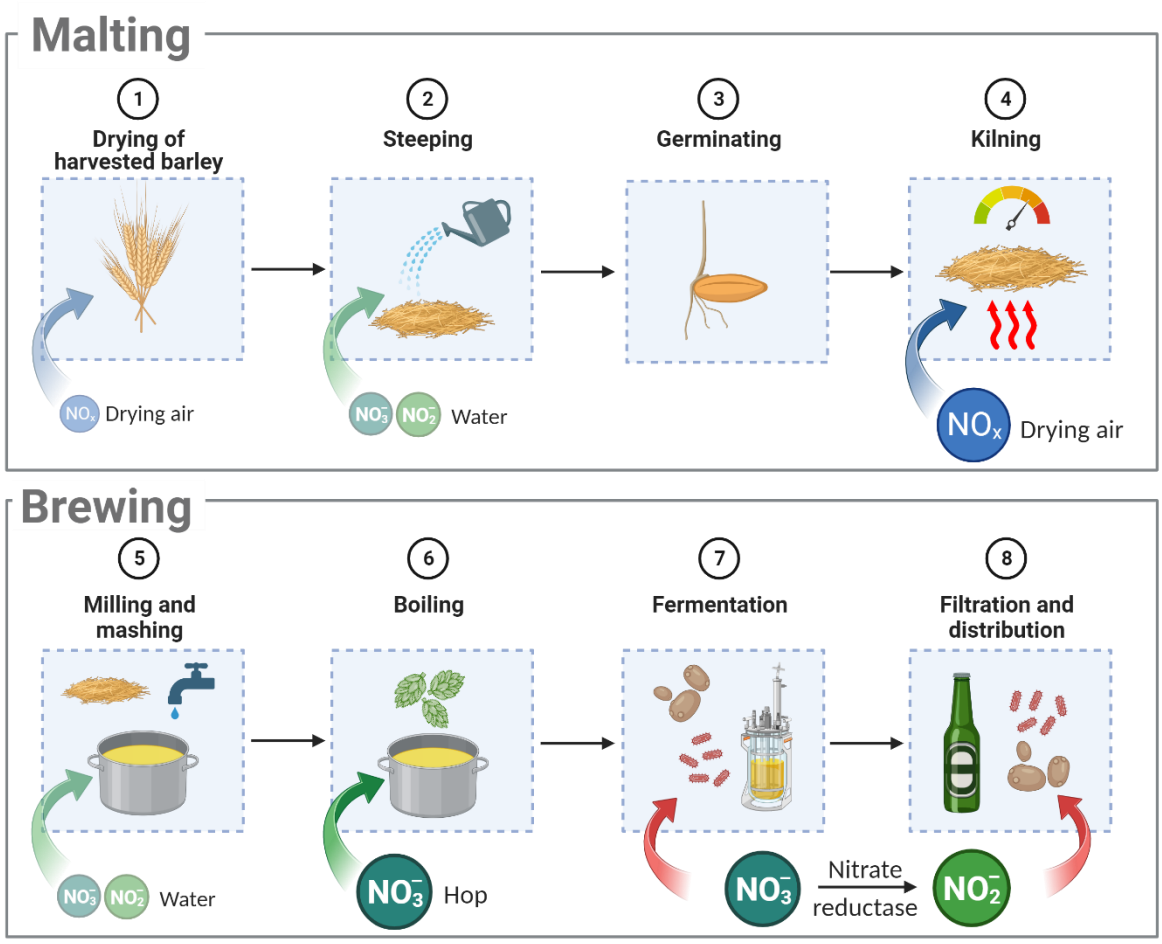

Figure 3. Possible sources of nitrosation reagents during malting and brewing processes.

Understanding the chemistry and eliminating nitrite exposure during brewing is desirable. The same applies to nitrates, as they can be easily reduced to nitrites by enzymatic reactions from bacteria. However, complete elimination is limited since both are naturally present in water or other raw materials [40]. For instance, brewing water follows up legislative levels of nitrates (<50 mg/L) and nitrites (<0.5 mg/L); hence, its contribution to NOCs formation can be suggested as negligible (**Figure 3: steps 2, 5**) [50, 51]. Nitrite/nitrate natural content in malt is also insignificant [52]. However, nitrates can occur in hops in significant concentrations ranging up to 2-18 g/kg (**Figure 3: step 6**) [52, 53]. The nitrate extractability into wort was nearly quantitative and proportional to the wort boiling time. Therefore, to stay under the recommended maximum nitrate residual level in the final beer, it is recommended to calculate the used hop before brewing, as nitrate concentrations in beers were up to 87 mg/L [42, 51, 53].

A failure to maintain the proper hygienic principles during brewing can introduce microbial contamination. The contamination of brewing yeast can be so low that it does not even affect the organoleptic properties of the final beer [15, 43]. When nitrate and specific nitrate-reducing bacteria are present, the formation of ATNC-positive compounds and non-volatile NOCs is nearly inevitable (**Figure 3: steps 7, 8**). For instance, even a relatively low presence of nitrates in wort (<5 mg/L) together with the bacteria *Obesumbacterium proteus* in brewing yeast (<0.03 %) was able to form relatively high ATNC (39 µg(NNO)/kg) [17]. The analyses of bacterially treated beer showed a higher occurrence of *C*-nitroso compounds but did not affect NDMA concentration [15, 20]. However, coincidences of ATNC with NDMA concentrations were found in sweet wort contaminated by *Bacillus coagulans* [54]. Additionally, nitrate-reductase enzymes were inactive in wild yeast, and no significant increase of ATNC was observed (< 10 µg(NNO)/kg) [55].

1.3.2. Nitrosation reagents

As mentioned above, there are various resources of nitrosation reagents, nitrogen oxides (NO_x = N_2O, NO, N_2O_3, NO_2, N_2O_4), and nitrite (NO_2^-) or, eventually, nitrate ions (NO_3^-). From these, the direct nitrosation agents are subsequently formed. N_2O does not cause nitrosation and exists in the following equilibria (see **Figure 4**). N_2O_3 and N_2O_4 are direct nitrosation and, eventually, nitration agents, and their formation increases when NO_x is dissolved in an aqueous solution, as proved by the determination of dissociation constants for N_2O_3 and N_2O_4 [49].

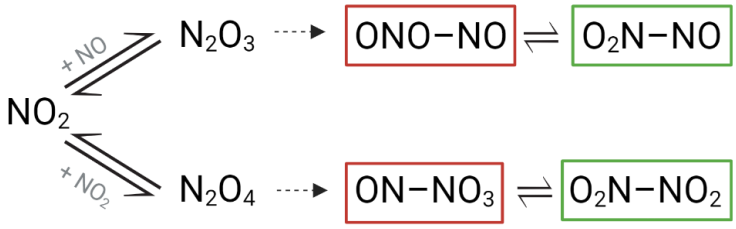

Figure 4. Equilibrium reactions of nitrogen oxides form direct nitrosation agents (N_2O_3 and N_2O_4). As proposed, the first red structural conformation leads to nitrosation, and the second green conformation leads to nitration.

Nitrite ion is not a direct nitrosation agent but coexists in equilibria with many other direct nitrosation agents, such as N_2O_3, N_2O_4, ^+NO, $^{\bullet}NO$, and $^+H_2NO_2$ **(Figure 5)** [40, 46, 56].

pH plays an essential role in nitrosation as it affects both the reagent and the substrate. For instance, at acidic conditions (pH<5), nitrosation occurs more frequently since the equilibrium reaction is driven to the formation of nitrosonium (^+NO) and nitrosacidium cations ($^+H_2NO_2$). In neutral/alkaline conditions, the formation of other nitrosation agents, such as N_2O_3 and N_2O_4, also occurs [2, 49]. Nitrite is believed to be the primary reagent responsible for forming our target compounds, ATNC-positive compounds, and non-volatile NOCs. Their potential precursors are polyphenols, vitamins, amino acids, and similar (will be discussed later) [49].

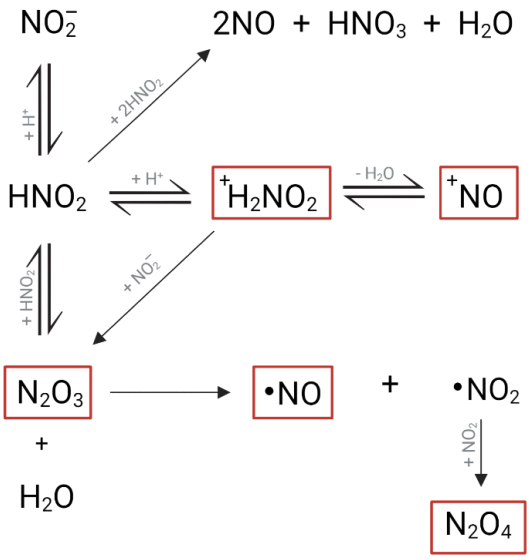

Figure 5. Equilibria of nitrite in acidic aqueous solution. Direct nitrosating agents are highlighted in red.

Although nitrates are always present in beer, nitration reactions and the formation of nitro compounds are barely discussed along with nitrosation. However, the nitration and nitrosation reactions can compete, as shown in **Figure 6** [40]. For instance, when a low concentration of gaseous NO_2 is present, nitration is a more favourable reaction to nitrosation since NO_2 cannot form a dimer of N_2O_4. Another possible source of nitration reagents (see **Figure 4**) is specific structural conformations of N_2O_3 and N_2O [49].

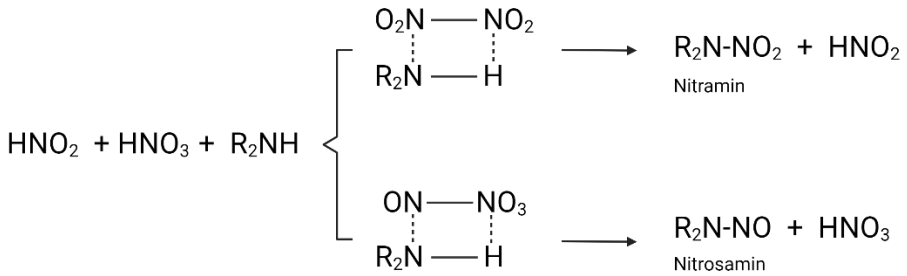

Figure 6. Possible simultaneous formation of nitramines and nitrosamines.

1.3.3. Chemistry of *N*-nitrosation

The mechanism of nitrosation by N_2O_3 and N_2O_4 forming *N*-nitrosamines is described via transition states (**Figure 6**). It is most common for secondary amines and, eventually, tertiary amines. Such reactions in malt and beer have been comprehensively studied and described (especially for NDMA) [23, 46, 49]. Other mechanisms include *N*-nitrosation as a nucleophilic substitution of hydrogen (from N-H) by electrophilic agents, such as nitrosonium cation (NO^+). The suitable precursor molecules for this reaction are then amines, hydroxylamines, and less frequently (hetero)amides, carbamates, hydrazides, ureas, guanidine, some amino acids, and aromatic N-H moieties (pyrroles or tetrazoles). Another alternative mechanism is the oxidation of hydrazones and hydrazines or the reduction of *N*-nitro compounds [56].

The intramolecular rearrangement of the nitrosyl group in phenolic *N*-nitrosamines can demonstrate the substantial effect of pH on a substrate. At acidic conditions (2-8M HCl), *N*-nitroso-*N*-methyl aniline underwent intramolecular shift leading to two main products, *p*-nitroso-*N*-methyl aniline (*C*-nitroso compound) and *N*-methyl aniline (product of trans-nitrosation to suitable acceptor) [57].

1.3.4. Chemistry of *C*-nitrosation

The mechanism of *C*-nitrosation was described as an electrophilic attack of ^+NO or $^+H_2NO_2$ ions on favourable nucleophile sites of a substrate. The substrate can be any electron-rich hydrocarbons, such as in olefines, enolates, and molecules with aromatic rings [58, 59]. A kinetic study of amino acid nitrosation by the N_2O_3 transition state led to two *C*-nitroso and *N*-nitroso products. An intramolecular migration of the nitroso group

can also happen if amino acids form a five- or six-carbon ring transition state [60]. Favourable *C*-nitrosation precursors generally are molecules with nucleophilic carbon sites, such as phenolic and polyphenolic compounds, some amino acids, etc. [61-63]. Regarding the *C*-nitrosation of phenols, acidic conditions drive nitrosation into *orto*- positions, whereas alkaline conditions drive it to *para*-positions [64].

C-nitrosation is often discussed as a competing reaction to *N*-nitrosation. One of the reasons might be that protonated secondary amines (precursors *N*-nitrosamines) are inactive for *N*-nitrosation at pH<5.6. Hence, especially in acidic conditions, *C*-nitrosation is preferable. Compounds rapidly undergoing *C*-nitrosation are sometimes called *N*-nitrosation inhibitors or nitrite scavengers since they prevent harmful *N*-nitrosamine formation [40]. The most inhibiting properties were proved for ascorbic acid (vitamin C) and its derivatives [32, 65-70].

Similarly, α-Tocopherol (vitamin E) inhibited undesired *N*-nitrosation at acidic conditions (pH~3), but at pH>5, showed the opposite effect [67]. Erythorbic acid, a stereoisomer of ascorbic acid, and ascorbyl palmitate, an antioxidant soluble in fat, also showed inhibiting properties when tested individually. However, when combined, no synergic effect was shown [71, 72]. An inhibitive effect of alcohols (methanol, ethanol, n-propanol, isopropanol) was also observed during the *N*-nitrosation of tyramine [73].

1.4 Possible precursors in beer and raw materials

The molecules formed after *C*-nitrosation, or the products of inhibition reaction, are barely discussed in the literature, and their properties remain unknown. Possible reaction products are *C*-nitroso compounds or their tautomers (oximes), sometimes even without the nitroso group. The following section will discuss possible precursors, their products after reactions with nitrite, and their health-effect properties if known [49, 74, 75].

1.4.1 Phenols

Phenolic compounds are known for their antioxidant activities. The inhibition of undesired *N*-nitrosamine formation was observed for caffeic, dihydrocaffeic, ferulic, and protocatechuic acids. Lower inhibitive properties were determined for coumaric acid and chlorogenic acid [67]. On the contrary, di- and trihydric phenols (at alkalic conditions) or cinnamic acid, eugenol, and vanillic acid showed catalyzing properties [67, 76]. However, comparing inhibitive activity against antioxidant activity did not reveal any correlation [77].

The inhibition of undesired *N*-nitrosation is simply a preferable nitrosation or nitration reaction of phenols. The reactivity of phenols can increased by electron-donating substituents on aromatic rings (such as alkyl, methoxy, hydroxy, and amine), which preferably orient *C*-nitrosation into *ortho*- and *para*-positions. More potent inhibition properties showed phenols with olefine or vicinal hydroxyl groups [67]. Halogen, carboxyl, carbonyl, or cyano- substituents have the electron-withdrawing effect and drive *C*-nitrosation into *meta*-position [59, 78]. In addition, at acidic conditions (pH<4), various aromatic compounds (phenol, aniline, p-toluidine, and 1,2,4-trihydroxy benzene) formed even free cyanide ions via several consecutive reactions [79].

Beer and its raw materials are naturally rich in phenolic compounds (4-ethylphenol, 4-ethyl guaiacol, pyrocatechol, pyrogallol, syringic acid, salicylic acid, *p*-hydroxyphenyl acetic acid), derivatives of cinnamic acid (caffeic, *p*-coumaric, chlorogenic, sinapic, and ferulic acid), and derivatives of benzoic acid (p-hydroxybenzoic, protocatechuic, and vanillic acid) [80-83]. The nitrosated phenolic compounds are colourful products that can contribute to the final beer colour [84].

1.4.2 Polyphenols

The mechanism of polyphenol nitrosation was suggested by the nitric oxide radical (·NO) attack producing nitroso and dinitroso derivatives. The suggested inhibitors

of undesired *N*-nitrosamine formation are catechins, procyanidins, or less efficient rutin [67, 85]. Catechin, epicatechin, epicatechin gallate, myricetin, kaempferol, quercetin, and rutin are polyphenols in beer and beer raw materials [83]. They are also effective antioxidants, and their reactions with nitrite were mostly simulated under gastric conditions. Catechin with nitrous acid yielded dinitroso derivative 6,8-dinitrosocatechin, which was further oxidized to a quinone. The nitrite reaction product of quercetin was 2-(3,4-dihydroxybenzoyl)-2,4,6-trihydroxy-3(2H)-benzofuranon. However, the health-effects of these products were not investigated [75]. Similarly, reactions of beer **tannins** with nitrite were also investigated, but the inhibition and health effects were not evaluated [84].

1.4.3 Amino acids and biogenic amines

Amino acids and their derivatives are another extensive group of reactive substances that can undergo nitrosation reactions. Some products, such as NPRO and NSAR, were already mentioned in beer or malt. In aqueous solutions, the nitrosation reaction of proline, 4-hydroxyproline, and sarcosine decreases at higher pH but increases with higher NO_x concentration [86]. Thioproline showed a higher affinity to form *N*-nitroso derivate than proline in the presence of nitrite at physiological conditions. In the presence of nitrates, NPRO and *N*-nitrosothioproline are formed even faster [70]. Trans-nitrosation from NPRO to glutathione and tyrosine molecules was also observed, and the products were S-nitroso glutathione and 3-nitrotyrosine, respectively [87, 88].

Amino acids can also be inhibitors of *N*-nitrosamine formation, and the inhibition efficiency decreased in order cysteine > serine > alanine and proline (which had almost no effect) [67]. S-allyl cysteine in garlic suppressed NPRO formation, and the suggested nitrosation product was N-acetyl-S-allyl cysteine [89]. Nitrosation products of amino acids were described as not colouring compounds, and their contribution to beer colour is negligible [84]. This observation did not agree with our experience when tyrosine, after reaction with nitrite, formed a yellowish-to-brown solution. Depending on specific amino

acids and their derivatives, they can undergo *N*-nitrosation, *C*-nitrosation, or even distinct reaction products without a nitroso group. Nitrite reactions with tyramine, a decarboxylated tyrosine, at stomach conditions led to many reaction products, from which *o*-nitroso tyramine and 3-diazo tyramine were of mutagenic behaviour [59, 73]. Tryptophol, a metabolic intermediate of tryptophan, reacted with nitrite (at pH=3) to form *N*-nitroso derivative (*N*-nitroso tryptophol) and *C*-nitro derivative (6-nitro tryptophol). Both products showed mutagenic properties on *Salmonella* tester strains [90].

Histidine in reaction with sodium nitrite (at pH = 4) yielded five reaction products, and one of them (*N*-nitroso-1H-imidazol-4-yl)acetohydroxamic acid showed some specific mutagenic properties in *Salmonella typhimurium*. In this case, mutagenicity was suggested for *N*-nitroso and hydroxamic groups [91]. Other alternative nitrosation products of aliphatic amino acids (α-,β-,γ-) resulted in the formation of α-hydroxy acids or, α-,β-,γ-lactones and corresponding lactones also showed potential alkylating features [92-95]. Alternatively, it was suggested that nitrosation products in the amine group have higher potency to be alkylating agents than a product where nitrosation occurs in the amide or indole group in the amino acid molecule [93].

1.4.4 Saccharide derivatives

Regarding sugars or their derivatives, Amadori compounds are usually mentioned. Amadori compounds are intermediates of Maillard reactions and consist of monosaccharides and amino acid units. Their highest concentration can be detected in malts, as these compounds are formed at high temperatures during kilning, with temperatures up to 200 °C. They decompose significantly during mashing and wort boiling but not during fermentation [35]. Amadori compounds can react with nitrite at pH = 3, forming *N*-nitroso derivatives; however, their health-effect is currently unknown [96-98].

2. Experimental considerations

The following section discusses the experimental considerations that led to the final experiments. As discussed above, target-unknown non-volatile NOCs are broad and complex groups of organic compounds, and the primary aim was to characterize them structurally. Since the natural content of NOCs is in ppb levels, there was a demand to prepare beer matrices with a higher content of target compounds [20]. The artificial addition of nitrites into beer or exposure of malt to nitric oxides was a promising approach, and the final procedures are described in the experimental parts. The following studies will discuss non-volatile NOCs or potentially ATNC-positive compounds as N-products since they were detected in beer after nitrite-related reactions and not all contain specific nitroso groups.

When artificial beer and malt were prepared, the next task was extracting the broadest spectrum of N-products possible and distinguishing them from the interferents. N-products are medium-polar to polar and small to medium in size; therefore, they can be determined by gas chromatography (GC).

2.1 Derivatization and extraction

Chemical derivatization of N-products was necessary to improve the volatility of target compounds. An appropriate derivatization method was needed, considering the chosen instrumentation, N-product complexity, and chemical composition. The aim was to enhance the overall volatility of hydroxyls, carboxyles, and amino groups. In past NPRO, NSAR, and NPIC determinations, methylation reagents diazomethane and BF3-methanol were used [21, 22]. Nowadays, silylation reactions are more common. Its efficiency increases in order: amides < amines < carboxylic acids < phenols < alcohols. Common silylation agents are BSA, BSTFA, MTBSTFA, and, less frequently, MSA and MSTFA. The efficiency of BSTFA is higher than BSA since it has higher silyl-donor strength, and

its by-products are more volatile [99, 100]. Derivatization yields for some compounds can vary in two ways. The first is an insufficient solubility of a compound in a solvent, resulting in the analyte's absence in the solution. The second is the silylating strength, which depends on the type of derivatized functional group and total solvent mixture [101]. A silylation catalyst such as trimethylchlorosilane can avoid the latter effect and facilitate the derivatization of groups with low affinities, such as amines [100].

Different extraction methods were applied for malt and beer depending on the initial matrix. Solid-liquid phase extraction was chosen for malt samples and was described previously [102]. Solid-phase extraction (SPE) was chosen for beer samples and is commonly used for *N*-nitrosamine determinations. As sorbents were used, polymer cartridges (e.g., LiChlorut EN, WAX-SPE, molecularly imprinted polymer) and RP-SPE cartridges [89, 103, 104]. Since our target NOCs are supposed to have different properties and functional groups, a universal C18-SPE (Discovery DSC-18, 500 mg, Supelco) was selected.

2.2 Chromatographic methods

Determination of NDMA and other volatile *N*-nitrosamines by GC is widespread and used in many matrices, such as beer, malt, rubber, cosmetics, drugs, water, or meat [4, 8, 11, 105-108]. They usually employ mid-polar to non-polar GC columns with cyanopropyl or phenyl active sites (5-14%), such as DB-624 DB-1701, DB-5, or HP-5MS, to enhance retention of either semi-polar compound. For trace analysis of target unknown NOCs, an HP-5MS UI column was selected for its universal use and suitability for mass spectrometry [11, 20, 89, 104, 105, 109]. GC is mainly coupled with a nitroso-specific chemiluminescence detector (GC-NCD) and mass spectrometry for these applications.

Liquid chromatography (HPLC) is also suitable for determining NOCs because of their higher polarity. For instance, HPLC-NCD was used to determine *N*-nitroso amino acids and other *N*-nitroso derivatives of carboxylic acids in meat [110, 111]. Other HPLC detectors

for detecting NOCs were fluorescence or mass spectrometry [103, 105, 112-114]. Although HPLC could be a sufficient method for non-volatile NOCs determination, the preliminary experiments by GC-NCD showed sufficient response of silylated target compounds and the possibility of methods translation to GC-MS/MS [20].

In our studies, the GC-MS/MS was used since mass spectrometry has the great advantage of structural information, which recently led to the structural identification of *N*-nitrosoproline ethylester [20]. The information from MS/MS fragmentation experiments can result in various proposed molecular structures, which must be confirmed by GC-MS standards analysis. Preparation of such standards in satisfactory purity can be time-consuming and costly and often does not produce the desired confirmation. Because the molecular structure is closely associated with the retention index, any tool that can suggest a retention index based on the proposed molecular structure could be helpful, not only in the area of the present study. A computational tool, DeepReI, was developed in the present study. The DeepReI can predict retention indices in GC for the semi-standard non-polar columns using the Simplified Molecular Input Line Entry System (SMILES) as an input [115]. Its architecture consists of deep-learning neural networks and is comprehensively described in the third paper attached in **Supplementary data – Appendix 1**. DeepReI was extensively used to confirm suggested molecule structures of studied unknown N-products in the first study. In the second study, mass spectrometric data of identified N-products were used for developing the GC-MS/MS method to monitor the natural occurrence of N-products in beers and malts (untreated by nitrite or nitrogen oxides).

2.3 Specific detector for NOCs and ATNC determination

The great advantage of NOCs is the possibility of precise detection provided by nitroso-specific chemiluminescence detector, NCD (also known as a Thermal Energy Analyzer, TEA). Detection consists of a thermal cleavage of the nitrosyl group from

a molecule moiety. Then, oxidation of evolved nitrosyl radicals by ozone forms excited nitrogen dioxide (NO_2*). When NO_2* returns to the ground energy state, the emitted near-infrared light is detected, and its intensity is proportional to the concentration of released nitrosyl groups [110, 116].

The NCD is used in ATNC determination, which is the routine method of determination used to monitor the presence of non-volatile NOCs in beer and other matrices. Method modifications include different cleaving mixtures, such as acidic iodine/iodide or HBr/acetic acid mixture [15, 23, 113, 116]. The linear response to NOCs was proved over six orders of magnitude [110]. Although ATNC should be solely specific for *N*-nitroso compounds, the possibility of false-positive compounds was already mentioned. The summary of NCD-positive compounds, including *N*-nitroso and other NOCs, is listed in **Supplementary data – Appendix 2: Table 1**. The false-positive NCD responses were estimated for nitrothiols and nitrolic acids [12]. Due to the potential existence of false-positive ATNC compounds, the second study aimed to compare the N-products with ATNC concentrations in beer.

3. Results and discussion

The following section comprises the results achieved in two publications. The first publication focuses on the structural elucidation of N-products in artificially nitrosated beer. Based on gathered GC-MS/MS fragmentation, a specific detection method for N-products was developed to monitor their natural occurrence in untreated beers and malts. N-products were monitored on commercially available 191 beer samples and 198 malt samples. Both publications include final experimental procedures along with results and discussion. Supporting information for both papers is in **Supplementary data – Appendices 3 and 4**.

JOURNAL OF AGRICULTURAL AND FOOD CHEMISTRY

pubs.acs.org/JAFC Article

Characterization of Nitrite-Related Reaction Products in Beer

Michaela Malečková, Tomáš Vrzal,* Jana Olšovská, and Jana Sobotníková

Cite This: *J. Agric. Food Chem.* 2021, 69, 11687−11695 Read Online

ACCESS | Metrics & More | Article Recommendations | Supporting Information

ABSTRACT: The effect of nitrites in foods and beverages still raises discussion due to the possible formation of harmful nitroso compounds. However, as most of these compounds in beer were not structurally characterized yet, the research about their toxicological relevance for consumers is limited. This study is focused on identification of the products formed by nitrite (or isotopically labeled nitrite ^{15}N) reactions in beer using gas chromatography with tandem mass spectrometry. In total, 19 products were identified, and some of them were structurally characterized and confirmed by comparing retention indices and mass spectra of standard/synthesized compounds. Identified compounds were representatives of nitroso, nitro, oxime, and even cyano compounds. For the peaks which were not structurally identified, primary structural characteristics were also listed. Found products were further screened in 16 authentic beer samples which showed the apparent occurrence of found compounds in non-treated beers.

KEYWORDS: *nitrite, beer, nitroso compounds, gas chromatography, tandem mass spectrometry*

INTRODUCTION

The possible health risk of nitrite in foods still raises discussions. While some studies consider naturally occurred nitrites as beneficial for gastrointestinal, immune, and cardiovascular functions,[1,2] other ones are concerned about the formation of carcinogenic compounds (especially volatile *N*-nitrosamines) from the compounds present in foods or beverages, such as meat products and beer.[3,4] Ways how nitrites are brought into contact with natural compounds in foods vary. For instance, in meat production, sodium nitrite (E250) is added purposely to prevent microbial growth. Conversely, non-treated vegetables and fruits could naturally contain nitrite in considerable amounts.[5] Also, in the case of beer, a higher concentration of nitrites is usually a consequence of the contamination.[6] Several studies found a correlation between microbial contamination of beer and Apparent Total Nitroso Compound concentration (ATNC, a determination of all nitroso functional groups in the sample).[7] For instance, increased ATNC was observed in beers contaminated by various bacteria, such as from the genera *Bacillaceae*, *Enterobacteriaceae*, and *Obesumbacterium*.[6,8,9] The above-mentioned bacteria reduced nitrate to nitrite, which might react with beer compounds to form ATNC responsive products. Although ATNC concentrations in beer are usually lower than 20 μg (N−NO)/L, occasionally, they may be significantly higher as a study from 2014 observed.[6] This may be the result of microbial contamination with combination of a higher level of nitrate in beer or raw materials. The most possible nitrate-donating raw material may be hop since the transfer of nitrates from hop (during wort boiling as well as dry hopping) was found to be almost quantitative.[10]

The products of nitrite reactions in beer are generally assumed to be non-volatile nitroso compounds approximately quantitated by ATNC. Known volatile *N*-nitrosamines (such as *N*-nitrosodimethylamine) contribute to ATNC only by 1%, and their origin was proved to be different.[11,12] Therefore, the remaining ATNC content is supposed to be formed by unknown compounds.[13] Their precursors are hypothesized to be phenols, amines, amino acids, or peptides, and depending on their concentration, chemical nature, and ambient conditions, they might be nitrosated, nitrated, or oxidized.[12] Since specific products of these reactions are so far unknown, the study of their toxicology relevance and the advancement of their detection is limited.

Several attempts to develop a new method for their characterization were reported previously.[14,15] One study used liquid chromatography and gas chromatography (GC), combined with a nitrogen chemiluminescence detector (NCD) and mass spectrometry (MS), respectively. As a result, the MS spectrum of one unknown *N*-nitroso compound was published.[14] In our previously published study, GC combined with pyrolytic profiling NCD was used to classify chromatographic peaks into *C*-nitroso, *N*-nitroso, and interferent compound groups, which gave primary structural information about detected analytes. Another important finding was structural characterization of unknown compounds based on MS/MS fragmentation experiments, which led to the identification of two most significant peaks as *N*-nitrosoproline (NPRO) and its ethyl ester (NPRO−Et).[15] However, except for *N*-nitrosoproline, its ethyl ester, and two more unknown nitroso compounds, the other compounds of interest remained unidentified.

This study is focused on the identification of the products formed by the reaction of nitrite with naturally occurring compounds in beer. The aim is to prepare products of nitrite

Received: July 22, 2021
Revised: September 13, 2021
Accepted: September 14, 2021
Published: September 24, 2021

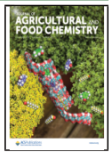

reactions directly in the beer matrix, to detect them by GC−MS, and to characterize their chemical structures by tandem MS. Knowing structures of these compounds could bring new opportunities for the analytical method development as well as the study of their toxicological relevance.

The study was carried out in three stages: (i) detection of the products formed by the reaction of nitrite in beer and their structural study based on the MS/MS analyses (as well as isotopically labeled experiments),[16] (ii) detection and characterization of the products formed by the reaction of nitrite with standard compounds previously described in beer, and (iii) a brief screening of detected products in real beer samples. Besides using general rules for structural elucidation from GC−MS/MS fragmentation, a new computational tool DeepReI [for retention index (RI) prediction according to SMILES notation] was used as well.[17] Additional information regarding RI prediction (RI_{pred}), all MS and MS/MS spectra of the products, and the results of the screening experiment are listed in the Supporting Information.

MATERIALS AND METHODS

Reagents and Materials. All used reagents, sodium nitrite (97%), isotopically labeled sodium nitrite ^{15}N (98 atom % ^{15}N, 95%), a solution of C_7−C_{30} saturated *n*-alkanes (1000 μg/mL in hexane), *N*,*O*-bis(trimethylsilyl)trifluoroacetamide with trimethylchlorosilane (BSTFA + TMCS, 99:1, 98.5%), 2-ethylphenol (99%), 2-methoxyphenol (98%), pyruvic acid oxime (98%), tyrosine (≥98.0%), hydroxylamine hydrochloride (99%), pyridine (≥99.0%), 4-cyanophenol (95%), 2-cyclohexen-1-one (≥95.0%), 4-nitrosophenol (95%), and DL-phenylalanine-1-^{13}C (99 atom % ^{13}C), were purchased from Sigma-Aldrich, Germany. Hydrochloric acid (37%), ammonium amidosulfonate (>99%), and sulfuric acid (96%) were obtained from Merck, Germany. Acetonitrile, dichloromethane, ethyl acetate, *n*-hexane, and methanol used as solvents were of reagent grade, obtained from Honeywell, USA. Deionized water was obtained using a Milli-Q system.

Reaction of Nitrite with a Beer Sample. A sample of lager beer (500 mL, obtained from the local manufacturer) was treated with 4 mL of 37% hydrochloric acid and 2.0 g of sodium nitrite. The beer was stored in the dark at room temperature for 1 month to obtain enough reaction product yield. The same procedure was applied to prepare parallel beers (with isotopically labeled sodium nitrite addition and blank beer without any nitrite addition). Before sample extraction, a beer sample (6 mL) and 1 mL of 0.2 mol/L ammonium amidosulfonate in 0.2 mol/L sulfuric acid were left 15−30 min at room temperature in the dark to remove unreacted nitrites. Meanwhile, an SPE sorbent (Discovery DSC-18, 500 mg, Supelco) was conditioned with 6 mL of methanol and 6 mL of water. The whole beer sample (7 mL) was loaded on a conditioned SPE cartridge, washed with 1 mL of water, and gently dried by vacuum, and retained compounds were eluted from the SPE cartridge by 12 mL of dichloromethane. The obtained extract was evaporated to dryness by a gentle argon flow (Air Products, Czech Republic) at 45 °C. The dry residuum was dissolved in 0.2 mL of BSTFA, and derivatization was performed for 1 h at 65 °C.

Reactions of Standard Compounds. Oximation and derivatization of pyruvic acid and 2-cyclohexen-1-one were performed according to a previous study.[18] The standard (39 μL) was mixed with 200 μL of 3.5 mol/L hydroxylamine hydrochloride solution in pyridine. The mixture was left in an ultrasonication bath for 1 min and incubated at 35 °C for 3 h in the dark. Derivatization was performed by 500 μL of BSTFA addition to the cooled sample, and the mixture was left at 70 °C for 2 h.

Parallel samples of tyrosine, histidine, phenylalanine, 2-ethylphenol, and 2-methoxy phenol (15.0 mg) with the addition of sodium nitrite (17.5 mg) were dissolved in 1 mL of methanol and acidified by 20 μL of hydrochloric acid (37%), separately. The mixture was left over 72 h at room temperature in the dark. The liquid mixture was then transferred into a new vial and evaporated under a gentle argon flow at 50 °C. The dry residuum was dissolved in 500 μL of BSTFA and incubated at 65 °C for 1 h. The reaction of vanillic acid with sodium nitrite was described in the previous study.[17] 4-Nitroso phenol (40.5 mg) and 4-cyano phenol (18.1 mg) were dissolved in 500 μL of BSTFA, separately, and both mixtures were incubated at 65 °C for 1 h. If necessary, the samples were diluted by *n*-hexane before GC−MS analyses.

GC−MS/MS Analyses. Samples were analyzed using a gas chromatograph Agilent 7890 B with a 7000D triple quadrupole mass spectrometric detector (Agilent Technologies, Santa Clara, USA). Separations were carried out on a capillary column HP-5MS UI [(5% phenyl)-methylpolysiloxane, 30 m × 0.25 mm × 0.25 μm]. Injections were performed in a split mode (5:1) at 250 °C, with a constant helium flow at 1 mL/min (Air Products, Czech Republic). A gradient temperature program was set to 50 °C (1.5 min)—20 °C/min—150 °C (5 min)—10 °C/min—210 °C (3 min)—10 °C/min—320 °C (5 min), and the interface temperature was 250 °C. Two conditions of electron impact ionization were used, standard (70 eV, 230 °C) and soft (20 eV, 180 °C), to decrease the fragmentation rate and improve the relative intensity of molecular ions. A full scan mode of detection was maintained in the range of m/z 40−600, and MS/MS experiments in a product or precursor ion mode were performed at a collision energy of 15 eV.

Methodology for Structure Elucidation of the Products. Peaks of the interest products were identified according to a comparison of chromatograms and MS full scan spectra of parallel beer samples after the reaction with sodium nitrite and isotopically labeled sodium nitrite ($Na^{15}NO_2$). If some parallel MS spectra differ by m/z units, it points out isotopic nitrogen in the molecule originating from the nitrite reaction. The beer sample (without nitrite addition) was analyzed as a blank control. Recorded MS spectra of the detected peaks were compared to a reference library (NIST 14 MS Library). In peak coelution, the deconvoluted spectra were preferably used for searching in the reference library. After the detection of the products, RIs were calculated according to the definition using saturated *n*-alkanes (C_7−C_{30}).[19] For structural elucidation of the reaction products, many MS/MS experiments were performed. For instance, precursor ion spectra were used to identify a molecular ion. Structures of unknown products were suggested based on fragmentation, which was drafted according to product ion spectra and isotopically labeled fragments. The suggested structure (from the fragmentation path and/or reference library search) was transformed into the SMILES notation by ACD/ChemSketch software (version 12.01, Advanced Chemistry Development, Inc., Canada), according to which RI was predicted by DeepReI tool.[17] If experimental RI matched the predicted RI interval, the molecule was synthesized to confirm/disprove the assumed structure. Otherwise, the suggested molecule fragmentation pattern and molecule had to be redesigned.

Semiquantitation of the Products in Non-treated Beers. Semiquantitation of detected products in 16 commercial beer samples was performed by normalizing the peak response area to the internal standard (IS) response area (calculated as the ratio of peak area of the analyte to peak area of IS). Tested commercial beers were obtained from foreign and local manufacturers, including industrial breweries, microbreweries, and homebrewers (Table S3). Beer samples (non-acidified and non-treated by nitrite) were prepared and analyzed according to the procedures described above. The IS addition of 100 μL of DL-phenylalanine-1-^{13}C (100 mg/L) was performed to all beer samples immediately after SPE elution. Products were detected in a multiple-reaction-monitoring mode (MRM). Collision energies (CEs) for all MRM transitions were optimized individually for CEs ranging from 5 to 60 eV (Table S4). Relative abundances of the products were calculated by the ratio of the product peak area to the peak area of the IS. Each sample was prepared and analyzed in duplicates.

Safety Considerations. Substances studied in the present study are of unknown toxicity; however, because they are supposed to have some structural characteristics similar to those of toxic *N*-nitrosamines, they should be treated as potentially toxic for a human. Safety

https://doi.org/10.1021/acs.jafc.1c04421
J. Agric. Food Chem. 2021, 69, 11687−11695

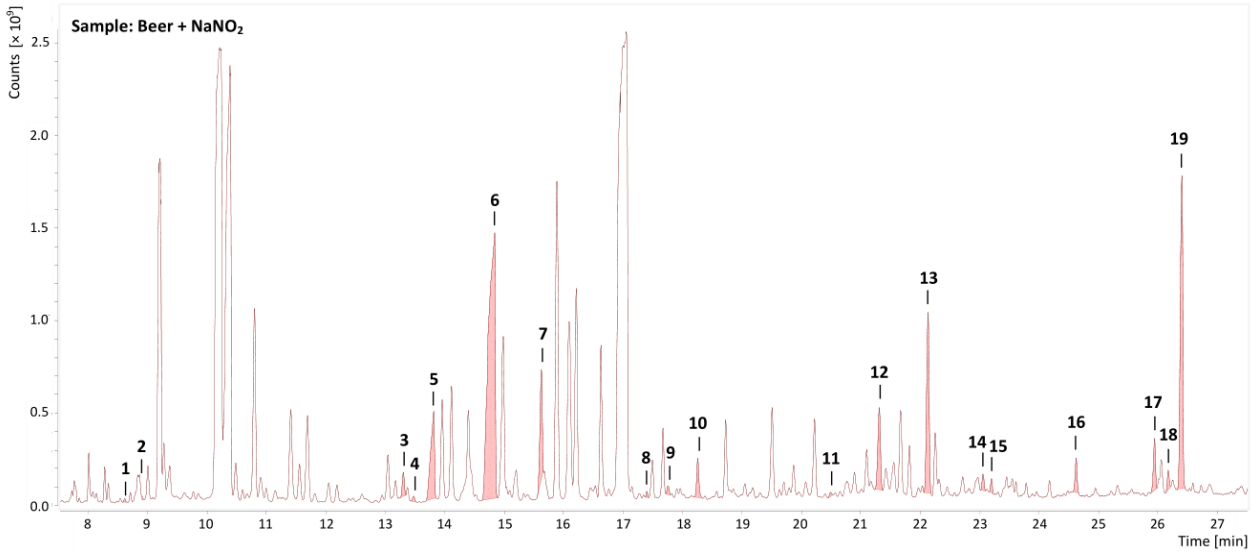

Figure 1. Chromatogram of the beer sample—products of the sodium nitrite reactions are highlighted by numbers.

Table 1. List of Products Formed by the Reaction of Nitrite in a Beer Sample

no.	RT [min]	MW [g/mol]	RI_{exp}	RI_{pred} [a]	RI_{lib} [b]	name of the product	precursor compound
1	8.6	183	1116			unknown	
2	8.9	247	1146	1211	1157	pyruvic acid oxime, 2TMS	
	12.3[c]	195	1348	1470		4-nitrosophenol	
3	13.3	191	1399	1384	1365	4-cyanophenol, TMS	tyrosine
4	13.5	212	1408			unknown	
5	13.7	172	1422	1418		*N*-nitrosoproline ethyl ester	proline
6	14.7	216	1471	1446		*N*-nitrosoproline, TMS	proline
	15.0[c]	223	1488	1481		2-ethyl-6-nitrosophenol	2-ethylphenol
7	15.6	230	1524			unknown	
	16.8[c]	225	1596	1611		2-methoxy-3-nitrosophenol	vanillic acid, guaiacol
8	17.4	239	1627			unknown	
9	17.7	218	1655			unknown	
10	18.2	241	1687	1706	1698	2-methoxy-5-nitrophenol, 1TMS	vanillic acid
11	20.5	306	1821			unknown	tyrosine
12	21.3	269	1866			unknown	
13	22.1	327	1912			unknown	
14	23.0	286	1972			unknown	
15	23.2	341	1981			unknown	tyrosine
16	24.6	357	2082			unknown	tyrosine
17	25.9	443	2189			unknown	tyrosine
18	26.2	389	2209			unknown	tyrosine
19	26.4	443	2230			unknown	tyrosine

[a]Value predicted by the DeepReI tool. [b]According to the reference library (semistandard non-polar). [c]Found as a product of nitrite reaction with the precursor standard compound.

precautions, protective equipment, and handling of samples in a fume hood to prevent exposure must be employed while manipulating with these substances.

RESULTS AND DISCUSSION

Reaction Products of Nitrite and Beer Compounds. Using the methodology described in the previous section led to the identification of 19 reaction products found in beer samples after reaction with nitrite. The corresponding peaks are shown in the beer sample chromatogram (Figure 1), and their characteristics are summarized in Table 1.

Identified Compounds. Compounds **5** and **6** have notably similar full scan spectra with previously published MS spectra of NPRO−Et and NPRO−TMS esters (Figures S1a,d and S2a,d).[15] For the assurance, these peaks' identities were checked by comparison of experimental RIs (RI_{exp}) and RI_{pred} (of the proposed chemical structures), and both matched within HDI[95] prediction intervals, compare Tables 1 and S1. Further, m/z ratio shift, for example, ions m/z 172 (173) and 99 (100), agreed with the proposed fragmentation of NPRO−Et (Figure S1b,c). The same approach applied to shifted fragments m/z 216 (217), 201 (202), 157 (158), and 99 (100) in the mass spectra of compound **6** also supported

https://doi.org/10.1021/acs.jafc.1c04421
J. Agric. Food Chem. 2021, 69, 11687−11695

fragmentation of NPRO−TMS (Figure S2b,c). Considering that the presence of these substances (especially NPRO) in beer was described in several studies[11,15,20] and isotopic experiments supported the fragmentations, peaks **5** and **6** might be affiliated to NPRO−Et and NPRO−TMS esters, respectively. Structures of these compounds (as non-silylated) are shown in Figure 2.

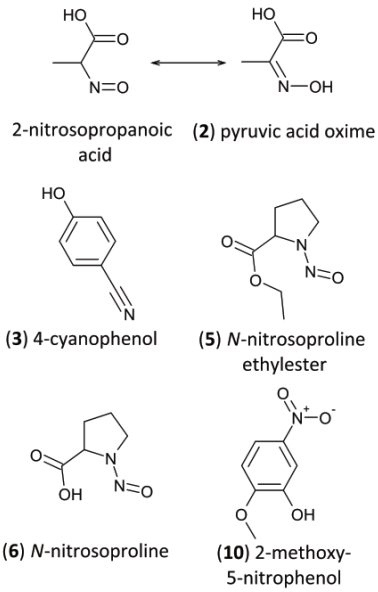

Figure 2. Structures of identified products formed by the reaction of nitrite in a beer sample. Numbers of the analytes correspond to peak numbers listed in Figure 1 and Table 1.

The mass spectrum of peak **7** may be assigned to a previously published spectrum of the unknown nitroso compound (Figure S3a−c).[15] The MS spectrum of this peak showed similar fragmentation to NPRO−TMS ester, with a difference that this peak's fragments were higher by 14 m/z units. Hence, it was affiliated to *N*-nitrosopyroglutamic acid−TMS (NPGA−TMS) or any isomer of *N*-nitrosopipecolic acid−TMS (NPIC−TMS) as standard NPIC−TMS nearly did not match in retention on the TG-200MS column.[15] For this reason, the RI_{exp} and RI_{pred} for all possible structures were compared and showed the best match with NPIC−TMS and NPGA−TMS. Therefore, the other isomers were due to RI comparison denied (Figure S3d). Since predicted RIs of NPIC−TMS and NPGA−TMS were very similar, it was impossible to distinguish which substance more likely corresponded to the unknown peak. Hence, the preparation and analysis of NPGA−TMS were performed; however, except for pyroglutamic acid's chromatographic peak, no product from the nitrite reaction was detected. It might be the result of poor stability and/or the slow rate of pyroglutamic acid with the nitrite reaction. It was described that the NPGA formation could be accelerated by thiocyanate, citrate, or tartrate in the reaction mixture; however, the product was still considerably unstable within studied pH 1−6.[21] Since the NPGA formation might be more favorable in complex samples than in standard solutions, its stability in beer could be also supported. Furthermore, although the standard of NPIC did match at retention on the HP5-MS UI column, this peak remains unidentified until an additional comparison with NPGA can be performed.

The mass spectra comparison of peak **2** (Figure S4a,b) with the reference library found the best match with pyruvic acid oxime, the bis-trimethylsilyl derivative (87.7%, MW 247). Although RI_{exp} was similar to RI_{lib} (suggested by the reference library), RI_{pred} was not in such agreement (Table 1). For this reason, the result of the library search was first checked by MS and MS/MS spectra. The molecular ion (m/z 247) was confirmed by the precursor ion spectrum of m/z 73 (Figure S4c). According to the product ion spectra of m/z 232 and 204, the fragmentation and molecule structure were suggested (Figure S4d−f). Considering the fact that the sample was derivatized by the silylation reagent, the spherically close trimethylsilyl moieties were evident from the abundant fragments m/z 73 and 147.[22] The isotopic experiment and the nitrogen rule (odd molecular mass) confirmed the nitrogen atom in the molecule. Second, the chromatographic and mass spectrometric properties of the unknown peak and synthesized pyruvic acid oxime−2TMS were compared, and the synthesized molecule perfectly matched the chromatographic and mass spectrometric properties of the unknown peak. Hence, pyruvic acid oxime−2TMS (a tautomer of 2-nitrosopropanoic acid) was concluded as the molecule represented by peak **2**, and both (non-silylated) structures are shown in Figure 2. It should be noted that this substance was also detected in GC−MS chromatograms performed on samples during a previous study, where an artificially contaminated beer sample by *Obesumbacterium proteus* (a known microbial agent responsible for the production of nitroso compounds in beer)[9] was analyzed.[15]

Mass spectra of peak **3** (Figure S5a,b) showed the highest match with 4-cyanophenol−TMS (98.3%, MW 191). Although the comparison of RI_{exp} matched RI_{pred}, it did not match RI_{lib} (Table 1). Hence, the molecular structure was further structurally elucidated. The nitrogen atom was obvious from the isotopic experiment and the nitrogen rule. The molecular ion (m/z 191) was identified according to the precursor ion spectrum of m/z 160 [M − 15 − 16] (Figure S5c). The pattern of the full scan spectra, namely, the base peak [M − 15], indicated a structure of a phenolic compound,[23] which was further supported by the product ion spectra of ions m/z 176 and 160 (Figure S5d,e). The target peak showed similar fragmentation as phenol−TMS with a difference that studied peak fragments were higher by 25 m/z units (agreed to the −CN moiety substituting a hydrogen atom).[22] This peak's identity was finally confirmed by the MS spectrum and retention of the 4-cyanophenol−TMS standard. Based on our experiments, this substance was also found among tyrosine reaction products (Figure S5f). Therefore, tyrosine may be a possible precursor for this compound in beer, and the formation of the cyano-functional group could take place according to the proposed mechanism.[24]

The mass spectra comparison of peak **10** (Figure S6a,b) with the reference library resulted in the best match with 2-methoxy-5-nitrophenol−TMS (86.0%, MW 241), and RI_{pred}, RI_{exp}, and RI_{lib} matched each other (Table 1). The nitrogen atom was evident from the isotopic experiment and nitrogen rule. This product matched perfectly (by spectral and retention properties) with the reaction product of vanillic acid nitrosation (Figure S6c).[17] Thus, vanillic acid could be a possible precursor for this compound in beer.

https://doi.org/10.1021/acs.jafc.1c04421
J. Agric. Food Chem. 2021, 69, 11687−11695

Consequently, except NPRO, NPRO−Et, and NPIC (or NPGA), the compounds above were identified in beer first. Their non-derivatized structures are summarized in Figure 2. The assumption about the formation of strictly nitroso compounds is questionable since all products belong to various groups of compounds (oximes, nitroso, cyano, and nitro). Due to this, a follow-up study is needed to confirm the contribution of these compounds to the ATNC.

Detected and Unidentified Compounds. Since a full scan of peak **1** was significantly influenced by baseline noise and coelution, its mass spectra are shown as product ion spectra of m/z 168 (m/z 169 in the isotopic experiment) in Figure S7a,b. The precursor ion spectrum of m/z 168 [M − 15] revealed an unstable molecular ion (m/z 183) (Figure S7c). The suggested compound from the reference library was denied due to the comparison of molecular weights, RIs, and the nitrogen atom presence (from the isotopic experiment together with the nitrogen rule, Table S2). The fragments highlighted by an asterisk represent structures bearing nitrogens originating from the nitrite reaction (Figure S7b). The base peak m/z 94 [M − 89] is probably formed by the loss of the $(CH_3)_3Si{-}O^{\bullet}$ fragment, and the TMS moiety is also apparent from abundant m/z 75 [$(CH_3)_2Si{-}OH^+$]. The product ion spectrum of m/z 94 showed two main fragments, m/z 66 and 39 (Figure S7d), which agreed with the fragmentation of 2-pyrrole-2-carboxaldehyde.[25] However, other unsaturated cycles, such as cyclopentene or cyclohexene, also fitted into the possible fragmentation patterns. Therefore, RI_{pred} of four suggested molecules were compared to RI_{exp}; however, none of them matched sufficiently (Figure S7e). Also, analysis of cyclohex-2-en-1-oxime−TMS denied this molecule to be the identity of this peak as it did not match by spectral neither chromatographic comparison. Hence, the structure of the molecule at 8.6 min remained unknown.

The mass spectrum of peak **4** is shown in Figure S8a. The stable molecular ion m/z 212 was identified by the precursor ion spectrum of m/z 141 (Figure S8b). The suggested compound from the reference library was denied due to the comparison of molecular weights, RIs, and the number of nitrogens (Table S2). Based on the nitrogen rule, this compound has even nitrogen atoms; however, only one nitrogen originated from the nitrite reaction (highlighted by an asterisk), as was obvious from product ion spectra of m/z 212 (m/z 213 in the isotopical experiment). The fragment m/z 141 [M − 71] is formed by the loss of isotopic nitrogen, possibly as simultaneous loss of m/z 44 + 27 (HCN) or 28 ($HC^{15}N$) in the isotopic experiment (Figure S8c,d). Further, abundant fragments m/z 73 and 75 probably correspond to $(CH_3)_3Si^+$ and $(CH_3)_2Si{-}OH^+$ fragments, respectively.[22] However, despite obtained information, the structure of molecule **4** remained unknown.

The comparison of the mass spectrum of peak **8** (Figure S9a) with the reference library revealed the highest match with 4-nitrobenzoic acid, a TMS derivative. The molecular weight and RI of the proposed compound by the reference library matched well with experimental values (Table S2). The molecular ion m/z 239 was identified by the precursor ion spectrum of m/z 224 [M − 15] (Figure S9b). The suggested compound from the reference library was also supported by product ion spectra of m/z 224 and 225 in the isotopic experiment (Figure S9c,d), where the formation of ions m/z 178 [M − 15 − 46] and 150 [M − 15 − 74] could be the losses of $^{\bullet}CH_3$ + $^{\bullet}NO_2$ or $(CH_3)_2Si{=}O$, respectively.[22,26] Therefore, RIs predicted for 4-/3-/2-nitrobenzoic acid isomers were compared to RI_{exp}; the best match was observed for 2-nitrobenzoic acid (Figure S9e). Hence, peak **8** might be a positional isomer of nitrobenzoic acid; however, it should be additionally confirmed by a standard compound.

The mass spectrum of peak **9** is shown in Figure S10a. The molecular ion (m/z 218) was identified by the precursor ion spectrum of the base peak m/z 203 [M − 15] (Figure S10b). The suggested compound from the reference library was denied based on the comparison of molecular weights, RIs, and the number of nitrogens (Table S2). By comparing product ion spectra of m/z 218 and m/z 219 in the isotopic experiment, an even number of nitrogens was observed. However, only one nitrogen (highlighted by an asterisk) originated from the nitrite reaction. The fragments m/z 175 [M − 43] and 144 [M − 74] might be formed by losses of $^{\bullet}CH_3$ + CO and $(CH_3)_2Si{=}O$, respectively (Figure S10c,d). However, despite obtained structural information, the structure of molecule **9** remained unknown.

The MS spectrum of peak **11** is shown in Figure S11a. A molecular ion (m/z 306, also the base peak) was indicated by the precursor ion spectrum of m/z 276 [M − 30] (Figure S11b). The suggested compound from the reference library was denied based on the comparison of molecular weights, RIs, and nitrogens (Table S2). Comparing the product ion spectra of m/z 306 and 308 from the original and isotopic experiments revealed the presence of two nitrogen atoms, both from the nitrite reaction (Figure S11c,d). The product ion spectrum of m/z 291 [M − 15] showed two main fragments, m/z 191 [M − 15 − 100] and 176 [M − 15 − 115], which might correspond to a simultaneous loss of the HCN + $(CH_3)_3Si^{\bullet}$ or $(CH_3)_4Si$ moiety, respectively, as the fragment m/z 264 [M − 15 − 27] was formed by the loss of $^{\bullet}CH_3$ + HCN. In addition, the ion of m/z 276 [M − 30] was formed by the loss of the $^{\bullet}NO$ radical, compare Figure S11b−d. Although this substance was also found as a tyrosine reaction product (Figure S11f), its structure remained unknown.

Mass spectra of peak **12** are shown in Figure S12a,b. The molecular ion (m/z 269) was indicated by the precursor ion spectrum of m/z 223 [M − 46] (Figure S12c). The suggested compound from the reference library was denied based on the comparison of molecular weights, RIs, and the number of nitrogen atoms (Table S2). By comparing the precursor ion spectra of m/z 223 in the original and isotopic experiments, an odd number of nitrogen atoms was observed, and one originated from the nitrite reaction. The ion m/z 223 might originate from the simultaneous loss of $^{\bullet}CH_3$ + HNO or the loss of NO_2 (Figure S12c,d). Also, the TMS moiety is indicated by the m/z 73 fragment.[22] However, despite obtained structural information, the structure of molecule **12** remained unknown.

MS spectra of peak **13** could be assigned to the previously published spectrum, where its primary structural characteristics were described (Figure S13a,d).[15] Unlike the previous study, the molecular ion (m/z 342) was identified by the precursor ion spectrum of m/z 327 [M − 15] (Figure S13c). The suggested compound from the reference library was denied based on the comparison of molecular weights, RIs, and the number of nitrogen atoms (Table S2). By comparing the original and isotopic experiments, an odd number of nitrogens was observed, where one originated from the nitrite reaction (Figure S13a,b). However, despite obtained structural information, the structure of molecule **13** remained unknown.

https://doi.org/10.1021/acs.jafc.1c04421
J. Agric. Food Chem. 2021, 69, 11687−11695

Mass spectra of peak **14** are shown in Figure S14a,b. The molecular ion (m/z 286) was confirmed by the precursor ion spectrum of m/z 271 [M − 15] (Figure S14c). The suggested compound from the reference library was denied based on the comparison of molecular weights, RIs, and the number of nitrogens (Table S2). MS spectra comparison of the original and isotopic experiments revealed even nitrogens, two originating from the nitrite reaction (Figure S14d,e). Nitrogen atoms possibly corresponded to nitro and nitroso groups as indicated by MS spectra of the product ions m/z 225 [M − 15 − 46], 271 [M − 15], and 273 [M − 15] in the isotopic experiment. For instance, m/z 225 (226 in the isotopic experiment) was formed by the loss of 46 (NO_2) from m/z 271. Further losses from m/z 225 included nitrogen as well, compare, for example, m/z 137 [M − 15 − 88] in the original and isotopic experiments (Figure S14f,g). In addition to fragments mentioned above, the fragment m/z 75 probably corresponds to the $(CH_3)_2Si^+{=}OH$ moiety as the samples were silylated.[23] However, despite obtained structural information, the structure of molecule **14** remained unknown.

MS spectra of peak **15** are shown in Figure S15a,b. The molecular ion (m/z 341) was confirmed by the precursor ion spectrum of m/z 326 [M − 15] (Figure S15c). The suggested compound from the reference library was denied based on the comparison of molecular weights, RIs, and the number of nitrogens (Table S2). The nitrogen atom (originating from the nitrite reaction) and its loss could be observed in product ion spectra of m/z 326 (or 327 in the isotopic experiment, Figure S15e,f). Further, fragments such as the base peak [M − 15] and others, [M − 59], [M − 105], and [M − 133], were frequently observed for polyfunctional carboxylic acids.[23] According to fragmentation, peak **15** was suggested as nitroso vanillic acid. DeepReI predicted RIs for nitroso vanillic acid isomers, and some of them matched with RI_{exp} (Figure S15g). Therefore, the reaction of nitrite with vanillic acid was performed; however, an identical product at 23.2 min was not observed. The performed synthesis led to the confirmation of peak **10** as 2-methoxy-5-nitrophenol.[17] In addition, compound **15** was also found among tyrosine reaction products (Figure S15d), so tyrosine may be a possible precursor for this compound in beer.

The remaining peaks **16**, **17**, **18**, and **19** also had a common possible precursor—tyrosine. The suggested compounds from the reference library were denied based on the comparison of molecular weights, RIs, and the number of nitrogens (Table S2). MS spectra of peak **16** are shown in Figure S16a,b. The molecular ion (m/z 357) was identified by the precursor ion spectrum of m/z 342 [M − 15] (Figure S16c), and it corresponds to the base peak frequently observed in MS spectra of aromatic phenols or amines.[23] The remaining fragments were of significantly lower intensities, including m/z 73, which is usually of a higher intensity, indicating more stable incorporation of the TMS moiety. Further, it could indicate good resonance stability of the [M − 15] base peak. This compound has only one nitrogen originating from the nitrite reaction, and its loss is noticeable by further fragmentation of m/z 342 (m/z 343 in the isotopic experiment), where fragments [M − 89] and [M − 119] were formed by nitrogen loss (Figure S16e,f).

Mass spectra of peak **17** are shown in Figure S17a,b. The molecular ion (m/z 443) was identified by the precursor ion spectrum m/z 413 [M − 30] (Figure S17c). Fragments [M − 15] and [M − 30] and low-intense fragment [M − 43] could indicate losses of $^{\bullet}CH_3$, $CH_3{-}CH_3$, and $^{\bullet}CH_3$ + CO, respectively.[23] Highly abundant fragments m/z 73 and 147 indicated spherically close TMS moieties.[22] This product has only one nitrogen originating from the nitrite reaction, and its loss is apparent by further fragmentation of m/z 236 (eventually 237 in the isotopic experiment), forming [M − 58] (assumed loss of $^{\bullet}NO$ + CO or C_2H_4, Figure S17e,f).

MS spectra of peak **18** are shown in Figure S18a,b. The molecular ion (m/z 389) was identified by the precursor ion spectrum of m/z 338 (Figure S18c). Another but highly abundant fragment, m/z 374 [M − 15], had a typical isotopic pattern indicating the presence of chloride, which could be supported by loss of HCl forming m/z 338 [M − 15 − 36]. It has only one nitrogen originating from the nitrite reaction, and its losses are apparent from further fragmentation of m/z 374 (or more precisely m/z 375 in the isotopic experiment). The most significant loss of nitrogen led to the formation of m/z 179 [M − 15 − 195]; compare product ion spectra of m/z 374 and 375 in Figure S18e,f. However, based on the information of the mentioned MS/MS spectra, the specific group containing nitrogen was not revealed, as well as the compound structure.

MS spectra of peak **19** are shown in Figure S19a,b. The molecular ion (m/z 443) was confirmed by the precursor ion spectrum m/z 400 [M − 43] (Figure S19c). The peak has fragments typical for polyfunctional carboxylic acids [M − 15], [M − 43], [M − 90], [M − 105], and [M − 133] and for aminoacids [M − 15], [M − 43], and [M − 117] mostly formed by alpha-cleavage. Also, the fragment m/z 218 represented by TMS−N(H)−C(H)$^+$−C(O)−O−TMS was previously mentioned to be typical for α-amino acids;[23] hence, m/z 219 [M − 224]$^{\bullet+}$ could be of a similar structure of TMS−O−C(H)$^+$−C(O)−O−TMS. Its opposite fragment 224 [M − 219]$^+$ (bearing nitrogen from the reaction with nitrite) has similar intensity. Mentioned fragments were not found in other product ion spectra of abundant fragments; hence, these fragments might be the results of competitive cleavages. Highly abundant fragments m/z 73 and 147 indicated spherically close TMS moieties.[22] The molecule has one nitrogen that originated from the nitrite reaction. The loss of this nitrogen (supposedly as a $^{\bullet}NO$ or HNO together with another small molecule loss) is obvious from the product ion spectra of m/z 208 (m/z 209 of the isotopic experiment) and 238 (m/z 239 of the isotopic experiment) (Figure S19e−h). Based on proposed fragmentation, the peak was suggested to be a nitro derivative (and TMS derivative) of 2-hydroxy-3-(4-hydroxyphenyl)propanoic acid, having a nitro group bonded to an aromatic ring. Based on previous studies about nitrosation of tyrosine,[27,28] the formation of a 3-nitro derivative was suggested, and the RI prediction was performed (Table S1). Although RI_{exp} (2230) did not match the RI_{pred} HDI^{95} prediction interval calculated by DeepReI (2142-2222), the RI_{exp} was still very close; hence, the suggested molecule was not denied. However, an additional confirmation/rejection of the structure based on analysis by more specific techniques is advised. Furthermore, peaks **18** and **19** had common several MS/MS spectra, such as product ions of m/z 338, 293, 264, 249, 222, 219, and 179, indicating the same molecular basis.

Reaction Products of Nitrite with Standard Compounds. In addition to the study of nitrite reaction products in the complex beer matrix, there was simultaneously paid attention to the substances formed by the nitrite reaction with few compounds previously described in beer.[29−31] These

https://doi.org/10.1021/acs.jafc.1c04421
J. Agric. Food Chem. 2021, 69, 11687−11695

substances were 2-ethyl phenol, 2-methoxy phenol (guaiacol), vanillic acid, and amino acids (tyrosine, phenylalanine, and histidine). They were chosen with a criterion to contain a substituted aromatic ring, which is supposed to be favorable to form *C*-nitroso compounds.[32−34]

The reactions of amino acids with sodium nitrite yielded many unknown products. However, for structure elucidation, only reaction products of tyrosine were selected because some of the products were notably similar to several unknown products in beer samples. They were peaks **3**, **11**, **15**, **16**, **17**, **18**, and **19** (Table 1). Their MS spectra are individually shown in the Supporting Information in Figures S5f, S11f, and S15d−S19d. It should be highlighted that peak **3** was structurally characterized above as 4-cyanophenol (a TMS derivative). Hence, tyrosine could be a precursor of this substance. Nevertheless, further study is desired to resolve individual tyrosine reaction products as more comprehensive fragmentations were already discussed in the previous section.

The chromatogram of 2-ethylphenol with sodium nitrite reaction showed one product at 15.0 min and unreacted 2-ethylphenol (9.7 min, NIST 14 match 80.3%), see Table 1. According to the MS spectral pattern in Figure S20a, both substances followed fragmentation as monosubstituted phenolic compounds, such as stable molecular ions and [M − 15] ions.[22] The reaction product was assumed to be 2-ethyl-nitrosophenol due to a difference $\Delta m/z$ 29 between both molecular ions (it might correspond to the −NO moiety substituting a hydrogen atom). Hence, RI_{pred} of four possible positional isomers of 2-ethylnitrosophenol were compared to RI_{exp} (Figure S20b). The most similar RI_{pred} had 2-ethyl-6-nitrosophenol trimethylsilyl ether. Apart from the ethyl substituent, the hydroxyl group activates an aromatic ring to allow *C*-nitrosation into ortho- and para-positions. Since the ethyl group occupies one ortho-position, the second one is available to form 2-ethyl-6-nitroso substituted phenol.[35]

The reaction of guaiacol with sodium nitrite yielded the formation of one main product at 16.8 min (Table 1) and unreacted 2-methoxy phenol (10.2 min, NIST 14 match 94.1%) (Figure S21a). The same assumption as for 2-ethylphenol was applied. Hence, RIs for all four possible positional isomers were predicted (Figure S21b). The most similar RI_{pred} had 2-methoxy-5-nitrosophenol trimethylsilyl ether. Although both methoxy and hydroxyl groups activate an aromatic ring to allow *C*-nitrosation into ortho- and para-positions, predicting a more favorable nitrosation product is questionable as these substituents are mutually in the ortho-position. Since an identical product was found recently (in the reaction of vanillic acid with nitrite) at the same retention (16.8 min) and had the same MS spectrum (Figure S21a) and its second product was identified as 2-methoxy-5-nitrophenol (RT = 18.2 min), the corresponding peak could be substituted equally.[17]

Semiquantitative Determination of the Products in Commercial Beers. The GC−MS/MS method for determining the products (mentioned in the previous sections and listed in Table 1) was developed to demonstrate the research's practical relevance. The list of analytes found in beer was extended by 4-nitroso phenol (Figure S22) and 2-methoxy-5-nitrosophenol (both as trimethylsilyl ethers). In this preliminary screening, 16 commercial beers from local and foreign manufacturers were analyzed to investigate these compounds' relative amounts in non-treated beer. The semiquantitative results of target compounds are summarized in Table S5. Most analytes were found at a level <1.0 of the relative unit, which corresponded to the peaks with responses lower than the IS response. Compounds **3** (4-cyanophenol), **10** (2-methoxy-5-nitrophenol), and **15** exceeded abundances up to <10 of relative units (normalized to IS), and the mentioned peaks were detected in all samples. Higher relative units (>10) were found for compound **1**, which was detected in most studied samples. Regarding 4-cyanophenol (13.3 min), some tested samples also exceeded relative units of 10. Peak **13** showed the highest relative units (>50); however, it was detected only in six samples. Based on the results, further attention should be paid to elucidating the molecules with higher relative amounts in commercial beers. The present paper structurally described two analytes of desired interest: peaks **3** and **10** were among newly identified compounds. The primary screening supported the study's importance as most analytes were detected in commercial beer samples. However, observing these compounds in beer should not bear any harmful consequence for beer consumers since the compounds' toxicological relevance is not currently known.

Based on the results, nitrite in beer led to the formation of various nitrogen-containing compounds. Besides *N*-nitroso compounds, the representatives of oxime, *C*-nitroso, nitro, and nitrile group-containing compounds were identified and also detected in beer samples. As beer is brewed from natural resources, the studied compounds may be possibly found in other foods, especially plant-based. Although most compounds were not completely structurally characterized, the primary structure characteristics were estimated to all products. The possible health risk resulting from the consumption of beer/foods containing the compounds studied in this study should be analyzed in the future.

■ ASSOCIATED CONTENT

Supporting Information

The Supporting Information is available free of charge at https://pubs.acs.org/doi/10.1021/acs.jafc.1c04421.

Results of predicted RI by DeepReI according to proposed structures of studied compounds; remaining unidentified peaks and their best match results of MS spectra comparison with the reference library; list of beers used for primary monitoring of the identified products; list of monitored compounds, supplemented by MRM transitions at optimal CEs; semiquantitation results of the products in beer samples; MS spectra of peak **5** and the same peak in the isotopic experiment found in beer samples; proposed fragmentation and MS spectrum of the peak identified as NPRO−Et copied from a previous publication;[1] MS spectra of peak **6** (a) and the same peak in the isotopic experiment found in beer samples; proposed fragmentation and MS spectrum of the peak identified as NPRO−TMS copied from the previous publication;[1] MS spectra of peak **7** and the same peak in the isotopic experiment found in beer samples; MS spectrum of the peak found in artificially nitrosated beer at 14.7 min copied from the previous publication;[1] comparison of the peak's experimental RI and predicted RIs of NPIC−TMS (first three isomers) and NPGA−TMS (second three isomers); MS spectra of peak **2** and the same peak in the isotopic experiment found in beer samples; precursor ion spectrum of m/z 73 and product ion spectra of m/z 232 (d) and m/z 204

https://doi.org/10.1021/acs.jafc.1c04421
J. Agric. Food Chem. 2021, 69, 11687−11695

(e) of the same peak; suggested fragmentation of pyruvic acid oxime−2TMS; MS spectra of peak **3** (a) and the same peak in the isotopic experiment; precursor ion spectrum of m/z 160, product ion spectra of m/z 176, and m/z 160 of the same peak; MS spectrum of the product from tyrosine with the nitrite reaction; MS spectra of peak **10** and the same peak in the isotopic experiment; MS spectrum of the product from vanillic acid with the nitrite reaction, copied from a previous study;[2] product ion spectra of m/z 168 (a) and m/z 169 in the isotopic experiment of peak **1**; precursor ion spectrum of m/z 168 (c) and the product ion spectrum of m/z 94; comparison of the peak's experimental RI and predicted RIs of proposed structures; MS spectrum of peak **4** and the precursor ion spectrum of m/z 212; product ion spectra of m/z 212(c) and m/z 213 in the isotopic experiment of the same peak; MS spectrum of peak **8** and the precursor ion spectrum of m/z 224; product ion spectra of m/z 224 (c) and m/z 225 in the isotopic experiment of the same peak; comparison of the peak's experimental RI and predicted RIs of proposed structures; MS spectrum of peak **9** and the precursor ion spectrum of m/z 203; product ion spectra of m/z 218 (c) and m/z 219 in the isotopic experiment of the same peak; MS spectrum of peak **11** and the precursor ion spectrum of m/z 276, product ion spectra of m/z 306, m/z 308 in the isotopic experiment, and m/z 291 of the same peak; MS spectrum of the product from tyrosine with the nitrite reaction; MS spectra of peak **12** and the same peak in the isotopic experiment; precursor ion spectra of m/z 223 and m/z 223 in the isotopic experiment of the same peak; MS spectra of peak **13** and the same peak in the isotopic experiment; precursor ion spectrum of m/z 223 and the MS spectrum of the peak at 18.3 min found in artificially nitrosated beer;[1] MS spectra of peak **14** and the same peak in the isotopic experiment, precursor ion spectrum of m/z 271, product ion spectra of m/z 271, m/z 273 in the isotopic experiment, m/z 225, and m/z 226 in the isotopic experiment; MS spectra of peak **15** and the same peak in the isotopic experiment, precursor ion spectrum of m/z 326, and MS spectrum of the product from tyrosine with the nitrite reaction; product ion spectra of m/z 326 (e) and m/z 327 in the isotopic experiment; comparison of the peak's experimental RI and predicted RIs of proposed structures; MS spectra of peak **16** and the same peak in the isotopic experiment, precursor ion spectrum of m/z 342, and MS full scan spectrum of the product from tyrosine with the nitrite reaction of the same peak; product ion spectra of m/z 342 and m/z 343 in the isotopic experiment; MS spectra of peak **17** and the same peak in the isotopic experiment, precursor ion spectrum of m/z 413, and MS spectrum of the product from tyrosine with the nitrite reaction of the same peak; product ion spectra of m/z 236 and m/z 237 in the isotopic experiment; MS spectra of peak **18** and the same peak in the isotopic experiment, precursor ion spectrum of m/z 338, and MS spectrum of the product from tyrosine with the nitrite reaction; product ion spectra of m/z 374 and m/z 375 in the isotopic experiment of the same peak; MS spectra of peak **19** and the same peak in the isotopic experiment, precursor ion spectrum of m/z 400, and MS spectrum of the product from tyrosine with the nitrite reaction; product ion spectra of m/z 238, m/z 239 in the isotopic experiment, m/z 208, and m/z 209 in the isotopic experiment of the same peak; chromatogram of the 2-ethyl phenol after the reaction with sodium nitrite and MS spectra of the reaction products; comparison of the peak's experimental RI and predicted RIs of proposed structures; chromatogram of guaiacol after the reaction with sodium nitrite and MS spectra of the reaction products; comparison of the peak's experimental RI and predicted RIs of proposed structures; and chromatogram of 4-nitroso phenol tri(methyl)silyl ether and its MS spectrum (PDF)

AUTHOR INFORMATION

Corresponding Author

Tomáš Vrzal − *Research Institute of Brewing and Malting, 120 00 Prague, Czech Republic;* orcid.org/0000-0001-5866-1520; Email: tomas.vrzal@beerresearch.cz

Authors

Michaela Malečková − *Research Institute of Brewing and Malting, 120 00 Prague, Czech Republic; Faculty of Science, Department of Analytical Chemistry, Charles University, 128 43 Prague, Czech Republic*

Jana Olšovská − *Research Institute of Brewing and Malting, 120 00 Prague, Czech Republic;* orcid.org/0000-0003-4938-3666

Jana Sobotníková − *Faculty of Science, Department of Analytical Chemistry, Charles University, 128 43 Prague, Czech Republic*

Complete contact information is available at: https://pubs.acs.org/10.1021/acs.jafc.1c04421

Notes

The authors declare no competing financial interest.

ACKNOWLEDGMENTS

This study was supported by the Ministry of Agriculture of the Czech Republic within the institutional support MZE-RO1918 and by the project of Specific University Research SVV260560.

REFERENCES

(1) Hord, N. G.; Tang, Y.; Bryan, N. S. Food sources of nitrates and nitrites: the physiologic context for potential health benefits. *Am. J. Clin. Nutr.* **2009**, *90*, 1−10.

(2) Björne, H.; Weitzberg, E.; Lundberg, J. O. Intragastric generation of antimicrobial nitrogen oxides from saliva—Physiological and therapeutic considerations. *Free Radic. Biol. Med.* **2006**, *41*, 1404−1412.

(3) Sindelar, J. J.; Milkowski, A. L. Human safety controversies surrounding nitrate and nitrite in the diet. *Nitric Oxide* **2012**, *26*, 259−266.

(4) Olšovská, J.; Jandovská, V.; Běláková, S.; Kubizniaková, P.; Vrzal, T.; Štěrba, K. Monitoring of potential contaminants in beer from the Czech Republic. *Kvasny Prum.* **2019**, *65*, 84−96.

(5) Carocho, M.; Barreiro, M. F.; Morales, P.; Ferreira, I. C. F. R. Adding Molecules to Food, Pros and Cons: A Review on Synthetic and Natural Food Additives. *Compr. Rev. Food Sci. Food Saf.* **2014**, *13*, 377−399.

(6) Olšovská, J.; Matoulková, D.; Čejka, P.; Jurková, M. Beer and Health. *Kvasny Prum.* **2014**, *60*, 174−181.

(7) Massey, R. C.; Key, P. E.; McWeeny, D. J.; Knowles, M. E. The application of a chemical denitrosation and chemiluminescence

detection procedure for estimation of the apparent concentration of total N-nitroso compounds in foods and beverages. *Food Addit. Contam.* **1984**, *1*, 11−16.
(8) Calderbank, J.; Hammond, J. R. M. Influence of Nitrate and Bacterial Contamination on the Formation of Apparent Total N-nitroso Compounds (ATNC) During Fermentation. *J. Inst. Brew.* **1989**, *95*, 277−281.
(9) Smith, N. A. Cambridge Prize Lecture Nitrate Reduction and N-nitrosation in Brewing*. *J. Inst. Brew.* **1994**, *100*, 347−355.
(10) Kippenberger, M.; Hanke, S.; Biendl, M.; Stettner, G.; Lagemann, A. Transfer of nitrate and various pesticides into beer during dry hopping. *Brew. Sci.* **2014**, *67*, 1−9.
(11) Čulík, J.; Horák, T.; Čejka, P.; Jurková, M. Non-volatile N-nitrosamines in brewing industry. Part 1. - Arrising and methods of estimation. *Kvasny Prum.* **2012**, *58*, 6−12.
(12) Wainwright, T. Nitrosamines in Malt and Beer. *J. Inst. Brew.* **1986**, *92*, 73−80.
(13) Vrzal, T.; Olšovská, J. N-nitrosamines in 21st Century. *Kvasny Prum.* **2016**, *62*, 2−8.
(14) Johnson, P.; Pfab, J.; Massey, R. C. Development of Medhods for the Characterization of Non-volatile N-nitroso Compounds in Malt. *J. Inst. Brew.* **1988**, *94*, 19−22.
(15) Vrzal, T.; Olšovská, J. Pyrolytic profiling nitrosamine specific chemiluminescence detection combined with multivariate chemometric discrimination for non-targeted detection and classification of nitroso compounds in complex samples. *Anal. Chim. Acta* **2019**, *1059*, 136−145.
(16) Clarke, D. B.; Startin, J. R.; Hasnip, S. K.; Crews, C.; Lloyd, A. S.; Dennis, M. J. Progress towards the characterisation of faecal N-nitroso compounds. *Anal. Methods* **2011**, *3*, 544−551.
(17) Vrzal, T.; Malečková, M.; Olšovská, J. DeepReI: Deep learning-based gas chromatographic retention index predictor. *Anal. Chim. Acta* **2021**, *1147*, 64−71.
(18) Mastrangelo, A.; Ferrarini, A.; Rey-Stolle, F.; García, A.; Barbas, C. From sample treatment to biomarker discovery: A tutorial for untargeted metabolomics based on GC-(EI)-Q-MS. *Anal. Chim. Acta* **2015**, *900*, 21−35.
(19) van Den Dool, H.; Dec Kratz, P. A generalization of the retention index system including linear temperature programmed gas—liquid partition chromatography. *J. Chromatogr. A* **1963**, *11*, 463−471.
(20) Johnson, P.; Pfab, J.; Massey, R. C. A method for the investigation of free and protein-bound N-nitrosoproline in beer. *Food Addit. Contam.* **1988**, *5*, 119−125.
(21) Yamada, T.; Yamamoto, M.; Tanimura, A. Reaction of Pyroglutamic Acid with Sodium Nitrite. *Food Hyg. Saf. Sci.* **1981**, *22*, 404−408.
(22) Harvey, D. J.; Vouros, P. Mass Spectrometric Fragmentation of Trimethylsilyl and Related Alkylsilyl Derivatives. *Mass Spectrom. Rev.* **2020**, *39*, 105−211.
(23) Lai, Z.; Fiehn, O. Mass spectral fragmentation of trimethylsilylated small molecules. *Mass Spectrom. Rev.* **2018**, *37*, 245−257.
(24) Zheng, A.; Dzombak, D. A.; Zheng, R. G. Effects of Nitrosation on the Formation of Cyanide in Publicly Owned Treatment Works Secondary Effluent. *Water Environ. Res.* **2004**, *76*, 197−204.
(25) Schreyen, L.; Dirinck, P.; Van Wassenhove, F.; Schamp, N. Volatile flavor components of leek. *J. Agric. Food Chem.* **1976**, *24*, 336−341.
(26) Fulkrod, J. Electron impact induced multiple rearrangements of aralkyl nitro and nitroso compounds and multiple hydrogen rearrangements in cumyl and related cations. Dissertation Thesis, Iowa State University, 1971.
(27) Bartesaghi, S.; Radi, R. Fundamentals on the biochemistry of peroxynitrite and protein tyrosine nitration. *Redox Biol.* **2018**, *14*, 618−625.
(28) Radi, R. Nitric oxide, oxidants, and protein tyrosine nitration. *Proc. Natl. Acad. Sci. U.S.A.* **2004**, *101*, 4003−4008.
(29) Scholtes, C.; Nizet, S.; Collin, S. Guaiacol and 4-Methylphenol as Specific Markers of Torrefied Malts. Fate of Volatile Phenols in Special Beers through Aging. *J. Agric. Food Chem.* **2014**, *62*, 9522−9528.
(30) Nardini, M.; Garaguso, I. Characterization of bioactive compounds and antioxidant activity of fruit beers. *Food Chem.* **2020**, *305*, 125437.
(31) Ferreira, I.; Guido, L. Impact of Wort Amino Acids on Beer Flavour: A Review. *Fermentation* **2018**, *4*, 23.
(32) Fernández-Liencres, M. P.; Calle, E.; González-Mancebo, S.; Casado, J.; Quintero, B. Nitrosation kinetics of phenolic components of foods and beverages. *Int. J. Chem. Kinet.* **1997**, *29*, 119−125.
(33) González-Mancebo, S.; Lacadena, J.; García-Alonso, Y.; Hernández-Benito, J.; Calle, E.; Casado, J. Nitrosation of Phenolic Compounds: Effects of Alkyl Substituents and Solvent. *Monatsh. Chem.* **2002**, *133*, 157−166.
(34) Gowenlock, B. G.; Richter-Addo, G. B. Preparations of C-Nitroso Compounds. *Chem. Rev.* **2004**, *104*, 3315−3340.
(35) González-Jiménez, M.; Arenas-Valgañón, J.; García-Santos, M. d. P.; Calle, E.; Casado, J. Mutagenic products are promoted in the nitrosation of tyramine. *Food Chem.* **2017**, *216*, 60−65.

https://doi.org/10.1021/acs.jafc.1c04421
J. Agric. Food Chem. 2021, 69, 11687−11695

JOURNAL OF AGRICULTURAL AND FOOD CHEMISTRY

pubs.acs.org/JAFC Article

Natural Occurrence of Nitrite-Related Compounds in Malt and Beer

Michaela Malečková, Tomáš Vrzal,* Tomáš Vaško, Jana Olšovská, and Jana Sobotníková

Cite This: J. Agric. Food Chem. 2023, 71, 17321−17329 Read Online

ACCESS | Metrics & More | Article Recommendations | Supporting Information

ABSTRACT: Despite sufficient control of volatile *N*-nitrosamines in foods and beverages, little attention remained on nonvolatile nitroso compounds, which are mostly unknown and relative to nitrite reactions. In a recent study, new compounds related to reactions of nitrite in beer were pyruvic acid oxime, 4-nitrosophenol, 4-cyanophenol, *N*-nitrosoproline ethyl ester, nitrosoguaiacol, and 2-methoxy-5-nitrophenol, as well as the already known *N*-nitrosoproline. The present study is intended to observe their natural occurrence in commercial beers and malts. All 22 nitrite-related products (N-products) were monitored in almost 200 samples of beers and malts. As many as 17 N-products were detected in malts, and all 22 N-products were found in beers. The hierarchical clustering grouped samples based on similarities of detected N-products by frequency of their appearance and level of response. Between N-products and *N*-nitrosodimethylamine concentrations in malts, only moderate Pearson correlations were found. The same applied to N-product correlations with the apparent total nitroso compound determination in beers.

KEYWORDS: *ATNC, beer, malt, NDMA, nitrite, nitroso compounds*

INTRODUCTION

Nitroso compounds (NOCs) remain a continuing problem in foods and beverages. They are formed by reactions of nitrosation agents, namely, nitric oxides and nitrites, with naturally present compounds. The first concern about volatile *N*-nitrosamines was explicitly received due to their known carcinogenic and mutagenic properties, and some representatives, e.g., *N*-nitrosodimethylamine (NDMA), were also found in malt and beer.[1−3] Volatile *N*-nitrosamines are primarily formed in malt, but some residues can remain in beer. The formation was associated with reactions of nitric oxides in drying air (from direct kilns) with precursors presented in barley. Thanks to technological improvements, such as replacing direct kilns with indirect kilns or sulfuring, the levels of volatile *N*-nitrosamine were significantly minimalized. Nowadays, typical concentrations of NDMA in malts are units of parts per billion (ppb) or less and in beers are less than units of ppb.[1]

Besides volatile *N*-nitrosamines, a significant part of total NOCs in beer consists of nonvolatile representatives, which are structurally nearly unknown. They are associated with nitrite reactions with midpolar/polar compounds presented in beer or its raw materials. The precursors are suggested to be amino acids, phenolic acids, polyphenols, or derivatives of saccharides.[3−5] Their formation was severally proven and monitored during fermentation, indicating a side effect of microbial contamination.[2,3] The principle is an enzymatic reduction of nitrates into nitrites, which further react with the named precursors, yielding nonvolatile *N*-nitroso and *C*-nitroso compounds.[1,6] The source of nitrates can be a hop, from which nitrate transfer during wort boiling is almost quantitative.[7,8] Therefore, when the higher nitrate content hop is combined with contaminated yeast, nonvolatile NOCs may be registered in considerable amounts (up to hundreds of ppb).[3]

Comprehensive research on volatile *N*-nitrosamines was carried out due to their simple determination by gas chromatography, mostly coupled with nitroso-specific chemiluminescence detection (GC-NCD) and, more importantly, the accessibility of analytical standards. Since most nonvolatile NOCs are unknown compounds, analytical standards do not exist, which limits further qualitative and quantitative investigations, leading to more exact health-safety assumptions and food quality control. Although methods to determine total NOCs exist (ATNC from apparent total *N*-nitroso compounds), they are based on the cleavage of R-NO bonds (by chemical or ultraviolet (UV) irradiation) and provide only an apparent estimation of the nitroso group content.[3,9] For instance, NDMA and *N*-nitrosoproline (NPRO, one of the few known representatives of nonvolatile NOCs in malt and beer) contributed to ATNC concentration by less than 1 and 10%, respectively.[10]

Although known representatives of nonvolatile NOCs did not show the same mutagenic properties as NDMA, other studies presented different potential risk mechanisms. They were, namely, *trans*-nitroso reactions or intramolecular shifts.[11] For instance, NPRO may undergo thermal decarboxylation, forming mutagenic *N*-nitrosopyrrolidine, and thus can be a potential precursor in dark malts, which are kilned at higher temperatures. A similar may apply to NDMA formation from *N*-nitrososarcosine.[12,13] Furthermore, NPRO may also endogenously undergo trans-nitrosation, leading to carcinogenic *N*-nitroso-*N*-methylurea when thiourea is present (e.g., from beer

Received: July 27, 2023
Revised: October 20, 2023
Accepted: October 25, 2023
Published: November 4, 2023

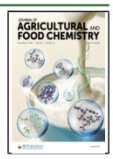

or other sources).[14,15] Nitrosation of amino acid histidine resulted in various compounds, from which one product (1-nitroso-1*H*-imidazol-4-yl)acetohydroxamic acid exhibits mutagenic properties.[16] Alternatively, nitroso derivatives of Amadori compounds or indoles committed mutations by trans-nitrosation directly to purine bases.[17,18] Based on the named examples, there should be awareness of the potential risk of some nonvolatile NOCs. It was severely advised that the characterization of individual representatives of nonvolatile NOCs would improve the health-safety assessment of foods and other products where NOCs occur.[3,10,19]

One of the first attempts to reveal representatives of nonvolatile NOCs in beer was performed by combinations of high-performance liquid chromatography-NCD (HPLC-NCD), GC-flame ionization detector (GC-FID), GC-NCD, and GC-mass spectrometry (GC-MS) and provided one mass spectrum of unknown NOCs.[20] Later, a novel method combining GC-NCD with discriminant analysis classified registered chromatographic peaks into *N*-nitroso, *C*-nitroso, and *C*-nitro/*C*-nitroso groups and distinguished them from interferents. It confirmed the first *N*-nitrosoproline ethyl ester (NPRO-O-Et) and the presence of *C*-nitroso or *C*-nitro/*C*-nitroso compounds. These findings were found in artificially nitrosated and contaminated beer by *Obesumbacterium proteus*.[6] The preceding study of the present paper used parallel nitrosation of beer by nitrite and nitrite-^{15}N, which led to identifying more than 20 unknown products containing nitrogen (later as N-products since not all contain nitroso group). Besides NPRO and NPRO-O-Et, other newly characterized N-products were 4-cyanophenol, 4-nitrosophenol, pyruvic acid oxime, 2-methoxy-5-nitrophenol, and nitrosoguaiacol (3-methoxy-5-nitrosophenol). Proline, tyrosine, and vanillic acid were suggested as their precursors. N-products were structurally studied by MS/MS fragmentation and confirmed by a retention index and mass spectrum of laboratory-prepared compounds or standards. Collected structural mass information allowed the development of the specific detection method described in the mentioned paper.[21] The present study applied this method for a semiquantitative screening of found N-products in commercial samples of malts and beers (nearly 200 samples each). The aim was to observe a natural occurrence within different beer/malt types. Malts exposed to exceeded nitrogen dioxide were also screened to observe if nitrogen oxides also form identical N-products. The study further compares N-products relative to standard determinations of NOCs, such as NDMA in malts and ATNC in beers. Consequently, results from this observational study strongly support the previous study that focused on a structural characterization/identification of N-products and reveal their existence in beer and malt for the first time.

MATERIALS AND METHODS

Reagents and Materials. Used reagents and chemicals: hydrochloric acid (37%), ammonium amidosulfonate (>99%), hydrogen bromide in glacial acetic acid (33%), sulfuric acid (96%), pyridine (≥99.8%), DL-phenylalanine-1-^{13}C (99%), *N*,*O*-bis(trimethylsilyl)-trifluoroacetamide with trimethyl-chlorosilane (99:1, BSTFA), *N*-nitrosodipropylamine (100 μg/mL in methanol, certificated reference standard), 4-nitrosophenol (95%), 4-cyanophenol (95%), and NDMA (100 μg/mL in methanol, certificated reference standard) were obtained from Merck-Agilent, Germany. *N*-nitrosoproline (100 μg/mL) was purchased from Isconlab, Germany. Potassium hydroxide (85%) was obtained from Penta, Czech Republic. Ethyl acetate, acetonitrile, and methanol were of reagent grade and obtained from Honeywell. Milli-Q system was used to produce deionized water.

Malt Sample Preparation for GC-MS/MS Analyses. Analyzed malt samples (198) were mainly obtained from industrial malthouses, providing malts for commercial use. Regarding malt styles, 50% were representatives of Pilsner malts, 14% were Munich malts, and 23% were unspecified by a supplier. However, based on the visual observation of grain color, the unspecified malts were assumed to represent Pilsner and Munich malts. The remaining 13% of the samples consisted of not only special malts, such as caramel, coloring, smoked, and wheat malts, but also contained culms and barley. The origin of malts was predominantly the Czech Republic (78%) and other European countries (18%), such as France, Poland, Slovakia, and Serbia. In 4% of the samples, a supplier did not specify a country of origin.

Malt grains were finely ground with an electronic mixer. Homogenized malt powder (50 mg) was extracted in 50 μL of pyridine: acetonitrile mixture (3:2, v/v) for 30 min at 65 °C. Subsequently, 150 μL of BSTFA was added, and derivatization took 30 min at 65 °C. After centrifugation (12,000 rpm, 5 min), the extract was transferred into a new vial and subjected to GC-MS/MS analyses. Internal standard (ISTD) phenylalanine-1-^{13}C (10 μg) was derivatized with 200 μL of BSTFA at 65 °C for 1 h separately and injected with a malt sample in a dual-injection mode. Each sample was duplicated, and four replicate analyses were carried out for each malt sample.

Beer Sample Preparation for GC-MS/MS Analyses. Analyzed beers (191 in total) were mainly obtained from the commercial market; the beers were produced by industrial breweries (71%), craft breweries (16%), and homebrewers (13%). Regarding beer styles, 61% were representatives of bottom-fermented beers (Lagers and Bocks) and 30% consisted of top-fermented beers (Ales, Wheat, Stout, Porter, and Trappist). The rest were nonalcoholic beers (8%), lambic (0.5%), and ciders (0.5%). The origin of beers was mainly the Czech Republic (61%), other European countries (32%, namely, Belgium, Bulgaria, Denmark, England, France, Germany, Hungary, Ireland, Italy, Netherlands, Norway, Poland, Romania, and Slovakia), and other world continents such as America (3%, namely, Brazil, Mexico, and USA) or Asia (4%, South Korea and Nepal).

At first, beer samples (6 mL) were mixed with 1 mL of ammonium amidosulfonate (0.2 M, dissolved in 0.2 M sulfuric acid) to remove nitrite. The nitrite-eliminating reaction was carried out at room temperature for 15−30 min and was prevented from light exposure. Subsequently, an SPE cartridge (Discovery DSC-18, 500 mg, Supelco) was conditioned with 6 mL of methanol and 6 mL of water. The sample was loaded on the conditioned SPE sorbent and washed with 1 mL of water; a flow-through was discarded, and the sorbent was gently dried by vacuum. Next, elution was achieved with 6 mL of a mixture of dichloromethane: ethyl acetate (1:3, v/v). Finally, ISTD phenylalanine-1-^{13}C (100 μL, 100 mg/L) was added to the eluent, and the mixed solution was immediately fully evaporated by a gentle argon flow (Air Products, Czech Republic) at 45 °C and recovered in 200 μL of BSTFA at 65 °C for 1 h. Each sample was duplicated, and four replicate analyses were carried out for each beer sample.

Nitrosated Malt and Congress Wort Preparation. Nitrosated malt was prepared in two different conditions: at a low temperature (∼40 °C) and a high temperature (∼80 °C). Congress wort was prepared from malt (nitrosated at a high temperature) by a miniaturized standard procedure instituted by the European Brewing Convention (Analytics EBC: Method 4.5.1). Detailed procedures are described in the Supporting Information (SI): Sections 1.1 and 1.2 (Schemes A and B). N-product extractability from malt to wort was estimated on 16 repetition samples; malts and wort were prepared in 8 repetitive samples, and each sample was analyzed in duplicate. N-product's area responses were standardized by weight of malt. N-product extractability into wort was estimated as the ratio of standardized responses of wort samples to malt samples.

GC-MS/MS Analyses. Analyses were carried out by a gas chromatograph Agilent 7890 B on a capillary column HP-5MS UI

https://doi.org/10.1021/acs.jafc.3c05217
J. Agric. Food Chem. 2023, 71, 17321−17329

Table 1. List of N-Products Formed by the Reaction of Nitrite in a Beer Sample[21]

sample ID	RT [min]	M_w [g/mol]	retention index	name of the product	precursor compound	specific functional groups[a]	occurrence in malt/beer[b] [%/%]	extraction into wort [%]
N-01	8.6	183	1116			cycloalkene	100/100	87
N-02	8.9	247	1146	pyruvic acid oxime, 2× TMS, isomer 1		=N−OH, COOH	100/91[c]	72
N-03	9.1	247	1159	pyruvic acid oxime, 2× TMS, isomer 2		=N−OH, COOH	100/100[c]	77
N-04	12.3	195	1348	4-nitrosophenol		−NO, OH	35/25	
N-05	13.3	191	1399	4-cyanophenol, 1× TMS	tyrosine	−CN, OH	96/100	103
N-06	13.5	212	1408			−CN	2/71	101
N-07	13.7	172	1422	*N*-nitrosoproline ethyl ester	proline	−NO, COO-Et	0/81	
N-08	14.7	216	1471	*N*-nitrosoproline, 1× TMS	proline	−NO, COOH	82/62	97
N-09	15.6	230	1524	*N*-nitrosopipecolic/*N*-nitrosopyroglutamic acid	-	−NO, COOH	51/70	101
N-10	16.8	225	1596	nitrosoguaiacol (2-methoxy-3-nitrosophenol)	vanillic acid	−NO, OH, O-Me	42/73	[d]
N-11	17.4	239	1627			$-NO_2$	64/26	105
N-12	17.7	218	1655				50/77	54
N-13	18.2	241	1687	2-methoxy-5-nitrophenol, 1× TMS	vanillic acid	$-NO_2$, OH, O-Me	92/97	104
N-14	20.5	306	1821		tyrosine	−CN, −NO	2/4	45
N-15	21.3	269	1866			$-NO/-NO_2$	1/57	190
N-16	22.1	327	1912				100/100	94
N-17	23.0	286	1972			$-NO, -NO_2$	0/20	83
N-18	23.2	341	1981		tyrosine	−COOH	13/77	117
N-19	24.6	357	2082		tyrosine	−COOH	6/74	103
N-20	25.9	443	2189		tyrosine	−NO	0/6	93
N-21	26.2	389	2209		tyrosine	−Cl	0/3	105
N-22	26.4	443	2230		tyrosine	$-COOH, -NO_2$	1/4	100

[a]Estimations based on MS/MS fragmentation mechanisms; hence, other species may still be possible. [b]A percentage of samples in which a specific N-product was detected. The total number of malt samples was 198 and of beer samples was 191. [c]The number of beer samples where the analyte was monitored is 69. [d]The N-product was detected only in the congress wort.

((5% phenyl)-methylpolysiloxane, 30 m × 0.25 mm × 0.25 μm) and detection by an Agilent 7000D triple quadrupole mass spectrometric detector (Agilent Technologies, Santa Clara). Injections (2 μL) were performed in a split mode (5:1) at 250 °C, with a constant helium flow rate of 1 mL/min (Air Products, Czech Republic). The set temperature program was as follows: 50 °C (1.5 min) - 20 °C/min - 150 °C (5 min) - 10 °C/min - 210 °C (3 min) - 10 °C/min - 320 °C (5 min), and the interface temperature was 250 °C. Conditions of multiple-reaction monitoring are specified in Table S1. Although analytes were detected in trimethylsilyl forms, original nonsilylated forms were listed and discussed for clarity.

NDMA and ATNC Determinations. The determination of NDMA in malts was carried out according to a standard operating procedure of TIBM based on the analytical method MEBAK 2.6.4.2. According to the described method, ATNC was determined in beers on a miniaturized apparatus.[22]

Data Processing. Data were acquired in an Agilent Mass Hunter and processed by an R (version 4.2.1) environment (R-Studio, version 2022.07.2). The ISTD peak area was monitored by a Shewart control chart. The detection limit was estimated as three times the noise level, and peaks below this limit were labeled nondetected. Data were further standardized as relative responses calculated as a ratio between an analyte peak area to the ISTD peak area and the amount of the sample (weight of malt or volume of the beer sample). Data visualizations and multivariate analyses were performed on the log-scaled average responses of samples. For two-dimensional (2D) hierarchical cluster analysis, the metric Euclidean distance and Ward method for the clustering algorithm were used. Correlation coefficients were calculated by using the Pearson method. More information regarding used R packages was named in Section 1.3. Approximate estimation of NPRO, 4-cyanophenol, and 4-nitrosophenol concentrations was performed by a one-point calibration on standards added to the beer matrix. In addition, two isomers of pyruvic acid oxime were added to the detection method later when analyses were already in progress. For this reason, they were monitored in only 69 beer samples but in all malt samples. Chromatograms and mass spectra of both isomers are shown in Figure S1.

Safety Considerations. There should be awareness of the potential risk of the studied compounds; hence, maintaining general laboratory safety protection, such as wearing protective equipment and sample manipulation in a fume hood, was essential.

RESULTS AND DISCUSSION

N-Products in Artificially Nitrosated Malt. In a previous study, the addition of nitrite into a beer sample led to the formation of 22 N-products. Their identification and structural characterization were individually performed in the previous publication and are summarized in Table 1.[21] A similar treatment was applied to malt when moist malt grains were exposed to nitrogen dioxide under different conditions. First, malt nitrosated at high temperature was incubated at 40 °C and dried at 80 °C since the kilning temperature is also associated with NDMA formation.[23] Second, malt nitrosated at low temperature was incubated at room temperature and dried at 40 °C. Temperatures were selected based on common kilning and drying temperatures used during malting.[24] Thus, in addition to nitrogen oxide reactivity, the temperature effect on N-product formation was also possible to observe.

An increase in N-product responses in nitrosated malts is shown in Figure 1. Compounds N-01, pyruvic acid oxime (N-

https://doi.org/10.1021/acs.jafc.3c05217
J. Agric. Food Chem. 2023, 71, 17321−17329

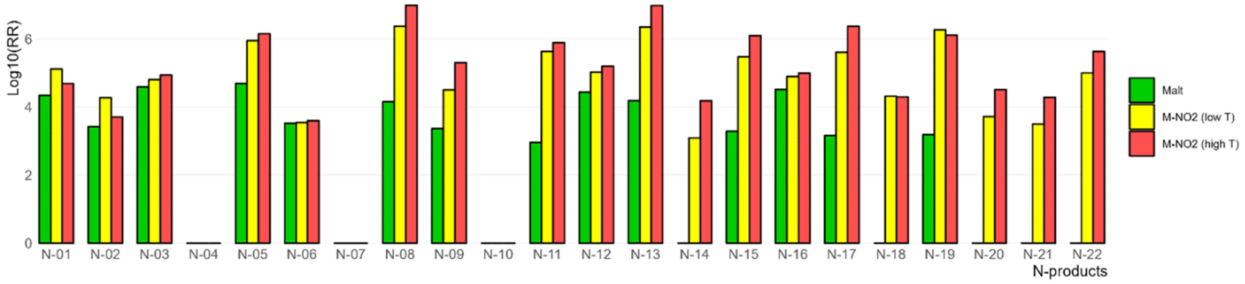

Figure 1. Comparison of N-product relative responses in original malt (green), nitrosated malt at a low temperature (~40 °C, yellow), and nitrosated malt at a high temperature (~80 °C, red).

02, N-03), N-06, N-12, and N-16 had similar responses in nitrosated malts as in the original malt (±10 orders of magnitude); hence, they were probably abundant already in the not-treated malt. Whereas some nitrosation products of tyrosine (N-14, N-18, N-20, N-21, and N-22) needed more extreme conditions to create. Malting procedure and treatment with nitrogen dioxide probably did not lead to the formation of 4-nitrosophenol (N-04), NPRO-O-Et (N-07), and nitrosoguaiacol (N-10) since they were not detected in any malt (untreated and nitrosated).

Responses of most N-products (Figure 1) were proportional to the nitrogen dioxide treatment and higher temperature. Based on that, the formation of N-product (or nonvolatile NOCs) is not closely associated only with nitrite, as assumed by the literature.[3] 11 previous kinetic studies of nitrosation reactions suggested that nitrite and nitrogen oxides in aqueous solutions form complex reactions and direct nitrosation agents were their equilibrium products, such as ^{+}NO, $^{+}H_2NO_2$, $^{\bullet}NO$, N_2O_3, or N_2O_4. Since wet malt was exposed to nitrogen dioxide, the dissolved oxide probably contributed to the formation of these direct nitrosation agents, which was also previously described.[25−27]

Experimental N-product extractibility from nitrosated malt (at high temperature) into the condensed wort is also listed in Table 1. Most N-product (17 from 19 counts) extractability was over 70%, and the response of N-15 in the wort almost doubled (190%). Lower extractability (~50%) was observed only for N-12 and N-14. On the contrary, 4-nitrosophenol (N-04) and NPRO-O-Et (N-07) were detected neither in wort. It could be expected since they were not detected in nitrosated malts (Figure 1). However, the preparation of the congress wort probably led to the form of nitrosoguaiacol (N-10).

Nearly quantitative extraction from malt to congress wort may indicate that many N-products in beer could originate from malt. The solubility of N-products into wort is predictable, considering the polarity and solubility of their supposed precursors.[3−5,21] However, it should be noted that the design of the presented experiment included one rough assumption. Namely, the extraction efficiency of N-products from malt to organic solvent (pyridine: acetonitrile) is equivalent to extraction from wort through SPE. Therefore, different matrix effects and affinity to aqueous and organic solvents could have affected the final N-product responses.

Frequency and Intensity of N-Product Responses within Malt/Beer Styles. The natural occurrence of N-products in beers and malts was first demonstrated by the detection frequency of specific compounds within tested samples (see Table 1, occurrence in malt/beer). In total, 191 beer samples and 198 malt samples were examined. All 22 N-products were detected in beers, and only 17 N-products were detected in malts. It may point out that precursors of N-products not found in malts may originate from other raw materials (e.g., hop, yeast) and/or were exposed to insufficient conditions for their formation in malt.

Regarding individual N-products, pyruvic acid oxime isomers (N-02, N-03), as well as N-01, 4-cyanophenol (N-05), 2-methoxy-5-nitrophenol (N-13), and N-16, were among the most commonly found compounds as they were detected in more than 90% of examined beers and malts. On the contrary, NPRO-O-Et (N-07), N-17, N-20, N-21, and similarly N-06, N-14, N-15, N-18, N-19, and N-22 were detected in none or less than 15% of tested malts, respectively. However, some of the rarely detected N-products in malts (N-06, N-07 (NPRO-O-Et), N-15, N-18, and N-19) were more frequently (>50%) observed in beers. N-09, N-10 (nitrosoguaiacol), and N-12 were found more frequently (between 20 and 30%) in beers than in malts. The contrary effect was observed for N-04 (4-nitrosophenol), N-08 (NPRO), and N-11 (Table 1).

Considering the intensity of relative responses within the tested samples, it covered several orders of magnitude. A detailed overview of the N-product responses within malt and beer styles is shown in Figure S2 (M1−M22 for malts and B1−B22 for beers). N-products below the detection limit were also covered in the distribution plots to show the average response representing the natural occurrence. The highest responses in beers and malts had N-01 and N-16 (medians reaching nearly ~10^4 of relative units per kilogram or liter). Moreover, in malts, other intensive responses gave pyruvic acid oxime (N-02, N-03), 4-cyanophenol (N-05), N-09, N-12, 2-methoxy-5-nitrophenol (N-13), and N-18. Such N-products showed exceeding intensity, especially in coloring and caramel malts, barley, and culms, compared with median responses of other malt styles. The possible elucidations will be discussed later. Different N-product responses within specific beer styles were not observed regarding beer samples, except N-01, whose response in ciders was significantly lower (Figure S2, M1). It may support the assumption that N-01 in beers can originate from malt.

2D Hierarchical Cluster Analysis. Multivariate methods were applied due to many samples (198 malts and 191 beers) on which 22 variables (N-products) were determined. The previously discussed frequency and intensity of N-product responses can be summarized by 2D hierarchically clustered heatmaps for malts and beers shown in Figures 2 and 3, respectively. The heatmap grouped samples (as the z-score scaled by columns) according to similarities of detected N-products. High and average responses (positive and zero z-scores) of the corresponding analyte are signaled by yellow and

https://doi.org/10.1021/acs.jafc.3c05217
J. Agric. Food Chem. 2023, 71, 17321−17329

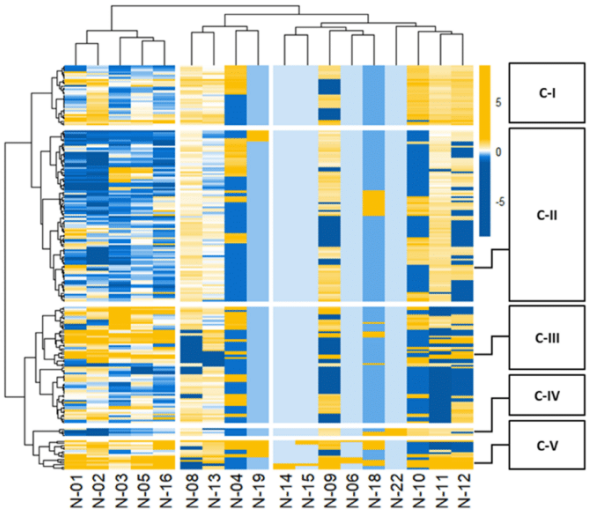

Figure 2. Hierarchically clustered heatmap of malt samples.

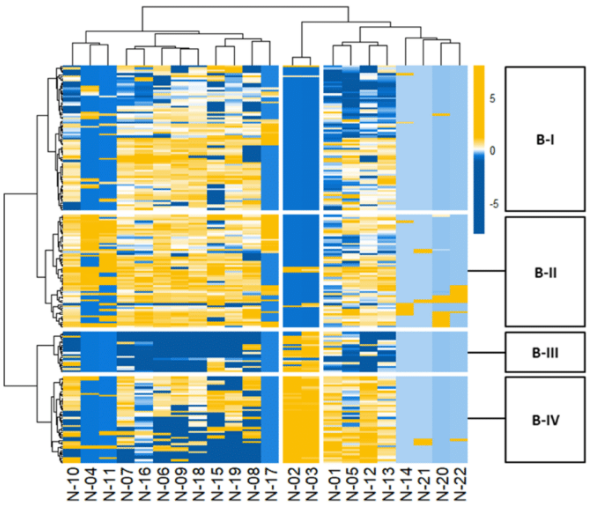

Figure 3. Hierarchically clustered heatmap of beer samples.

white, respectively, whereas low responses (negative z-score) are shown by blue. When an analyte was undetected in many samples, it appeared as a unicolor blue band in the heatmap.

Five groups were registered for malt samples differing from each other in N-product response intensities (Figure 2). Detailed compositions of individual clusters by malt style are shown in Figure S3. Based on the heatmaps, positive N-product responses (N-10, N-11, N-12) were typical for cluster C−I (31 samples). Similarly, high responses of N-01, N-02/N-03 (pyruvic acid oxime), N-05 (4-cyanophenol), and N-16 characterized groups C−III (60 samples) and C−V (15 samples). On the contrary, their lowest responses were typical for C−II (88 samples) and C−IV (4 samples). Rarely detected N-products (N-06, N-14, and N-15) were grouped into C−V, and samples containing N-22 were grouped into C−IV. The most prominent groups were C−II and C−III, covering 44 and 30% of all tested samples. Munich, Pilsner, and unspecified malts were similarly distributed within clusters C−I to C−V (except C−IV, which consisted of only Pilsner malts). Almost half of the caramel and coloring malts and culms were grouped into C−V. Similarly, barley and the other half of the caramel and wheat samples were grouped into C−III. As high responses of these specific malt styles were discussed above, their effect on sample clustering was evident.

Four clusters were registered in the heatmap of beers (Figure 3). Detailed compositions of individual clusters by beer style are shown in Figure S4. Based on the heatmaps, positive N-product responses (pyruvic acid oxime N-02, N-03) and (N-01, N-05, N-12, N-13) were typical for clusters B−III (20 samples) and B−IV (43 samples). Rarely detected N-products of tyrosine (N-14, N-20, N-21, and N-22) were distributed within all clusters except B−III. Clusters B−I (72 samples) and B−II (56 samples) comprised 38 and 29% of the tested samples and were typical for intensive responses for 4-nitrosophenol (N-04), NPRO-O-Et (N-07), NPRO (N-08), *N*-nitrosopipecolic acid/*N*-nitrosopyroglutamic acid (N-09), nitrosoguaiacol (N-10), or tyrosine-related products (N-18, N-19). Lagers and ales were proportionally distributed among all clusters. Nonalcoholic beers were also broadly distributed, probably due to their variable brewing technology and the inclusion of more nonalcoholic beer styles, such as nonflavored and flavored. However, specific clustering was observed for special beers (see Figure S4, clusters I−IV). Wort, cider, lambic, and part of the wheat beers were grouped in B−I. Several stouts, porter, bock, and one wheat beer fell into cluster B−II, three wheat beers into B−III, and two Trappists beers into B−IV.

Natural Occurrence of N-Products in Beer and Malt. Unknown compounds N-01 and N-16, followed by pyruvic acid oxime isomers (N-02, N-03), 4-cyanophenol (N-05), and 2-methoxy-5-nitrophenol (N-13), belong among the most significant compounds in both malts and beers, as proved by frequencies when detected (Table 1), response intensity (Figure S2), and also by heatmaps (Figures 2 and 3). It agreed with additional heatmaps grouped by N-products (as z-score scaled by rows; see Figure S5), where the most intense N-products were clearly shown. These mentioned N-products, and also N-04, N-06, and N-09 to N-13, had higher average responses in coloring and caramel malts, barley, and culms related to other malt styles (see Figure S2, M1-M6, M9, M13, M16). Grouping of caramel, coloring malts, and culms was also evidenced by 2D hierarchical clustering (Figure S3, cluster V). Such an effect may be associated with a technological treatment during malting (coloring and caramel malts) or natural composition (culms and barley). For instance, caramel and coloring malts are kilned at temperatures reaching 180 and 225 °C; then, the formation of some specific N-products can be accelerated.[28] Culms were described as naturally rich in the nitrogen compound content (22−25%), and a potential risk of NOCs and *N*-nitrosamine formation was already mentioned. Therefore, association with N-product formation may be predictable.[29] It agreed with a primary screening performed on 16 commercial beers in the prior study.[21] However, it does not necessarily imply that they are the most concentrated since each N-product poses a different unknown response factor. Relative responses in malts were generally higher than in beers, which could be possibly caused, among other reasons, by a matrix effect.[30]

Twelve N-products were also found in raw barley samples, and their responses were comparable with those of malt (see Figure S3, cluster III). The occurrence of N-products in barley is unclear but may be hypothetically associated with drying air applied on freshly harvested barley to reach desirable dryness

https://doi.org/10.1021/acs.jafc.3c05217
J. Agric. Food Chem. 2023, 71, 17321−17329

before malting.[24] Another hypothesis supposed a natural content of several N-products already in barley.[26] However, a matrix effect might have also affected the response magnitude.[30]

NPRO (N-08) occurred relatively frequently (82 and 62% in malts and beers, respectively); see Table 1. The lower frequency of NPRO in beers might be associated with NPRO esterification by ethanol, which leads to NPRO-O-Et (N-07) formation. Since ethanol is not present in malt, the suggested esterification cannot undergo, and N-07 was not found in malt samples.[6,31]

Although 4-nitrosophenol (N-04) and nitrosoguaiacol (N-10) were found neither in artificially nitrosated beer nor in nitrosated malt, they occasionally occurred naturally in malt and beer (Table 1). It may point out that their precursors (phenolic compounds) originate from other raw materials (e.g., hop) and/or insufficient conditions for their formation are in malt (such as nitrosoguaiacol formation during the preparation of congress wort; Table 1).[32]

Regarding N-products of tyrosine, the important reaction product was 4-cyanophenol (N-05, detected in all beers), followed by N-18 and N-19 (detected in up to 77% of tested beers; see Table 1). Based on the low detection frequency of remaining tyrosine products (N-14, N-20, N-21, N-22) and observation of nitrosated malt by nitrogen dioxide (Figure 1), the standard malting conditions supposedly do not lead to the formation of these structures.

Hierarchical cluster analysis visualizes the grouping of tested samples based on the frequency and intensities of the analyzed N-product. The frequency of analyte's occurrence and intensity of relative response (relative units based on weight or volume) were used as quantitative evaluation factors.[33] Because of the lack of available standards and different response factors, the estimation of concentrations based on the acquired data would be misleading. However, a rough concentration of NPRO, 4-cyanophenol and 4-nitrosophenol was estimated. In studied beer samples, NPRO ranged between 13 and 688 μg/L (with a median level of 32 μg/L). Our estimated average value was similar to a previously estimated average level of NPRO in beer (71 μg/L).[34] However, by comparison with other determinations, they were significantly higher. For instance, earlier studies found NPRO in levels between <1−11 μg/L (median 8 μg/L, 13 beer samples) or within the range <1−6 μg/L (average 1.7 μg/L, 28 beer samples).[10,12] Regarding 4-cyanophenol and 4-nitrosophenol, they ranged between <1−15 μg/L (median of <1 μg/L) and 2−138 μg/L (median of 8 μg/L), respectively. Since these compounds were not found in beer yet, no data to compare estimated levels were available. Hence, improvements to the current analytical method are in demand for quantitative determinations. Thus, the availability of analytical standards is highly required to achieve this task.

Results of NDMA Determination. Since malt is suggested as the primary source of NDMA in beer, the NDMA concentration in tested malts is shown in Figure 4.[1] NDMA was determined in 95% of tested samples (188 counts from 198 samples). In total, 28% of the samples (53 counts from 188) were below the quantification limit (0.2 μg/kg) of NDMA (all of them were representatives of special malts). If the NDMA concentration is assumed to be typical for a specific malt style, then the Munich malt generally has a higher median NDMA level than the Pilsner malt. Regarding the unspecified malt, the median concentration was closer to the median of Pilsner, indicating that they are probably similar in style.

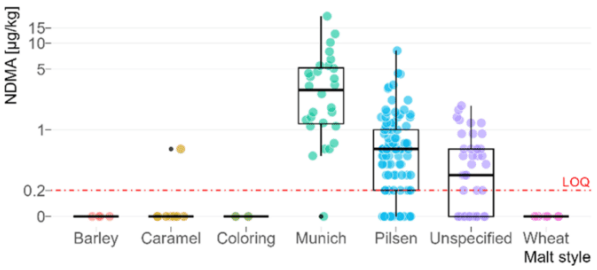

Figure 4. Concentrations of NDMA within malt styles. The red dashed line shows the limit of quantification (0.2 μg/kg).

Recommended maximum limits for NDMA concentrations exist but differ according to the country of origin. According to The Czech Beer and Malt Association, the maximum recommended level of NDMA in malt is 1.0 μg/kg, which exceeded 28% of tested samples (52 counts from 188),[11,35] whereas the U.S. Food and Drug Administration states a limiting value of up to 10.0 μg/kg, which exceeded only 1% of tested samples (3 counts from 188).[36] The range of determined NDMA concentration was from <0.2 up to 20.5 μg/kg. This range proves that contamination by *N*-nitrosamines may still occur in commercial malts. However, occasionally exceeding NDMA levels may indicate technological defects in malthouses.[11] It should be noted that NDMA formation in malts cannot be reduced entirely since the kilning air event at indirect heaters still contains traces of nitrogen oxides.[35] Moreover, since NDMA is volatile, its large part evaporates during brewing, and its final dilution was 5- to 10-fold less than in malt.[1]

Results of ATNC Determination. ATNC was determined in all tested beers. Concentrations below the quantification limit (10 μg(NNO)/l) were found in 30% of samples (58 counts from 191), and levels over 50 μg(NNO)/l were found in 25% of tested samples (47 counts from 191). The range of determined ATNC concentration was from <10 up to 649 μg(NNO)/L. The recommended but not legislatively supported limit is 20 μg(NNO)/L, and 51% of tested samples (97 counts from 191) did not meet this recommendation.[10,11] Exceeding ATNC concentrations still occur frequently in commercial beers, which supports this study's importance in revealing unknown representatives of others, especially non-volatile NOCs.

The association between ATNC and specific microbial contamination was mentioned in the introduction, as well as the higher frequency of exceeding ATNC levels within microbreweries.[3,19] Presented data also agreed with this observation as the median ATNC concentration of beers from homebrewers and microbreweries was higher than the median response (of all samples) from industrial breweries (Figure 5A). Furthermore, ATNC levels through individual breweries were also shown (Figure 5B), and they consisted of 25 industrial breweries and three microbreweries, from which more than one beer sample was analyzed. Other groups called "Industrial/Microbrewery/Homebrewers_mix" contain breweries where only one representative beer was analyzed. Noticeably higher medians of ATNC (shown by red points) were observed in several specific industrial breweries (Nos. 24, 07, 20, 22, 25, 08, and 19). A similar trend may also be

https://doi.org/10.1021/acs.jafc.3c05217
J. Agric. Food Chem. 2023, 71, 17321−17329

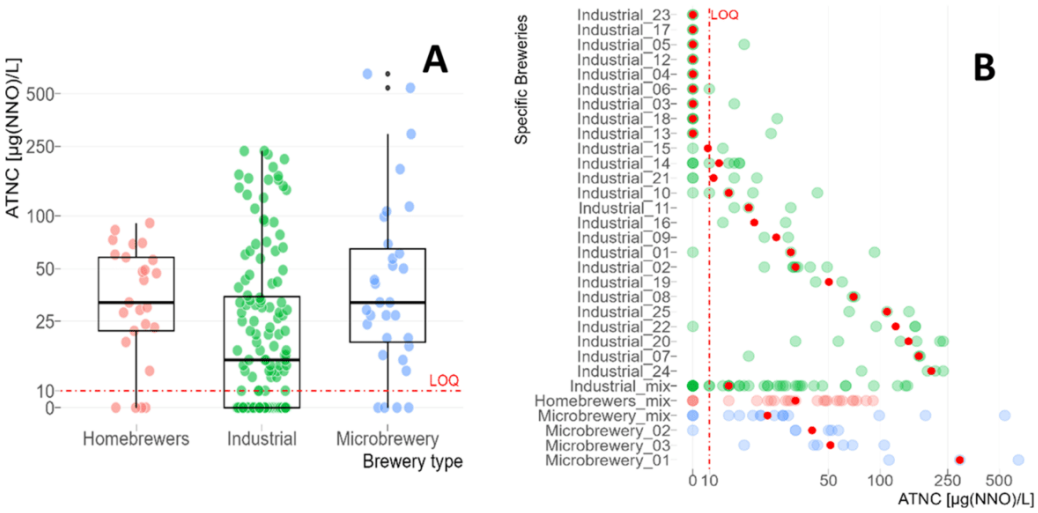

Figure 5. Comparison of ATNC concentrations. (A) Summarization of concentrations within all brewery types—industrial, microbrewery, and homebrewers. (B) Concentrations corresponding to individual specific breweries. The red dashed line shows the limit of quantification (10 μg (NNO)/L).

observed among representatives of microbreweries. In conclusion, higher ATNC concentrations seem not coincidental but could result from insufficient systematic microbial issues in specific breweries.

Correlation of N-Products. The Pearson correlation analysis was used to specify possible linear correlations to compare a natural occurrence of N-products within standard determinations of NOCs (NDMA and ATNC concentrations). Correlations were visualized by correlograms showing only significant correlations ($p < 0.05$). Individual correlation coefficients, p-values, and the number of observations for each pair of variables are listed in Table S2. The correlogram for malt samples (Figure S6) showed only positive correlations. The correlations were observed exclusively within N-01, N-02, N-03, N-04, N-05, N-08, N-09, N-10, N-11, N-12, N-13, N-16, N-18, and N-19. High correlations ($r > 0.8$) were found within 20 variable pairs. Regarding NDMA, only medium−low correlations ($r < 0.4$) were observed for N-08 (NPRO), N-10 (nitrosoguaiacol), and N-16.

Only positive correlations were observed among N-products in beers, except one (ATNC vs N-15; see Figure S7). For each variable in beer samples, at least two significant correlations were found with other variables. However, compared to malt sample correlations, high correlative variables from beer ($r > 0.8$) were observed only in four pairs (N-01 vs N-21, N-14 vs N-15, N-08 vs N-20, and N-12 vs N-21). Several medium correlations ($0.2 < r < 0.8$) were found between ATNC and N-03 (pyruvic acid oxime), N-05 (4-cyanophenol), N-13 (2-methoxy-5-nitrophenol), N-15 (negative correlation), N-16, and N-18. Individual correlation coefficients, p-values, and the number of observations for each pair of variables are listed in Table S3.

Fewer correlation pairs of N-products vs NDMA were found in malt samples compared to those of N-products vs ATNC in beer samples. Volatile *N*-nitrosamines (or NDMA) are known to be formed by different mechanisms than ATNC-positive compounds.[3,11] N-products that correlated with ATNC may simultaneously represent ATNC-positive compounds. However, several correlations may be affected by a third factor. For instance, a correlation of 4-cyanophenol with ATNC was found. However, the ATNC determination showed no valid response (<1.2 mA/mol, NCD detector response current per mol) even at 1.0 mg/mL of 4-cyanophenol. On the contrary, the NPRO (1.0 mg/mL) highly responded (up to 7000 mA/mol) during ATNC determination, but Pearson analysis showed no correlation. Finally, 4-nitrosophenol (1.0 mg/mL) did not show any valid response to ATNC (<1.4 mA/mol) nor correlation to ATNC (Figure S7). In conclusion, the correlations may be affected by third factors, such as the type of nitrosation reagents (gaseous nitric oxides and nitrate/nitrite in solution), concentrations of both reagents (nitrosation reagent and precursor), pH, or temperature. Hence, each of them may influence N-product formation in beer individually.

The present monitoring study confirmed the reliability of previously found N-related products in the beer matrix by their selective screening of nearly 200 beer and malt samples.[21] Most N-products (17 from 22) were found already in malt, and their extraction into wort was almost quantitative. Previously identified N-products, namely, pyruvic acid oxime, 4-cyanophenol, 4-nitrosophenol, nitrosoguaiacol, NPRO, NPRO-O-Et, and 2-methoxy-5-nitrophenol, were detected in the majority of tested samples.[21] There is still a need to reveal structures of unidentified N-products, such as highly abundant N-01 and N-16 or nitrosation products of tyrosine. Although most tyrosine-related N-products were rarely detected (N-14, N-19, N-20, N-21, and N-22), others, such as 4-cyanophenol, were among the abundant and newly found compounds.

The possible extension to other matrices is another important feature of the presented results and methodology. Promising are meat products since they similarly contain both volatile *N*-nitrosamines (NDMA, *N*-nitrosopyrrolidine, *N*-nitrosomorpholine, *N*-nitrosopiperidine) and nonvolatile *N*-nitroso compounds (NPRO, *N*-nitrososarcosine, *N*-nitrosopipecolic acid, *N*-nitrosohydroxyproline).[37−39] NOC formation in meat is related to nitrite, which is commonly added as a conservative additive (E250, E249) to avoid bacterial growth and elongate the desired fresh-color appearance.[38]

https://doi.org/10.1021/acs.jafc.3c05217
J. Agric. Food Chem. 2023, 71, 17321−17329

Heat treatment and added nitrite were proportional to their final concentrations, as observed in the nitrosated malt experiment (Figure 1).[40,41] Moreover, the discussed precursors, especially amino acids and amines, are present in meat in large amounts, and several identical N-products are highly probable.

Based on the presented observational study, several scopes for further studies can be suggested. (i) Structural elucidation of unknown N-products and their synthesis for qualitative confirmation. (ii) Simultaneously, improve quantitative determination to accurately estimate health safety in foods and other products where NOC may occur. (iii) Extension of the N-product list to perform similar screenings on other promising matrices, such as meat.

■ ASSOCIATED CONTENT

Supporting Information

The Supporting Information is available free of charge at https://pubs.acs.org/doi/10.1021/acs.jafc.3c05217.

> Experimental preparation of nitrosated malts at high and low temperatures (80 and 40 °C) (Section 1.1, Schemes A and B); preparation of congress wort (Section 1.2); conditions of multiple-reaction monitoring for N-product observation by GC-MS/MS (Table S1); and list of used R packages (Section 1.3). Chromatograms and mass spectra of laboratory-prepared pyruvic acid oxime and a beer sample treated by isotopically labeled nitrite-1-^{15}N (Figure S1); distributions of detected N-products (N-01−N-22) within malt and beer styles (Figure S2, M1−M22, B1−B22); distributions of N-products within individual clusters C−I to C−V from heatmap of malts (Figure S3); distributions of N-products within individual clusters B−I to B−IV from heatmap of beers (Figure S4); heatmap of malt and beer standardized by N-product response (Figure S5A,B); correlogram, correlation coefficients, *p*-values, and number of counts for NDMA and N-product Pearson correlation analysis in malts (Figure S6 and Table S2); and correlogram, correlation coefficients, *p*-values, and number of counts for NDMA and N-product Pearson correlation analysis in malts (Figure S7 and Table S3) (PDF)

■ AUTHOR INFORMATION

Corresponding Author

Tomáš Vrzal − *Research Institute of Brewing and Malting, 120 00 Prague, Czech Republic;* orcid.org/0000-0001-5866-1520; Email: tomas.vrzal@beerresearch.cz

Authors

Michaela Malečková − *Research Institute of Brewing and Malting, 120 00 Prague, Czech Republic; Faculty of Science, Department of Analytical Chemistry, Charles University, 128 43 Prague, Czech Republic;* orcid.org/0000-0002-2992-9580

Tomáš Vaško − *Faculty of Agrobiology, Food and Natural Resources, Department of Chemistry, Czech University of Life Sciences Prague, 165 00 Prague, Czech Republic*

Jana Olšovská − *Research Institute of Brewing and Malting, 120 00 Prague, Czech Republic;* orcid.org/0000-0003-4938-3666

Jana Sobotníková − *Faculty of Science, Department of Analytical Chemistry, Charles University, 128 43 Prague, Czech Republic;* orcid.org/0000-0003-1339-8583

Complete contact information is available at: https://pubs.acs.org/10.1021/acs.jafc.3c05217

Notes

The authors declare no competing financial interest.

■ ACKNOWLEDGMENTS

This study was supported by the Ministry of Agriculture of the Czech Republic through the institutional support of MZE-RO1918 and by the project of Specific University Research SVV260690.

■ REFERENCES

(1) Wainwright, T. Nitrosamines in malt and beer. *J. Inst. Brew.* **1986**, *92* (1), 73−80.

(2) Calderbank, J.; Hammond, J. Influence of nitrate and bacterial contamination on the formation of apparent total *N*-nitroso compounds (ATNC) During Fermentation. *J. Inst. Brew.* **1989**, *95* (4), 277−281.

(3) Massey, R.; Dennis, M.; Pointer, M.; Key, P. An investigation of the levels of N-nitrosodimethyl-amine, apparent total N-nitroso compounds and nitrate in beer. *Food Addit. Contam.* **1990**, *7* (5), 605−615.

(4) Johnson, P.; Pfab, J.; Massey, R. A method for the investigation of free and protein-bound N-nitrosoproline in beer. *Food Addit. Contam.* **1988**, *5* (2), 119−125.

(5) Johnson, P.; Pfab, J.; Massey, R. Development of medhods for the characterization of non-volatile *N*-nitroso compounds in malt. *J. Inst. Brew.* **1988**, *94* (1), 19−22.

(6) Vrzal, T.; Olšovská, J. Pyrolytic profiling nitrosamine specific chemiluminescence detection combined with multivariate chemometric discrimination for non-targeted detection and classification of nitroso compounds in complex samples. *Anal. Chim. Acta* **2019**, *1059* (1), 136−145.

(7) Kippenberger, M.; Hanke, S.; Biendl, M.; Stettner, G.; Lagemann, A. Transfer of nitrate and various pesticides into beer during dry hopping. *Brew. Sci.* **2014**, *67* (1), 1−9.

(8) Colomer, M. S.; Funch, B.; Solodovnikova, N.; Hobley, T.; Förster, J. Biotransformation of hop derived compounds by *Brettanomyces* yeast strains. *J. Inst. Brew.* **2020**, *126*, 280−288, DOI: 10.1002/jib.610.

(9) Massey, R. C.; Key, P.; McWeeny, D.; Knowles, M. The application of a chemical denitrosation and chemiluminescence detection procedure for estimation of the apparent concentration of total *N*-nitroso compounds in foods and beverages. *Food Addit. Contam.* **1984**, *1* (1), 11−16.

(10) Čulík, J.; Horák, T.; Čejka, P.; Jurková, M. Non-volatile *N*-nitrosamines in brewing industry. Part 1. - Arrising and methods of estimation. *Kvasny Prum.* **2012**, *58* (1), 6−12.

(11) Vrzal, T.; Olšovská, J. *N*-nitrosamines in 21st Century. *Kvasny Prum.* **2016**, *62* (1), 2−8.

(12) Sen, N. P.; Tessier, L.; Seaman, S. Determination of *N*-nitrosoproline and *N*-nitrososarcosine in malt and beer. *J. Agric. Food Chem.* **1983**, *31* (5), 1033−1036.

(13) Pollock, J. Acpects of nitrosation in malts and beers. I. Examination of malts for the presence of *N*-nitrosoproline, *N*-nitrososarcosine and *N*-nitrosopipecolinic acid. *J. Inst. Brew.* **1981**, *87* (6), 356−359.

(14) Nitz, S.; Moza, P.; Korte, F. A capillary gas-liquid chromatographic method for determination of ethylenethiourea and propylenethiourea in hops, beer, and grapes. *J. Agric. Food Chem.* **1982**, *30*, 593−596.

(15) Inami, K.; Shiino, J.; Hagiwara, S.; Takeda, K.; Mochizuki, M. Transnitrosation of non-mutagenic *N*-nitrosoproline forms mutagenic

N-nitroso-*N*-methylurea. *Bioorg. Med. Chem.* **2015**, *23* (13), 3297−3302.
(16) Danno, G.; Kanazawa, K.; Toda, M.; Mizuno, M.; Ashida, H.; Natake, M. A mutagen from histidine reacted with nitrite. *J. Agric. Food Chem.* **1993**, *41* (7), 1090−1093.
(17) Lucas, L.; Gatehouse, D.; Shuker, D. Efficient nitroso group transfer from *N*-nitrosoindoles to nucleotides and 2′-deoxyguanosine at physiological pH. A new pathway for *N*-nitrosocompounds to exert genotoxicity. *J. Biol. Chem.* **1999**, *274* (26), 18319−18326.
(18) Pignatelli, B.; Malaveille, C.; Friesen, M.; et al. Synthesis, structure-activity relationships and a reaction mechanism for mutagenic *N*-nitroso derivatives of glycosylamines and Amadori compounds–model substances for *N*-nitrosated early Maillard reaction products. *Food Chem. Toxicol.* **1987**, *25* (9), 669−680.
(19) Olšovská, J.; Matoulková, D.; Čejka, P.; Jurková, M. Beer and health. *Kvasny Prum.* **2014**, *60* (7), 174−181.
(20) Johnson, P.; Pfab, J.; Massey, R. Development of methods for the characterisation of non-volatile N-nitroso compounds in malt. *J. Inst. Brew.* **1988**, *94* (1), 19−22.
(21) Malečková, M.; Vrzal, T.; Olšovská, J.; Sobotníková, J. Characterization of nitrite-related reaction products in beer. *J. Agric. Food Chem.* **2021**, *69* (39), 11687−11695.
(22) Vrzal, T.; Malečková, M.; Olšovská, J. Miniaturized and improved method for apparent total *N*-nitroso compounds determination in beer. *Kvasny Prum.* **2021**, *67* (5), 498−502.
(23) Wainright, T. The chemistry of nitrosamine formation: Relevance to malting and brewing. *J. Inst. Brew.* **1986**, *92* (1), 49−64.
(24) Kunze, W. Malt production. In *Technology Brewing and Malting*, 3rd ed.; Springer: VLB: Berlin, Germany, 2004; Chapter 2, pp 97−188.
(25) Smith, N. A. Cambridge Prize Lecture Nitrate Reduction and *N*-nitrosation in Brewing. *J. Inst. Brew.* **1994**, *100* (5), 347−355.
(26) Kellner, V.; Čulík, J.; Basařová, G. *N*-nitrosaminy ve sladu - vznik a odstraňování. *Kvasny Prum.* **1983**, *29*, 28−31.
(27) López-Rodríguez, R.; McManus, J.; Murphy, N.; Ott, M.; Burns, M. Pathways for *N*-nitroso compound formation: Secondary amines and beyond. *Org. Process Res. Dev.* **2020**, *24* (9), 1558−1585.
(28) Basařová, G.; Psota, V.; Šavel, J.et al. Druhy sladů a jejich vlastnosti. In *Sladařství*; Havlíček Brain Team: Prague, Czech Republic, 2015; pp 369−370.
(29) Neylon, E.; Arendt, E.; Lynch, K.; Zannini, E.; Bazzoli, P.; Monin, T.; Sahin, A. Rootlets, a malting by-product with great potential. *Fermentation* **2020**, *6*, No. 117, DOI: 10.3390/fermentation6040117.
(30) Erney, D.; Gillespie, A.; Gilvydis, D.; Poole, C. Explanation of the matrix-induced chromatographic response enhancement of organophosphorus pesticides during open tubular column gas chromatography with splitless or hot on-column injection and flame photometric detection. *J. Chromatogr. A* **1993**, *638* (1), 57−63.
(31) Saito, Y.; Yamaki, T.; Kohashi, F.; Watanabe, T.; Ouchi, H.; Takahata, H. Simple and mild esterification of *N*-protected amino acids with nearly equimolar amounts of alcohols using 1-tert-butoxy-2-tert-butoxycarbonyl-1,2-dihydroisoquinoline. *Tetrahedron Lett.* **2005**, *46* (8), 1277−1279.
(32) Rothe, J.; Fischer, R.; Cotterchio, C.; Gastl, M.; Becker, T. Analytical determination of antioxidant capacity of hop-derived compounds in beer using specific rapid assays (ORAC, FRAP) and ESR-spectroscopy. *Eur. Food Res. Technol.* **2023**, *249* (1), 81−93.
(33) Ruiz-Hernández, V.; Roca, M.; Egea-Cortines, M.; Weiss, J. A comparison of semi-quantitative methods suitable for establishing volatile profiles. *Plant Methods* **2018**, *14*, No. 67, DOI: 10.1186/s13007-018-0335-2.
(34) Bogovski, P.; Rooma, M.; Kann, J.; Tatus, O. Research on environmental N-nitroso compounds in the USSR. *IARC Sci. Publ.* **1982**, *41*, 259−266.
(35) Čulík, J.; Jurková, M.; Horák, T.; Čejka, P.; Dvořák, J.; Olšovská, J. Volatile *N*-nitrosamines in malt, thing of the past? *Kvasny Prum.* **2011**, *57* (11), 413−416.
(36) CPG Sec 578.500 Dimethylnitrosamine (DMNA) in Barley Malt. U.S. Food & Drug Administrations. (https://www.fda.gov/regulatory-information/search-fda-guidance-documents/cpg-sec-578500-dimethylnitrosamine-dmna-barley-malt) (accessed September 14, 2023).
(37) Byun, M.; Ahn, H.; Kim.; et al. Determination of volatile *N*-nitrosamines in irradiated fermented sausage by gas chromatography coupled to a thermal energy analyzer. *J. Chromatogr. A* **2004**, *1054* (1−2), 403−407.
(38) Herrmann, S.; Duedahl-Olesen, L.; Granby, K. Simultaneous determination of volatile and non-volatile nitrosamines in processed meat products by liquid chromatography tandem mass spectrometry using atmospheric pressure chemical ionisation and electrospray ionisation. *J. Chromatogr. A* **2014**, *1330*, 20−29.
(39) Herrmann, S.; Duedahl-Olesen, L.; Granby, K. Occurrence of volatile and non-volatile *N*-nitrosamines in processed meat products and the role of heat treatment. *Food Control* **2015**, *48*, 163−169.
(40) Herrmann, S.; Granby, K.; Duedahl-Olesen, L. Formation and mitigation of *N*-nitrosamines in nitrite preserved cooked sausages. *Food Chem.* **2015**, *174*, 516−526.
(41) Drabik-Markiewicz, G.; Dejaegher, B.; De Mey, E.; Impens, S.; Kowalska, T.; Paelinck, H.; Vander Heyden, Y. Evaluation of the influence of proline, hydroxyproline or pyrrolidine in the presence of sodium nitrite on *N*-nitrosamine formation when heating cured meat. *Anal. Chim. Acta* **2010**, *657* (2), 123−130.

https://doi.org/10.1021/acs.jafc.3c05217
J. Agric. Food Chem. 2023, 71, 17321−17329

Conclusion

The stated aims of this investigation were achieved since nearly 22 N-products were observed in beer and malt for the first time. Several N-products can be representatives of studied non-volatile NOCs (*N*-nitroso, *C*-nitroso compounds, or oximes), but also representatives of nitro- and even cyano-compounds were characterized. The studied N-products were pyruvic acid oxime, 4-cyanophenol, 4-nitrosophenol, nitrosoguaiacol, NPRO, NPRO-O-Et, and 2-methoxy-5-nitrophenol. Possible precursors were amino acids (proline, tyrosine) or phenolic acids (vanillic acid). The following observational study supported the results from the first publication since the N-products were frequently detected in all commercial untreated beers, and up to 17 N-products were detected in commercial malts. Preliminary experiments revealed the N-product's good extractability into the wort. It was observed that several N-products can originate from malt, and some, such as *N*-nitrosoproline ethyl ester and 4-nitrosophenol, probably form during brewing. Comparisons of N-products with NDMA and ATNC determinations revealed only medium correlations, which other factors, such as concentrations of precursor and reagents, type of nitrosation reagents, temperature, or pH, can influence.

Although several N-products can be representatives of barely known non-volatile NOCs, further studies are necessary to prove the association between N-products and ATNC-positive compounds. Moreover, improvements in specific GC-MS/MS detection methods would also contribute to better health-assessment of beer. However, both mentioned scopes required analytical standards, which are currently unavailable for most N-products (except NPRO, 4-cyanophenol, and 2-methoxy-5-nitrophenol).

References

[1] V. Kellner, J. Čulík, L. Veselý and B. Špinar, Problems of *N*-nitroso compounds, *Kvasný Průmysl*, *37:7*, 193-196, **1991**.

[2] C. Hamlet and L. Liang, An Investigation to establish the types and levels of *N*-nitroso compounds (NOC) in UK consumed foods, *Food Standards Agency/Premier Analytical Services*, 1-79, **2017**.

[3] D. Schrenk, M. Bignami, L. Bodin, J. Chipman, J. del Mazo, C. Hogstrand, L. (Ron) Hoogenboom, J. Leblanc, C. Nebbia, E. Nielsen, E. Ntzani, A. Petersen, S. Sand, T. Schwerdtle, C. Vleminckx, H. Wallace, B. Romualdo, C. Fortes, S. Hecht, M. Iammarino, O. Mosbach-Schulz, F. Riolo, A. Christodoulidou and B. Grasl-Kraupp, Risk assessment of *N*-nitrosamines in food, *EFSA Journal*, *21:3*, 1-278, **2023**

[4] B. Spiegelhalder, G. Eisenbrand and R. Preussmann, Contamination of beer with trace quantities of *N*-nitrosodimethylamine, *Food and Cosmetics Toxicology*, *17:1*, 29-31, **1979**.

[5] D. Lachenmeier and D. Fügel, Reduction of nitrosamines in beer - Review of a success story, *Brewing Science*, *60:56*, 84-89, **2007**.

[6] T. Vrzal and J. Olšovská, *N*-nitrosamines in 21st century, *Kvasný Průmysl*, *62:1*, 2-8, **2016**.

[7] K. Kugemann, Nitrosamine in bier – Überblick, *Bayerisches Landesamt für Gesundheit und Lebensmittelsicherheit*, **2018**. [Online]. Available: https://www.lgl.bayern.de/lebensmittel/warengruppen/wc_36_biere/ue_2017_nitrosamine_in_bier_ueberblick.htm. [Accessed: 2023-11-30].

[8] J. Čulík, M. Jurková, T. Horák, P. Čejka, J. Dvořák and J. Olšovská, Volatile *N*-nitrosamines in malt, thing of the past?, *Kvasný Průmysl*, *57:11*, 413-416, **2011**.

[9] CPG Sec 510.600 Dimethylnitrosamine in malt beverages, *U.S. Food & Drug Administration*, **2005**. [Online]. Available: https://www.fda.gov/regulatory-information/search-fda-guidance-documents/cpg-sec-510600-dimethylnitrosamine-malt-beverages. [Accessed: 2023-11-30].

[10] CPG Sec 578.500 Dimethylnitrosamine (DMNA) in barley malt, *U.S. Food & Drug Administrations*, **2005**. [Online]. Available: https://www.fda.gov/regulatory-information/search-fda-guidance-documents/cpg-sec-578500-dimethylnitrosamine-dmna-barley-malt. [Accessed: 2023-11-30].

[11] C. Fan and T. Lin, *N*-nitrosamines in drinking water and beer: Detection and risk assessment, *Chemosphere*, *200*, 48-56, **2018**.

[12] R. Massey, P. Key, D. McWeeny and M. Knowles, The application of a chemical denitrosation and chemiluminescence detection procedure for estimation of the apparent concentration of total *N*-nitroso compounds in foods and beverages, *Food Additives and Contaminants*, *1:1*, 11-16, **1984**.

[13] M. Malečková, T. Vrzal and J. Olšovská, Development of a method for melamine determination in beer and beer-type beverages by GC-MS/MS, *Kvasný Průmysl*, *66:5*, 331-335, **2020**.

[14] B. Elefant and M. Hossain, Density of beer, *An encyclopedia of scientific essays*, **2000**. [Online]. Available: https://hypertextbook.com/facts/2000/BlairElefant.shtml. [Accessed: 2023-11-30].

[15] R. Massey, M. Dennis, M. Pointer and P. Key, An investigation of the levels of *N*-nitrosodimethylamine, apparent total *N*-nitroso compounds and nitrate in beer, *Food Additives & Contaminants*, *7:5*, 605-615, **1990**.

[16] J. Olšovská, D. Matoulková, P. Čejka and M. Jurková, Beer and health, *Kvasný Průmysl*, *60:7*, 174-181, **2014**.

[17] J. Calderbank and J. Hammond, Influence of nitrate and bacterial contamination on the formation of apparent total *N*-nitroso compounds (ATNC) during fermentation, *Journal of the Institute of Brewing*, *95:4*, 277-281, **1989**.

[18] J. Čulík, T. Horák, P. Čejka and M. Jurková, Non-volatile *N*-nitrosamines in brewing industry. Part 1. - Arrising and methods of estimation, *Kvasný Průmysl*, *58:1*, 6-12, **2012**.

[19] P. Johnson, J. Pfab and R. Massey, A method for the investigation of free and protein-bound *N*-nitrosoproline in beer, *Food Additives and Contaminants*, *5:2*, 119-125, **1988**.

[20] T. Vrzal and J. Olšovská, Pyrolytic profiling nitrosamine specific chemiluminescence detection combined with multivariate chemometric discrimination for non-targeted detection and classification of nitroso compounds in complex samples, *Analytica Chimica Acta*, *1059:1*, 136-145, **2019**.

[21] J. Pollock, Acpects of nitrosation in malts and beers. I.Examination of malts for the presence of *N*-nitrosoproline, *N*-nitrososarcosine and *N*-nitrosopipecolinic acid, *Journal of the Institute of Brewing*, *87:6*, 356-359, **1981**.

[22] N. Sen, L. Tessier and S. Seaman, Determination of *N*-nitrosoproline and *N*-nitrososarcosine in malt and beer, *Journal of Agricultural and Food Chemistry*, *31:5*, 1033-1036, **1983**.

[23] D. McWeeny, Nitrosamines in beverages, *Food Chemistry*, *11:4*, 273-287, **1983**.

[24] P. Johnson, J. Pfab and R. Massey, Development of methods for the characterization of non-volatile *N*-nitroso compounds in malt, *Journal of the Institute of Brewing*, *94:1*, 19-22, **1988**.

[25] N. Sagawa and T. Shikata, Are all polar molecules hydrophilic? Hydration numbers of nitro compounds and nitriles in aqueous solution, *Physical Chemistry Chemical Physics*, *16:26*, 13262-13270, **2014**.

[26] R. Loeppky, Nitrosamine and *N*-nitroso compound chemistry and biochemistry, *Nitrosamines and Related N-Nitroso Compounds*, *553*, 1-18, **1994**.

[27] K. Rostkowska, K. Zwierz and A. Rózański, Formation and metabolism of *N*-nitrosamines, *Polish Journal of Environmental Studies*, *7:6*, 321-325, **1998**.

[28] H. Kushida, K. Fujita and A. Suzuki, Metabolic activation of *N*-alkylnitrosamines in genetically engineered *Salmonella typhimurium* expressing CYP2E1 or CYP2A6 together with human NADPH-cytochrome P450 reductase, *Carcinogenesis*, *21:6*, 1227-1232, **2000**.

[29] Y. Li and S. Hecht, Metabolic activation and DNA interactions of carcinogenic *N*-nitrosamines to which humans are commonly exposed, *International Journal of Molecular Sciences*, *23:9*, **2022**.

[30] G. Bellec, Y. Dréano, P. Lozach, J. Ménez and F. Berthou, Cytochrome P450 metabolic dealkylation of nine *N*-nitrosodialkylamines by human liver microsomes, *Carcinogenesis*, *17:9*, 2029-2034, **1996**.

[31] A. Helguera, M. Cordeiro, M. Pérez, R. Combes and M. González, Quantitative structure carcinogenicity relationship for detecting structural alerts in nitroso-compounds: Species: Rat; Sex: male; route of administration: water, *Toxicology and Applied Pharmacology*, *231:2*, 197-207, **2008**.

[32] P. Smith, The occurence and formation of *N*-nitroso compounds *in vivo*, *Dissertation Thesis*, Surrey, **1986**.

[33] K. Inami, J. Shiino, S. Hagiwara, K. Takeda and M. Mochizuki, Transnitrosation of non-mutagenic *N*-nitrosoproline forms mutagenic *N*-nitroso-*N*-methylurea, *23:13*, 3297-3302, **2015**.

[34] S. Nitz, P. Moza and F. Korte, A capillary gas-liquid chromatographic method for determination of ethylenethiourea and propylenethiourea in hops, beer, and grapes, *Journal of Agricultural and Food Chemistry*, *30*, 593-596, **1982**.

[35] K. Eichner, M. Reutter and R. Wittmann, Detection of Amadori Compounds in Heated Foods, *Thermally Generated Flavors*, *5*, 42-54, **1993**.

[36] L. Lucas, D. Gatehouse and D. Shuker, Efficient nitroso group transfer from *N*-nitrosoindoles to nucleotides and 2'-deoxyguanosine at physiological pH. A new pathway for *N*-nitrosocompounds to exert genotoxicity, *The Journal of Biological Chemistry*, *274:26*, 18319-18326, **1999**.

[37] B. Pignatelli, C. Malaveille and M. Friesen, Synthesis, structure-activity relationships and a reaction mechanism for mutagenic *N*-nitroso derivatives of glycosylamines and Amadori compounds - model substances for *N*-nitrosated early Maillard reaction products, *Food and Chemical Toxicology*, *25:9*, 669-680, **1987**.

[38] S. Herrmann, L. Duedahl-Olesen and K. Granby, Occurrence of volatile and non-volatile *N*-nitrosamines in processed meat products and the role of heat treatment, *Food Control*, *48*, 163-169, **2015**.

[39] T. Wainwright, Nitrosamines in malt and beer, *Journal of the Institute of Brewing*, *92:1*, 73-80, **1986**.

[40] V. Kellner, J. Čulík and G. Basařová, *N*-nitrosaminy ve sladu - vznik a odstraňování, *Kvasný Průmysl*, *29*, 28-31, **1983**.

[41] J. Sindelar and A. Milkowski, Human safety controversies surrounding nitrate and nitrite in the diet, *Nitric Oxide*, *26:4*, 259-266, **2012**.

[42] M. Colomer, B. Funch, N. Solodovnikova, T. Hobley and J. Förster, Biotransformation of hop derived compounds by *Brettanomyces yeast* strains, *Journal of The Institute of Brewing*, *126*, 280-288, **2020**.

[43] R. Massey and P. Key, Examination of some fermented foods for the presence of apparent total *N*-nitroso compounds, *Food Additives and Contaminants*, *6:4*, 453-458, **1989**.

[44] N. Hord, Y. Tang and N. Bryan, Food sources of nitrates and nitrites: the physiologic context for potential health benefits, *The American Journal of Clinical Nutrition*, *90:1*, 1-10, **2009**.

[45] R. G. Liteplo, B. Meek, W. Windle, *N*-nitrosodimethylamine, *Concise International Chemical Assessment Document 38*, 1-47, **2002**.

[46] N. Smith, Cambridge prize lecture nitrate reduction and *N*-nitrosation in brewing, *Journal of the Institute of Brewing*, *100:5*, 347-355, **1994**.

[47] D. Seel, T. Kawabata, M. Nakamura, T. Ishibashi, M. Hamano, M. Mashimo, S. Shin, K. Sakamoto, E. Jhee and S. Watanabe, *N*-nitroso compounds in two nitrosated food products in Southwest Korea, *Food and Chemical Toxicology*, *32:12*, 1117-1123, **1994**.

[48] W. Kunze, Chapter 2 – Malt production, in *Technology brewing and malting*, 3rd ed., Berlin: VLB, 97-188, **2004**.

[49] T. Wainright, The chemistry of nitrosamine formation: Relevance to malting and brewing, *Journal of the Institute of Brewing*, *92:1*, 49-64, **1986**.

[50] COUNCIL DIRECTIVE 98/83/EC on the quality of water intended for human consumption, **1998**. [Online]. Available: https://eur-lex.europa.eu/legal-content/EN/TXT/PDF/?uri=CELEX:01998L0083-20151027&rid=2. [Accessed: 2023-11-30].

[51] J. Čepička, P. Baudyš, E. Víznerová and J. Krausová, Nitrate content in brewing waters and beers of eastern bohemian breweries, *Kvasný Průmysl*, *37:8*, 230-234, **1991**.

[52] M. Moll, S. Chevrier, N. Moll and J. P. Joly, Nitrate mass-balance in the brewing industry, *Developments in Food Science*, *29*, 427-436, **1992**.

[53] M. Kippenberger, S. Hanke, M. Biendl, G. Stettner and A. Lagemann, Transfer of nitrate and various pesticides into beer during dry hopping, *Brewing Science*, *67:1*, 1-9, **2014**.

[54] N. Smith, P. Smith and C. Woodruff, The role of bacillus sin *N*-nitrosamine formation during wort production, *Journal of the Institute of Brewing*, *98:5*, 409-414, **1992**.

[55] N. Smith, Nitrate reduction and ATNC formation by brewery wild yeasts, *Journal of the Institute of Brewing*, *98:5*, 415-420, **1992**.

[56] R. López-Rodríguez, J. McManus, N. Murphy, M. Ott and M. Burns, Pathways for *N*-nitroso compound formation: Secondary amines and beyond, *24:9*, 1558-1585, **2020**.

[57] T. Morgan and D. Williams, Kinetics and mechanism of the Fischer-Hepp rearrangement. Part I. Rearrangement of *N*-nitroso-*N*-methylaniline in hydrochloric acid, *Journal of the Chemical Society, Perkin Transactions* 2:1, 74-78, **1972**.

[58] J. Park and D. Williams, Kinetics of the reactions of nitrous acid with olefins. Kinetic identification of probable nitrosating agents, *Journal of the Chemical Society, Perkin Transactions 2:14*, **1972**.

[59] M. González-Jiménez, J. Arenas-Valgañón, M. García-Santos, E. Calle and J. Casado, Mutagenic products are promoted in the nitrosation of tyramine, *Food Chemistry*, *216*, 60-65, **2017**.

[60] R. Gil, J. Casado and C. Izquierdo, Structural effects on the *N*-nitrosation of amino acids, *International Journal of Chemical Kinetics*, *29:7*, 495–504, **1997**.

[61] S. González-Mancebo, M. García-Santos, J. Hernández-Benito, E. Calle and J. Casado, Nitrosation of phenolic compounds: Inhibition and enhancement, *Journal of Agricultural and Food Chemistry*, *47:6*, 2235-2240, **1999**.

[62] S. González-Mancebo, J. Lacadena, Y. García-Alonso, J. Hernández-Benito, E. Calle and J. Casado, Nitrosation of phenolic compounds: Effects of alkyl substituents and solvent, *Monatshefte fuer Chemie/Chemical Monthly*, 133:2, 157-166, 2002.

[63] M. Fernández-Liencres, E. Calle, S. González-Mancebo, J. Casado and B. Quintero, Nitrosation kinetics of phenolic components of foods and beverages, *International Journal of Chemical Kinetics*, *29*, 119-125, **1997**.

[64] T. Ishikawa, T. Watanabe, H. Tanigawa, T. Saito, K. Kotake, Y. Ohashi and H. Ishii, Nitrosation of phenolic substrates under mildly basic conditions: Selective preparation of *p*-quinone monooximes and their antiviral activities: Selective Preparation of *p*-quinone monooximes and their antiviral activities, *The Journal of Organic Chemistry*, *61:8*, 2774-2779, **1996**.

[65] S. Mirvish, L. Wallcave, M. Eagen and P. Shubik, Ascorbate-nitrite reaction: Possible means of blocking the formation of carcinogenic *N*-nitroso compounds, *Science*, *177:4043*, 65-68, **1972**.

[66] D. Williams, Comparison of the efficiencies of ascorbic acid and sulphamic acid as nitrite traps, *Food and Cosmetics Toxicology*, *16:4*, 365-367, **1978**.

[67] T. Rundlof, E. Olsson and A. Wiernik, Potential nitrite scavengers as inhibitors of the formation of *N*-nitrosamines in solution and tobacco matrix systems, *Journal of Agricultural and Food Chemistry*, *48*, 4381-4388, **2000**.

[68] H. Pourazrang, A. Moazzami and B. Bazzaz, Inhibition of mutagenic *N*-nitroso compound formation in sausage samples by using *L*-ascorbic acid and *α*-tocopherol, *Meat Science*, *62*, 479-483, **2002**.

[69] S. Mirvish, A. Grandjean, K. Reimers, B. Connelly, S. Chen, C. Morris, X. Wang, J. Haorah and E. Lyden, Effect of ascorbic acid dose taken with a meal on nitrosoproline excretion in subjects ingesting nitrate and proline, *Nutrition and Cancer*, *31:2*, 106-110, **1998**.

[70] M. Otsuka, Y. Sakashita, N. Arakawa and M. Tsuda, Studies on endogenous formation of *N*-nitroso compounds in the guinea pig supplemented with proline or thioproline and sodium nitrate, *Food and Chemical Toxicology*, *30:9*, 765-769, **1992**.

[71] C. Walters, M. Downes, M. Edwards and P. Smith, Determination of a non-volatile *N*-nitrosamine on a food matrix, *The Analyst*, *103:1232*, 1127-1133, **1978**.

[72] S. Herrmann, K. Granby and L. Duedahl-Olesen, Formation and mitigation of *N*-nitrosamines in nitrite preserved cooked sausages, *Food Chemistry*, *174*, 516-526, **2015**.

[73] M. Higashimoto, T. Yamamoto, T. Kinouchi, Y. Handa, H. Matsumoto and Y. Ohnishi, Mutagenicity of soy sauce treated with nitrite in the presence of ethanol or alcoholic beverages, *Mutation Research/Genetic Toxicology*, *345:3-4*, 155-166, **1995**.

[74] A. Malpica, M. Calzadilla and T. Cordova, Kinetics and mechanism of oxime formation from pyruvic acid, *13:3*, 162-166, **2000**.

[75] S. Veljovic-Jovanovic, F. Morina, R. Yamauchi, S. Hirota and U. Takahama, Interactions between (+)-catechin and quercetin during their oxidation by nitrite under the conditions simulating the stomach, *Journal of Agricultural and Food Chemistry*, *62:21*, 4951-4959, **2014**.

[76] E. Walker, B. Pignatelli and M. Friesen, The role of phenols in catalysis of nitrosamine formation, *Journal of the Science of Food and Agriculture*, *33:1*, 81-88, **1982**.

[77] D. Kim, G. Shin, Y. Lee, J. Lee, J. Cho, S. Baik and O. Lee, Assessment and comparison of the antioxidant activities and nitrite scavenging activity of commonly consumed beverages in Korea, *Food Chemistry*, *151*, 58-64, **2014**.

[78] P. Metivier and T. Schlama, The mechanisms of nitration of phenol, *The Roots of Organic Development*, *8*, 368-379, **1996**.

[79] A. Zheng, D. Dzombak and R. Zheng, Effects of Nitrosation on the Formation of Cyanide in Publicly Owned Treatment Works Secondary Effluent, *Water Environment Research*, *76:3*, 197-204, **2004**.

[80] I. Álvarez Gaona, M. Assof, V. Jofré, M. Combina and I. Ciklic, Mutagenesis, screening and isolation of Brettanomyces bruxellensis mutants with reduced 4-ethylphenol production, *World Journal of Microbiology and Biotechnology*, *37:6*, 1-9, **2021**.

[81] D. Szwajgier, J. Pielecki and Z. Targoński, The release of ferulic acid and feruloylated oligosaccharides during wort and beer production, *Journal of the Institute of Brewing*, *111:4*, 372-379, **2005**.

[82] J. Yu, T. Vasanthan and F. Temelli, Analysis of phenolic acids in barley by high-performance liquid chromatography, *Journal of Agricultural and Food Chemistry*, *49:9*, 4352-4358, **2001**.

[83] D. Šibalić, M. Planinić, A. Jurić, A. Bucić-Kojić and M. Tišma, Analysis of phenolic compounds in beer: from raw materials to the final product, *Chemical Papers*, *75:1*, 67-76, **2021**.

[84] J. Šavel and M. Prokopová, Change of beer colour due to effect of nitrite, *Kvasný Průmysl*, *38:11*, 321-325, **1992**.

[85] S. Hirota and U. Takahama, Reactions of polyphenols in masticated apple fruit with nitrite under stomach simulating conditions: Formation of nitroso compounds and thiocyanate conjugates, *Food Research International*, *75*, 20-26, **2015**.

[86] C. Janzowski, R. Klein, R. Preussmann and G. Eisenbrand, Nitrosation of sarcosine, proline and 4-hydroxyproline by exposure to nitrogen oxides, *Food and Chemical Toxicology*, *20:5*, 595-597, **1982**.

[87] A. Naka, T. Suzuki and S. Arimoto-Kobayashi, Nitrosation of glutathione and nitration of tyrosine by *N*-nitrosoproline with ultraviolet light, *Genes and Environment*, *32:4*, 75-84, **2010**.

[88] C. Oldreive, K. Zhao, G. Paganga, B. Halliwell and C. Rice-Evans, Inhibition of nitrous acid-dependent tyrosine nitration and DNA base deamination by flavonoids and other phenolic compounds, *Chemical Research in Toxicology*, *11:12*, 1574-1579, **1998**.

[89] K. Cope, H. Seifried, R. Seifried, J. Milner, P. Kris-Etherton and E. Harrison, A gas chromatography–mass spectrometry method for the quantitation of *N*-nitrosoproline and *N*-acetyl-S-allylcysteine in human urine: Application to a study of the effects of garlic consumption on nitrosation, *Analytical Biochemistry*, *394:2*, 243-248, **2009**.

[90] K. Tanaka, B. McConnell, W. Niemczura and H. Mower, Characterization and mutagenicity of 1-nitrosotryptophol and 6-nitrotryptophol possible genotoxic substances associated with smoking and alcohol consumption, *Cancer Letters*, *44:2*, 109-116, **1989**.

[91] G. Danno, K. Kanazawa, M. Toda, M. Mizuno, H. Ashida and M. Natake, A mutagen from histidine reacted with nitrite, *Journal of Agricultural and Food Chemistry*, *41:7*, 1090-1093, **1993**.

[92] S. Ulusoy, H. Ulusoy, D. Pleissner and N. Eriksen, Nitrosation and analysis of amino acid derivatives by isocratic HPLC, *RSC Advances*, *6:16*, 13120-13128, **2016**.

[93] M. García-Santos, E. Calle and J. Casado, Amino acid nitrosation products as alkylating agents, *Journal of the American Chemical Society*, *123:31*, 7506-7510, **2001**.

[94] M. García-Santos, S. González-Mancebo, J. Hernández-Benito, E. Calle and J. Casado, Reactivity of amino acids in nitrosation reactions and its relation to the alkylating potential of their products, *Journal of the American Chemical Society*, *124:10*, 2177-2182, **2002**.

[95] M. García Santos, E. Calle and J. Casado, A method for the kinetic study of amino acid nitrosation reactions, *Polyhedron*, *22:8*, 1059-1066, **2003**.

[96] K. Heyns, S. Röper, H. Röper and B. Meyer, *N*-nitroso sugar amino acids, *Angewandte Chemie International Edition in English*, *18:11*, 878-880, **1979**.

[97] J. Wang, B. Wu, M. Ding, Y. Yang, Z. Liu, F. Zhang, E. Tang and J. Duan, Aldehyde-mediated *N*-nitrosation of an amino acid, *ARKIVOC: Online Journal of Organic Chemistry*, *4*, 12-19, **2017**.

[98] M. Namiki, Chemistry of Maillard reactions: recent studies on the browning reaction mechanism and the development of antioxidants and mutagens, *Advances in Food Research*, *32*, 164-165, **1988**.

[99] J. Little, Artifacts in trimethylsilyl derivatization reactions and ways to avoid them, *Journal of Chromatography A*, *844*, 1-22, **1999**.

[100] H. Kataoka, Derivatization reactions for the determination of amines by gas chromatography and their applications in environmental analysis, *Journal of Chromatography A*, *733:1-2*, 19-34, **1996**.

[101] C. W. Gehrke and K. Leimer, Trimethylsilylation of amino acids, *Journal of Chromatography A*, *53:2*, 201-208, **1970**.

[102] M. Malečková, Vývoj miniaturizované extrakční metody pro screening netěkavých nitrososloučenin ve sladu pomocí GC-NCD, *Diploma Thesis*, Praha, **2018**.

[103] Z. Li, J. Wang, X. Chen, S. Hu, T. Gong and Q. Xian, A novel molecularly imprinted polymer-solid phase extraction method coupled with high performance liquid chromatography tandem mass spectrometry for the determination of nitrosamines in water and beverage samples, *Food Chemistry*, *292*, 267-274, **2019**.

[104] B. Jurado-Sánchez, E. Ballesteros and M. Gallego, Gas chromatographic determination of *N*-nitrosamines in beverages following automatic solid-phase extraction, *Journal of Agricultural and Food Chemistry*, *55:24*, 9758-9763, **2007**.

[105] K. Ikeda and K. Migliorese, Analysis of nitrosamines in cosmetics, *Journal of the Society of Cosmetic Chemists*, *41*, 283-333, **1990**.

[106] W. Altkofer, S. Braune, K. Ellendt, M. Kettl-Grömminger and G. Steiner, Migration of nitrosamines from rubber products - are balloons and condoms harmful to the human health?, *49:3*, 235-238, **2005**.

[107] D. Kocak, M. Ozel, F. Gogus, J. Hamilton and A. Lewis, Determination of volatile nitrosamines in grilled lamb and vegetables using comprehensive gas chromatography - Nitrogen chemiluminescence detection, *Food Chemistry*, *135:4*, 2215-2220, **2012**.

[108] M. Jones and C. Glover, A Fast Efficient Method to Determine the Presence of Nitrosamines in cosmetics, personal care, and consumer products, *Application Note*, 1-10, **2016**.

[109] S. Yurchenko and U. Mölder, *N*-nitrosodimethylamine analysis in Estonian beer using positive-ion chemical ionization with gas chromatography mass spectrometry, *Food Chemistry*, *89:3*, 455-463, **2005**.

[110] D. Fine, F. Rufeh, D. Lieb and D. Rounbehler, Description of the thermal energy analyzer (TEA) for trace determination of volatile and nonvolatile *N*-nitroso compounds, *Analytical Chemistry*, *47:7*, 1188-1191, **1975**.

[111] A. Tricker, M. Perkins, R. Massey, C. Bishop, P. Key and D. Mcweeny, Incidence of some non-volatile *N*-nitroso compounds in cured meats, *Food Additives and Contaminants*, *1:3*, 245-252, **1984**.

[112] L. Cárdenes, J. Ayala, V. González and A. Afonso, Fast microwave-assisted dansylation of *N*-nitrosamines Analysis by high-performance liquid chromatography with fluorescence detection, *Journal of Chromatography A*, *946*, 133-140, **2002**.

[113] D. Clarke, J. Startin, S. Hasnip, C. Crews, A. Lloyd and M. Dennis, Progress towards the characterization of faecal *N*-nitroso compounds, *Analytical Methods*, *3:3*, 544-551, **2011**.

[114] S. Herrmann, L. Duedahl-Olesen and K. Granby, Simultaneous determination of volatile and non-volatile nitrosamines in processed meat products by liquid chromatography tandem mass spectrometry using atmospheric pressure chemical ionization and electrospray ionization, *Journal of Chromatography A*, *1330*, 20-29, **2014**.

[115] T. Vrzal, M. Malečková and J. Olšovská, DeepReI: Deep learning-based gas chromatographic retention index predictor, *Analytica Chimica Acta*, *1147*, 64-71, **2021**.

[116] P. Kulshrestha, K. McKinstry, B. Fernandez and M. Feelisch, Application of an optimized total *N-n*itrosamine (TONO) assay to pools: Placing *N*-nitrosodimethylamine (NDMA) determinations into perspective, *Environmental Science & Technology*, *44*, 3369-3375, **2010**.

[117] J. Hotchkiss, J. Barbour, L. Libbey and R. Scanlan, Nitramines as thermal energy analyzer positive nonnitroso compounds found in certain herbicides, *Journal of Agricultural and Food Chemistry*, *26:4*, 884-887, **1978**.

Supplementary data

Appendix 1

Analytica Chimica Acta 1147 (2021) 64–71

Contents lists available at ScienceDirect

Analytica Chimica Acta

journal homepage: www.elsevier.com/locate/aca

DeepReI: Deep learning-based gas chromatographic retention index predictor

Tomáš Vrzal [a, *], Michaela Malečková [a, b], Jana Olšovská [a]

[a] Research Institute of Brewing and Malting, Plc., Lípová 511/15, 120 44, Prague 2, Czech Republic
[b] Charles University, Faculty of Science, Department of Analytical Chemistry, Albertov 6, 128 43, Prague 2, Czech Republic

HIGHLIGHTS

- Advanced model for retention indices prediction of compounds in GC was developed.
- The model is based on a convolutional neural network and advanced approaches.
- Median percentage error of prediction is ≤ 0.81%.
- The model is publicly available in the R package - DeepReI.

GRAPHICAL ABSTRACT

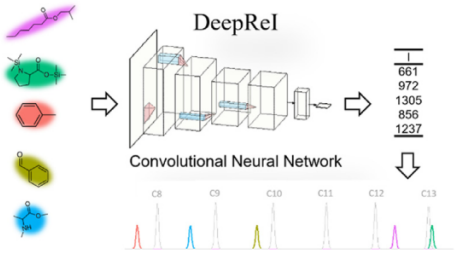

ARTICLE INFO

Article history:
Received 26 October 2020
Received in revised form
14 December 2020
Accepted 21 December 2020
Available online 29 December 2020

Keywords:
Artificial intelligence
Convolutional network
Deep learning
Gas chromatography
Retention index

ABSTRACT

Retention index in gas chromatographic analyses is an essential tool for appropriate analyte identification. Currently, many libraries providing retention indices for a huge number of compounds on distinct stationary phase chemistries are available. However, situation could be complicated in the case of unknown unknowns not present in such libraries. The importance of identification of these compounds have risen together with a rapidly expanding interest in non-targeted analyses in the last decade. Therefore, precise in silico computation/prediction of retention indices based on a suggested molecular structure will be highly appreciated in such situations. On this basis, a predictive model based on deep learning was developed and presented in this paper. It is designed for user-friendly and accurate prediction of retention indices of compounds in gas chromatography with the semi-standard non-polar stationary phase. Simplified Molecular Input Entry System (SMILES) is used as the model's input. Architecture of the model consists of 2D-convolutional layers, together with batch normalization, max pooling, dropout, and three residual connections. The model reaches median absolute error of prediction of the retention index for validation and test set at 16.4 and 16.0 units, respectively. Median percentage error is lower than or equal to 0.81% in the case of all mentioned data sets. Finally, the DeepReI model is presented in R package, and is available on https://github.com/TomasVrzal/DeepRel together with a user-friendly graphical user interface.

* Corresponding author.
E-mail address: tomas.vrzal@beerresearch.cz (T. Vrzal).

https://doi.org/10.1016/j.aca.2020.12.043
0003-2670/

1. Introduction

Retention index (RI) is a measure describing retention of substances in chromatographic systems. In comparison with more intuitive retention parameters like retention time and adjusted retention time which are specific for given experimental conditions, the RI is not highly influenced by these conditions. Therefore, reproducible results are obtained for a given substance across different laboratories. This nature of RI is very important since information about retention behavior of analytes can be spread among laboratories all over the world. In gas chromatography (GC), several retention indices were defined and mainly based on the approach of Kováts [1], and van den Dool and Kratz [2]. Since temperature-programed GC is usually adopted in a wide range of applications, the RI derived from the approach of van den Dool and Kratz is usually more frequently used. The main idea behind RI is that the values for n-alkanes are equal to 100 times the number of carbon atoms in a molecule. Hence, n-alkanes are widely used as RI references. The RIs of other substances (e.g. analytes) are usually calculated by linear interpolation between retentions of two n-alkanes. The mathematical definition of RI is described in Eq. (1) [2].

$$I = 100\left(\frac{t_s - t_n}{t_{n+1} - t_n} + n\right) \quad (1)$$

Where I is retention index, ts is retention time of a substance of interest, n is number of carbon atoms in shorter n-alkane, tn is retention time of n-alkane with n carbon atoms, tn+1 is retention time of n-alkane with n+1 carbon atoms. This approach strictly assumes linear course of RI between adjacent n-alkanes in a homologous series. However, this linearity could be more or less deviated when a complex temperature program is used. In such cases, non-linear regression could be a suitable alternative method.

Although, the RI of a given analyte is quite robust and reproducible parameter, it highly depends on chemistry of stationary phase in GC column due to different intensities of intermolecular forces during molecule retention in a stationary phase. Therefore, it is necessary to list RIs in different stationary phase types for a given substance. Standard non-polar, semi-standard non-polar and polar are the most commonly used stationary phase classifications in practice. The standard non-polar stationary phase mainly includes dimethylpolysiloxane, semi-standard non-polar phase mainly includes 5%-diphenyl-dimethylpolysiloxane, and polar phase polyethylene glycol [3]. Since these types of stationary phases are manufactured by many producers, minor differences in RIs can be observed due to the variations of stationary phase bonding and/or crosslinking. Due to the fact that GC columns with the semi-standard non-polar stationary phase (e.g. DB-5) are the most commonly used columns in many laboratories and are listed in a majority of scientific articles related to GC topics, the development described in this paper is focused on this type of stationary phase.

The identification of solutes in GC analysis is essential for a reliable analysis result in many fields, especially in non-targeted metabolomics or other “omic” technologies. In this way, RI provides valuable help in the identification of known unknown peaks together with mass spectral data (RI is referred as an orthogonal measure to mass spectra). On the other hand, unknown unknowns need a comprehensive elucidation procedure, usually based on a mass spectral interpretation, and subsequent molecular structure confirmation by checking spectral and chromatographic properties of standard or synthetized molecules. In spite of this procedure, it is still good practice to compare experimental RI of unknown peak with some reference, based on a suggested structure resulting from the interpretation of mass spectra, before financial resources will be spent on synthesis and/or purchase of chemicals. However, in case of unknown unknowns the situation is quite complicated due to the lack of RI values of such molecules in libraries. Hence, the only possibility is to calculate RI from intended molecular structure by some predictive tools and rely on the prediction quality which could hamper the whole identification if the quality is poor. Few methods for the gas chromatographic RI prediction/calculation are currently available. One of well-known methods is based on a simple linear group increment of all structural parts in a molecule on resulted RI [4]. Other authors published compound group-specific models for RI prediction (e.g. for alkenes, fatty acid methyl esters or coumarins solely) [5–7], which provide low prediction error but are useable only for limited number of substances. On the other hand, models applicable to compounds belonging to a broader spectrum usually do not achieve such a low prediction error [8,9]. All previously mentioned models were based on machine learning methods, relying mainly on feature quality and manual feature extraction. In contrast, deep learning models provide a more powerful, automated and precise alternative. At the same time, the training of deep learning models is usually computationally expensive and requires larger amount of training data [10]. Deep learning, as a part of artificial intelligence, is very effective in computer vision problems, prediction of time series or chemical related tasks. The latter mentioned example of the deep learning application was, for example, successfully used on detecting a chemical substructure in a molecule responsible for protein-binding with molecular representation in SMILES (Simplified Molecular Input Entry System) [11,12], component identification in a mixture from Raman spectra [13], peak alignment from complex GC analyses [14], molecules identification by improved library search [15], prediction of retention index [16,17], prediction of a molecular fingerprint from mass spectrum [17], and automated preprocessing of raw GC chromatogram for targeted analysis [18].

The aim of this paper is to develop a deep learning-based model in R [19] for gas chromatographic RI prediction of a broad spectrum of molecules on the semi-standard non-polar stationary phase from molecular representation in SMILES. The main motivation of this development is to obtain a model suitable for more precise identification purposes with a lower prediction error than currently available methods. The secondary aim is to make the resulted DeepRel model easily usable even for less experienced R users through a graphical user interface (GUI).

2. Experimental section

2.1. Reagents and chemicals

Following chemicals were used for experimental RI determination: *N*-nitrosodiethylamine, *N*-nitrosodiisopropylamine, *N*-nitrosodibutylamine, *N*-nitrosopyrrolidine, *N*-nitrosopiperidine, *N*-nitrosomorpholine, all 100 μg mL-1 in methanol (Agilent Technologies, Santa Clara, USA), nitrosobenzene (95%, Merck, Darmstadt, Germany), nitrosotoluene (97%, Sigma-Aldrich, Steinheim, Germany), *N*-nitrosohydroxyproline (100 μg mL-1), *N*-nitrososarcosine (100 μg mL-1), *N*-nitrosopipecolic acid (100 μg mL-1), *N*-nitrosoproline (100 μg mL-1, Isconlab, Germany), *N*-nitrosodiethanolamine (100 μg mL-1), *N*-nitrosodiisopropanolamine (100 μg mL-1, Neochema, Germany), melamine (99.95%, Sigma-Aldrich, Steinheim, Germany), N,O-Bis(trimethylsilyl) trifluoroacetamide with trimethylchlorosilane solution (99:1) (BSTFA) (Sigma-Aldrich, Steinheim, Germany), boron trifluoride in methanol solution (15%, Sigma-Aldrich, Steinheim, Germany), C7 – C30 saturated alkanes in hexane (1000 μg mL-1, Sigma-Aldrich, Steinheim, Germany).

Molecules bearing a hydroxyl, carboxyl and/or amino functional group were silylated by BSTFA and/or esterified by solution of boron

trifluoride in methanol according to the procedures described in Refs. [20,21].

2.2. Dataset

Retention indices on semi-standard non-polar stationary phases and respective molecule structures were obtained from NIST Mass Spectral/Retention Index Library (median from multiple RI values) [22]. Chemical structure of each compound was translated into a SMILES string by ACD/ChemSketch software (version 12.01, Advanced Chemistry Development, Inc., Canada). The molecules were classified into groups according to their chemical nature (number of molecules in brackets): alcohols (846), alkanes (39), alkenes (398), alkynes (105), amides (152), amines (260), amino acids (71), anhydrides (21), aromatic (303), branched-chain alkanes (260), carbonyls (338), cyclic (436), derivatized amino acids (2383), esters (5416), ethers (226), fatty acids (45), halogenated substances (6034 - limited to brominated, chlorinated and fluorinated substances), heterocycles (1555), nitriles (23), nitro substances (557), nitroso compounds (28), organic acids (87), oximes (14), phenolic acids (92), phosphates (70), saccharides (60), sterols (145), tert-butyldimethylsilyl derivatives (100), terpenes (86), thiols (40), vitamins (17) and others (62 - molecules not belonging to those groups). Each group contains not only original molecules (e.g. ethanol in a group of alcohols) but also derivatized molecules by trimethylsilyl moiety (e.g. ethanol, trimethylsilyl derivative). Since derivatization can lead to a different molecule classification (e.g. alcohol vs ether), and some molecules can belong to multiple groups, the classification used by the authors is not rigorous and it serves mainly for random stratification sampling purposes (see below). The minimal and maximal RI values in the original dataset were 85 (tetrafluoromethane) and 4355 (tridecaethylene glycol, diacetate), respectively. Both of these marginal objects were allowed to be a part of a training set in order to avoid extrapolation during the evaluation of prediction performance by validation and a test set.

The total number of objects (molecules) and their retention indices obtained from NIST 14 Library, together with retention indices determined experimentally, in the original dataset was 20269. The whole dataset was divided into three parts by stratified random sampling across compound groups: training set (17413 molecules; 179052 after data augmentation, see Data processing section), validation set (1878 molecules) and test set (978 molecules). Stratification sampling was used in order to obtain three different data sets with similar proportion of sample groups.

2.3. Instrumentation

For experimental RI estimation of substances listed in the Reagent and chemicals section, GC with the chemiluminescence detection (RI estimation of *N*-nitrosamines) and GC with mass spectrometry (for other types of compounds) were used according to the methods described previously [20]. The mentioned GC with chemiluminescence detection method was slightly modified in order to easily detect *N*-nitrosamines and n-alkanes – temperature of the pyrolytic tube was maintained at 500 °C for *N*-nitrosamine, and at 850 °C for n-alkanes analysis. All analyses were performed on HP-5MS UI column (5%-diphenyl-dimethylpolysiloxane, 30 m, 0.25 mm, 0.25 μm, Agilent Technologies).

Retention indices were calculated by Eq. (1) with n-alkanes (C7 – C30) as RI reference. These retention indices and their respective molecule description in the form of SMILES strings were used for dataset enhancement (most of them were assigned to the test set for the final model evaluation). The values of RI are in Table S1.

2.4. Data processing

Data were preprocessed through R (v. 4.0.1) environment in the RStudio (v. 1.1.456) [19,23] by corresponding R packages. Firstly, SMILES strings from the training, validation and test set were transformed into canonical form by the propOB function from the ChemmineR package (v. 3.40.0, together with ChemmineOB package v. 1.26.0) [24]. Subsequently, training set SMILES string augmentation was performed using SmilesEnumerator [25] in Python (v. 3.7). Accessibility of this function for R environment was carried out by a reticulate package (v. 1.16) [26]. During generation of augmented data, ten new versions of SMILES strings for each object were randomly generated and eventual duplicates were removed. This procedure led to 10.3 times the increase of a training set size – from 17413 to 179052 – including original (canonical) and rewritten SMILES strings (in average 10.3 different SMILES strings for each object). Since the input for RI prediction by the final model is canonical SMILES (in the form of one-hot code), the SMILES augmentation was performed only on an object from the training set. Finally, SMILES strings (in all data sets) were translated into one-hot code (vectorized representation) using the text_tokenizer function from the keras package (v. 2.3.00) [27] before feeding it into the convolutional model. Resulted dimensions of one-hot code matrices were driven by a) a number of symbols in the longest SMILES string in the training set (183 rows) and b) a number of unique SMILES symbols in the training set (32 columns representing the following symbols: C, c, O, o, N, n, S, s, H, P, F, Cl, Br, Si), (,], [, \,/, = , #, @, 1, 2, 3, 4, 5, 6, 7, 8, 9). Explicit order of the symbols (columns in a one-hot code matrix) is described in Supplementary Material.

2.5. Neural network architecture and training procedure

The core of DeepReI is a two-dimensional convolutional neural network with residual connections. The architecture consists of six convolutional blocks in the main skeleton, together the with rectified linear unit (ReLU) activation, batch normalization and max pooling. Three residual connections consisting mainly of convolution were added in order to avoid information loss along the main skeleton [28]. Flatten and fully connected dense layers were added on the top of the model architecture. Dropout layers, L1 and L2 kernel regularizers were added to increase the model generalization ability, and to avoid overfitting. The neural network architecture is schematically described in Fig. 1 and also as a source code in Supplementary Material.

The model was compiled with the ADADELTA optimizer [29]; the mean square error and mean absolute error were used as loss and monitoring metrics, respectively. The model training was performed on 500 epochs with the batch size 32 and triangular cyclical learning rate approach [30] with the step size of 5 epochs (learning rate rose from minimum to maximum, and vice versa, during 5 epochs). The minimal and maximal learning rates were at 1E-8 and 1, respectively. The training set loss (mean square error) was minimized during the model training by backpropagation algorithm.

Both, the neural network architecture construction and model training were performed in RStudio [23] by the keras package [27] and tensorflow backend (v. 2.2.0) [31]. Computations were performed by a device equipped with Intel® Core™ i7-8750H CPU, 16 GB RAM, NVIDIA GeForce RTX 2070 ~~8~~16 GB GPU and CUDA Toolkit.

2.6. Performance evaluation

Model performance was evaluated by the validation and test set.

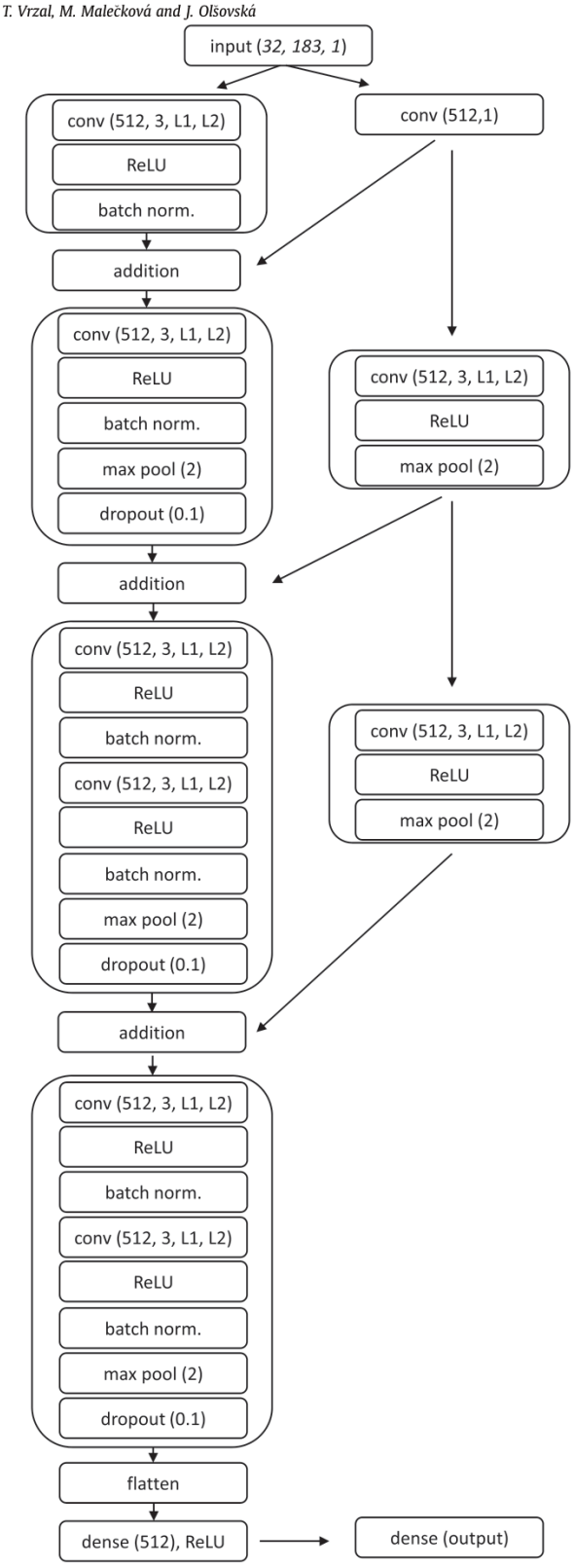

Fig. 1. Neural network architecture of the DeepRel model. Numbers in brackets: Input layer (input dimensions), conv layer (filters, kernel size, kernel regularizers), max pool layer (pool size), dropout layer (dropout rate), dense layer (units).

Model performance for the validation set was monitored during every model training after hyperparameter and/or architecture tuning. However, the test set was used only at the end of the project in order to avoid informational diffusion from the test set to the model during model tuning which could cause model overfitting and poor generalization [10]. After the final model training, retention indices of objects in the validation and test set were predicted. The resulted values were compared to the ones from the NIST Library by residual values computation and subsequent graphical and statistical analysis.

2.7. Graphical user interface

In order to build the DeepRel as a user-friendly tool even for less experienced R users, the developed model was incorporated into an application providing a clear user interface. The application was created on the basis of a Shiny package [32] and is available on GitHub repository (https://github.com/TomasVrzal/DeepRel) in the form of R package. The application enables to upload a SMILES table in.txt or.csv format for the RI prediction, and also to export or copy predicted values. The instructions for the installation and use are described in Supplementary Material and on GitHub.

3. Results and discussion

3.1. Dataset quality

The comparison of RI values distribution in the original, training, validation and test set (Table 1 and Fig. S1) exhibits a high degree of similarity. Therefore, together with a comparable proportion of each compound group in every dataset (obtained by stratified random sampling), the evaluation of prediction performance would not be highly influenced by different objects distribution in datasets. The most abundant compound groups are halogenated substances and esters, each forming nearly 30% of datasets. High number of possible combinations is the reason for a such high abundance of halogenated substances, as well as the fact that esters are one of the most common analytes in GC analysis (due to derivatization reactions). On the other hand, some groups are represented only by a few components, e.g. oximes group. However, boundaries among groups are not strict, and other compounds with oxime moiety are represented also in other groups.

Since precision of prediction by any machine learning or deep learning model highly depends on quality of training data, datasets had to be firstly inspected for erroneous RI values and appropriate cleaning step should be included. This inspection/cleaning step was carried out by training a shallow fully connected dense layer model (the model consisting of input layer, one hidden layer with 32 units, ReLU activation and output layer) on the original dataset; the stochastic gradient descent optimizer (learning rate 0.01), and the batch size of 32 and 100 epochs were used. This model was used for the calculation of residuals. Retention indices in the dataset with the highest obtained residuals were inspected in the meaning of the theoretical increase of RI values in respective homological series (increase by ~ 100 units with one aliphatic carbon addition) – the comparison of the inspected compound RI with RIs of other compounds in respective homological series from the NIST library. Several compounds with obviously erroneous RI were revealed by this procedure – mainly few esters of glutaric and terephthalic acid, all of them coming from only one experimental RI value. These compounds were removed from the original dataset (numbers of compounds shown in Experimental section are after such filtration). The removal of compounds was done only when a value was objectively concluded to be wrong (the difference between theoretical and actual value was more than 100 units), if not,

Table 1
Description of retention indices distribution in datasets.

dataset	I. Q	median	III. Q	min.	max.
Original	1601	2147	2631	85	4355
Training*	1602	2147	2633	85	4355
Validation	1617	2164	2618	177	3872
Test	1543	2112	2614	157	3774

compounds were left in the dataset. It should be emphasized, the filtration of such potential erroneous retention indices was done on the basis of RI prediction by the shallow, non-optimized, model, and the final DeepReI model uses absolutely different architecture. Hence, it could not be concluded that compounds were filtered out due to poor prediction by the developed model. This procedure allowed to obtain data of higher quality than blind usage of all retention values from the source, regardless their accuracy. Such cleaning step was essential as the purpose of the DeepReI model is to predict RI with sufficient precision. That in fact means the model needs to learn how RI is influenced by structural characteristics of molecules, and not how to predict all RI values from the library even if they are not correct.

3.2. Model development

During the model development, convolutional layers of neural network were tested (1D-convolution and 2D-convolution). During this preliminary test, the 2D-convolution provided slightly better results (data not shown). This observation is consistent with previously published studies [33,34] reporting the possible efficiency on 2D-convolution use on 1D-data. Therefore, firstly, two dimensional convolutional layers (with ReLU activation) alternating with average or max pool layers were trained on the training set without data augmentation and by the adamax optimizer. Output from the last layer was flattened and processed by a regressor consisting of fully connected dense layers (1–3 layers with 64 units, ReLU activation) and a final fully connected output layer with one unit. The resulted mean absolute error of prediction for the training and validation set ranged between about 70 and 110 without any improvements after an architecture change, hyperparameters tuning and/or the number of epochs during the training. Therefore, model architecture was further expanded, and batch normalization layers were also added. This expansion was done as the approach based on the idea that a sufficiently complex model that highly overfits, is able to carry a sufficient portion of complex information from the input data in order to effectively predict the target value after the implementation of tools against overfitting [10]. In particular, this approach is based on the fact that a complex overfitted model has number of parameters high enough to be able to model such a complicated task as a noise in the training input data (overfitting mainly occurs when the model memorizes data and/or starts to model even noise in the training data). Hence, such a model should theoretically be able to perform well on a given task after the implementation of dropout, regularization and/or data augmentation [10].

Based on the approach mentioned above, the model architecture was first expanded to the form of the main skeleton of the final DeepReI model except regularizations, dropout and addition layers (see Fig. 1). The training of such architecture resulted in the mean absolute error of prediction for the training and validation set of around 19 and 76, respectively. From these results, an underfitting tendency could be observed. Thus, three residual connections [28] were added together with addition layers (Fig. 1). The resulted architecture led to a slight improvement in the model performance on the training set, however, a tendency for overfitting was observed (data not shown). Since the model was overfitted, dropout, L1 and L2 regularization were implemented (also see Fig. 1). After these changes, the model performance improved (mean absolute error of prediction for validation set was 36). The next step in increasing the prediction quality was the implementation of data augmentation and a cyclical learning rate (described in Experimental section in detail), which led to the final model performance described in the next section.

3.3. Model performance

Metrics for the evaluation of performance of the DeepReI model are in Table 2 together with the graphical representation in Fig. 2. It is obvious that performances on the validation and test set are very close to each other, revealing very low likelihood of a significant informational leakage from the validation set into the model during the architecture and hyperparameters tuning. Concurrently, the differences between the mean absolute error and median absolute error are visible due to highly skewed distribution of absolute errors. In such cases, the mean loses its meaning as a centrality measure. Therefore, the values of absolute errors were mathematically transformed by natural logarithm to obtain a symmetrical distribution. The resulted mean absolute errors for the training, validation and test set (after the retransformation to the original scale) were 7.3, 14.4 and 14.4, respectively. These results confirm the median values in Table 2 as better metrics of performance, since the mean values are biased by extreme values of residuals. On the other hand, the mean absolute error was also used in the performance evaluation of previously published models, hence this parameter is also necessary to calculate for the comparison of different models. The most recently published and the most precise model for RI prediction in GC (also based on convolutional neural network) reached values of the mean absolute error, median absolute error, root mean square error and mean percentage error for the test set of 33.2, 18.0, 63.0 and 1.96, respectively [16]. In comparison, the DeepReI model, presented in this paper, reached better (lower) values of these parameters. Since Matyushin et al. [16] did not publish information about the prediction error variance, it is not possible to fully compare the performance of these two models based on these metrics. Conversely, it could be theoretically argued that when median absolute errors of two models are very close to each other, and the mean absolute errors are not so similar, the model with higher mean absolute errors has a higher proportion of high error values. Therefore, such a model with a lower mean absolute error could be theoretically considered as more precise (with lower proportion of high absolute errors). Since more direct comparison of the model would be highly beneficial, the test set was

Table 2
Model performance evaluation.

	Dataset		
	Training	Validation	Test
Mean absolute error	11.6	28.5	28.4
Median absolute error	9.0	16.4	16.0
Root mean square error	15.7	46.2	47.0
Root median square error	9.0	16.4	16.0
Mean percentage error	0.60%	1.63%	1.72%
Median percentage error	0.43%	0.80%	0.81%
		residua	
1. quartile	−8.6	−15.2	−14.6
median	0.4	0.5	1.3
3. quartile	9.5	17.1	17.2
5% quantile	−22.8	−69.9	−59.3
95% quantile	25.4	63.1	67.6

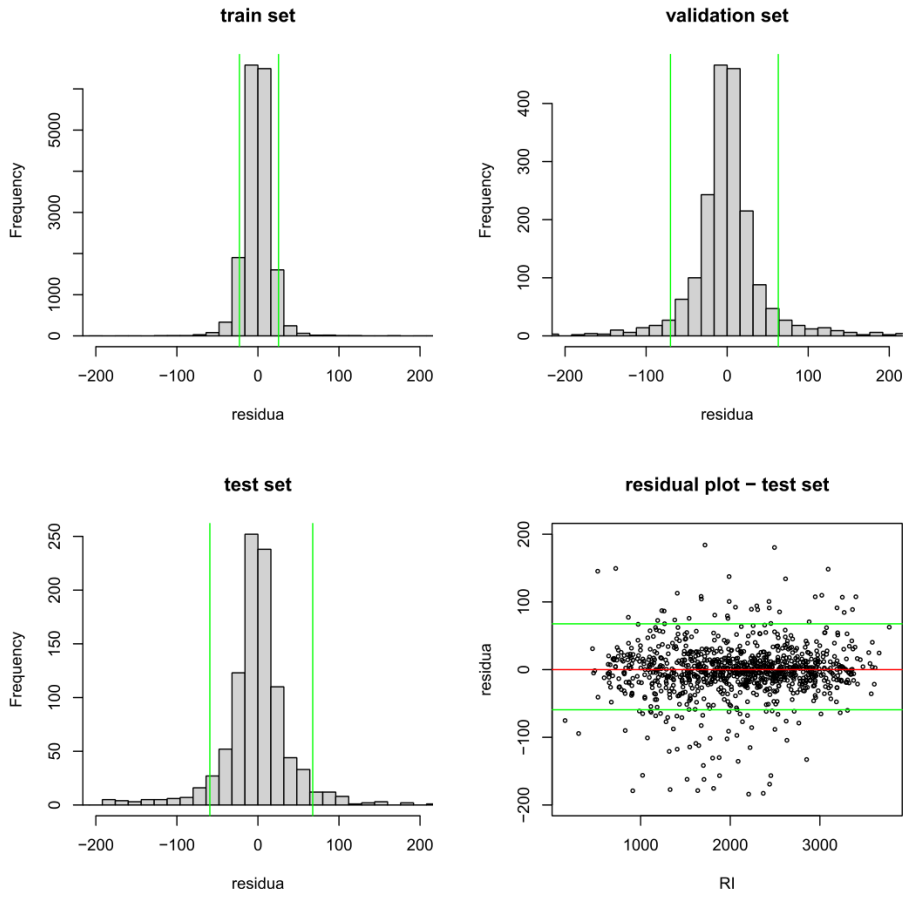

Fig. 2. Residuals distribution in the training, validation and test set. Green lines indicate corresponding 5th and 95th quantiles. Column width was set at 16.

used for prediction accuracy evaluation of the model published by Matyushin et al. [16]. The number of compounds in the test set was reduced (from 978 to 800) in the sense of removing of compounds presented in the training set used by the authors. Therefore, direct comparison of the models was performed on the same dataset not used for training of both models. The resulting mean absolute error, median absolute error, 5% and 95% quantile were 46.9, 29.2, −53.3 and 136.2, respectively. Comparison of these data with the data from Table 2 (results obtained by the use of reduced test set did not significantly differ from data in Table 2) show us that the DeepReI model outperforms the model previously published model. From these points of view, the DeepReI model performs better on RI prediction than previously published models, and it allows to further increase the probability of the accurate analyte identification (according to retention behavior and mass spectral data). As it can be seen from Table 2, the observed core of residuals (50% of all residuals between first and third quartile) for the validation and test set lies in quite a narrow interval. According to the previously published evaluation of RI quality on the semi-standard non-polar stationary phase performed for frequently reported compounds of plant essential oils (mainly alcohols, esters, aldehydes, ketones and terpenes) in the NIST RI library, 90% of RI values belong to the following interval: median ± 25.5 [35]. It means that the core of residuals mentioned above belong to the same interval as the evaluated 90% interval of RI quality. Of course, the remaining 50% of residuals, from which 25% belong to higher and 25% to lower residual values, should also be taken into consideration. Furthermore, 90% of residuals obtained during the DeepReI evaluation belonged to the interval between approximately ±70. In contrast, the same proportion of residuals in the case of the training set belongs to almost the same interval as was evaluated by Babushok et al. [35]. Therefore, based on the assumption of equal proportion of RI uncertainties for all types of compounds in the NIST RI library, it could be concluded that the DeepReI model learns well on the training data. However, the situation for unseen data (validation and test set) is commonly worse, since some degree of underfitting could be observed from Table 2. In order to evaluate this underfitting, the structures of molecules with the highest residuals in all datasets were inspected. The same structural pattern was found in such molecules – mainly an indole ring, and more specifically, a heterocyclic secondary amine group with an unsubstituted hydrogen atom. Hence, the DeepReI model does not perform sufficiently on this part of molecule, and high residuum is assumed when such molecule is presented for RI prediction.

Furthermore, the DeepReI model trained without data augmentation reached the mean absolute error of validation set at only 36 (see the Model development section). Hence, the effect of data augmentation on RI prediction together with its positive effect on the model robustness and generalization ability described in literature is obvious here [10]. Retention index uncertainty should also be taken into consideration during the molecule identification. According to the author's experience, one of the main factors

resulting in high RI uncertainty is the retention time shift between the analysis run and calculating RI on the peak maximum in the case of an unsymmetrical peak (given mainly by injection history, stationary phase exposure to air at high temperature, and overloaded column [36]).

Based on the previous, such RI deviations were simulated by the calculation of RI values - retention times of the peak maximum were shifted by the value of average peak width at the baseline of n-alkanes used as RI reference (see Experimental section). Absolute deviations of such simulated RIs ranged from 9 to 25 units depending on retention time in temperature-programmed GC (data not shown). The maximal deviation calculated by this simulation was comparable with the core of residuals obtained by the DeepReI, see Table 2. Consequently, the DeepReI performance almost hit the border of experimental precision of RI determination. The threshold for the component identification based on RI should be, therefore, set according to experimental and interlaboratory deviations as it was also mentioned in literature [36,37]. In fact, the majority of compounds in the NIST RI library has values from one source only, and it could also influence the predictive performance of the DeepReI model.

3.4. Example of the DeepReI application for unknown identification

A practical usage of the DeepReI model for unknown identification is demonstrated on products identification of vanillic acid reaction with sodium nitrite (see Supplementary Material for details). The reaction yields in two unknown products (peak at 16.75 and 18.18 min). The mass spectra of these chromatographic peaks (Figs. S3 and S4) were submitted to NIST MS Search 2.2 for library search and similarity calculation. Peak at 18.18 min showed relatively high similarity with TMS derivative of 2-methoxy-5-nitrophenol (Fig. S6). In order to confirm this first-step identification, the DeepReI was used for RIs prediction of four possible positional isomers of 2-methoxynitrophenol (Fig. S8). The highest similarity score (and the lowest difference between experimental and predicted RI value) was observed for 2-methoxy-5-nitrophenol. This result is consistent with the library search.

The best similarity for the peak at 16.75 min was 2,4-dimethoxyaniline, *N*-trimethylsilyl derivative (Fig. S5). However, the similarity score was insufficient (0.511). Based on the difference of the molecular ions of both peaks, the suggested structure of the peak at 16.75 min is nitroso derivative of 2-methoxyphenol. According to this assumption, RIs of four positional isomers were predicted (Fig. S8). Since NIST library does not include the mass spectrum of these nitroso derivatives, similarity was calculated only from RI values. The best match was obtained in the case of 2-methoxy-3-nitrosophenol.

4. Conclusions

It can be concluded that the developed DeepReI model is highly usable in RI prediction based on molecular structure and it exceeds the performance of previously published models. Since GC is an essential analytical technique in many areas, including petrochemistry, environmental chemistry, food chemistry, and many others, the model presented in this paper will find an application in a wide range of fields. Application of the DeepReI for routine usage was also enhanced by accessing it through user-friendly GUI available on https://github.com/TomasVrzal/DeepReI.

Author contributions

All authors have given the approval to the final version of the manuscript.

CRediT authorship contribution statement

Tomáš Vrzal: Data curation, programming, model architecture building, data preparation, Writing - original draft. **Michaela Malečková:** Data curation, Formal analysis, data preparation, GC analysis for retention index determination, Writing - original draft. **Jana Olšovská:** Writing - original draft.

Declaration of competing interest

The authors declare that they have no known competing financial interests or personal relationships that could have appeared to influence the work reported in this paper.

Acknowledgment

This study was supported by the Ministry of Agriculture of the Czech Republic within the institutional support MZE-RO1918.

Appendix A. Supplementary data

Supplementary data to this article can be found online at https://doi.org/10.1016/j.aca.2020.12.043.

References

[1] E. Kováts, Gas-chromatographische Charakterisierung organischer Verbindungen. Teil 1: retentionsindices aliphatischer Halogenide, Alkohole, Aldehyde und Ketone, Helv. Chim. Acta 41 (1958) 1915–1932.
[2] H. Van Den Dool, P. Dec Kratz, A generalization of the retention index system including linear temperature programmed gas-liquid partition chromatography, J. Chromatogr. 11 (1963) 463–471.
[3] V.I. Babushok, P.J. Linstrom, J.J. Reed, I.G. Zenkevich, R.L. Brown, W.G. Mallard, S.E. Stein, Development of a database of gas chromatographic retention properties of organic compounds, J. Chromatogr. A 1157 (2007) 414–421.
[4] S.E. Stein, V.I. Babushok, R.L. Brown, P.J. Linstrom, Estimation of Kováts retention indices using group contributions, J. Chem. Inf. Model. 47 (2007) 975–980.
[5] R.H. Rohrbaugh, P.C. Jurs, Prediction of gas chromatographic retention indexes of selected olefins, Anal. Chem. 57 (1985) 2770–2773.
[6] O. Farkas, I.G. Zenkevich, F. Stout, J.H. kalivas, K. Héberger, Prediction of retention indices for identification of fatty acid methyl esters, J. Chromatogr. A 11 (2008) 188–195.
[7] M. de Freitas Soares, F.D. Monache, V.E.F. Heinzen, R.A. Yunes, Prediction of gas chromatographic retention indices of coumarins, J. Braz. Chem. Soc. 10 (1999) 189–196.
[8] K.L. Goodner, Practical retention index models of OV-101, DB-1, DB-5, and DB-Wax for flavor and fragrance compounds, Lebensm. Wiss. Technol. 41 (2008) 951–958.
[9] E. Dossin, E. Martin, P. Diana, A. Castellon, A. Monge, P. Pospisil, M. Bentley, P.A. Guy, Prediction models of retention indices for increased confidence in structural elucidation during complex matrix analysis: application to gas chromatography coupled with high-resolution mass spectrometry, Anal. Chem. 88 (2016) 7539–7547.
[10] F. Chollet, J.J. Allaire, Deep Learning with R, Manning Publications Co., 2018.
[11] D. Weininger, SMILES, a chemical language and information system. 1. Introduction to methodology and encoding rules, J. Chem. Inf. Comput. Sci. 28 (1988) 31–36.
[12] M. Hirohara, Y. Saito, Y. koda, K. Sato, Y. Sakakibara, Convolutional neural network based on SMILES representation of compounds for detecting chemical motif, BMC Bioinf. 19 (2018) 526.
[13] X. Fan, W. Ming, H. Zeng, Z. Zhang, H. Lu, Deep learning-based component identification for the Raman spectra of mixtures, Analyst 144 (2019) 1789–1798.
[14] Li, M., Rosalind Wang, X. Peak alignment of gas chromatography-mass spectrometry data with deep learning. J. Chromatogr. A, 1604, 460476.
[15] D.D. Matyushin, A.Y. Sholokhova, A.K. Buryak, Deep learning driven GC-MS library search and its application for metabolomics, Anal. Chem. 92 (17) (2020), 11918 - 11825.
[16] D.D. Matyushin, A.Y. Sholokhova, A.K. Buryak, A deep convolutional neural network for the estimation of gas chromatographic retention indices, J. Chromatogr. A 1607 (2019) 460395.
[17] H. Ji, H. Deng, H. Lu, Z. Zhang, Predicting a molecular fingerprint from an electron ionization mass spectrum with deep neural networks, Anal. Chem. 92 (13) (2020) 8649–8653.
[18] A. Skarysz, Y. Alkhalifah, K. Darnley, M. Eddleston, Y. Hu, D.B. McLaren, W.H. Nailon, D. Salman, M. Sykora, C.L.P. Thoman, A. Soltoggio, Convolutional

Neural Networks for Automated Targeted Analysis of Raw Gas Chromatography-Mass Spectrometry Data, 2018, pp. 1–8, https://doi.org/10.1109/IJCNN.2018.8489539. International Joint Conference on Neural Networks (IJCNN), Rio de Janeiro.
[19] R Core Team, R: A Language and Environment for Statistical Computing, R Foundation for Statistical Computing, Vienna, Austria, 2019. HYPERLINK, https://www.R-project.org/, https://www.R-project.org/.
[20] T. Vrzal, J. Olšovská, Pyrolytic profiling nitrosamine specific chemiluminescence detection combined with multivariate chemometric discrimination for non-targeted detection and classification of nitroso compounds in complex samples, Anal. Chim. Acta 1059 (2019) 136–145.
[21] P. Araujo, T.-T. Nguyen, L. Frøyland, J. Wang, J.X. Kang, Evaluation of a rapid method for the quantitative analysis of fatty acids in various matrices, J. Chromatogr. A 28 (2008) 106–113.
[22] S. Stein, Y. Mirokhin, D. Tchekhovskoi, W. Mallard, A. Mikaia, O. Sparkman, P. Neta, E. White, V. Zaikin, X. Yang, D. Zhu, NIST/EPA/NIH Mass Spectral Library, 2014. Version 2.2, build Jun 10.
[23] RStudio Team, RStudio, Integrated Development for R. RStudio, Inc., Boston, MA, 2016. URL HYPERLINK "http://www.rstudio.com/, http://www.rstudio.com/, http://www.rstudio.com/. Version 1.1.456.
[24] Y. Cao, A. Charisi, L. Cheng, T. Jiang, T. Girke, ChemmineR: a compound mining framework for R, Bioinformatics 24* (15) (2008) 1733–1734, https://doi.org/10.1093/bioinformatics/btn307.
[25] E.J. Bjerrum, SMILES Enumerator as Data Augmentation for Neural Network Modeling of Molecules, 2017 arXiv:1703.07076vol. 2.
[26] Kevin Ushey, J.J. Allaire, Yuan Tang, reticulate: Interface to 'Python'. R package version 1.16, https://CRAN.R-project.org/package=reticulate, 2020.
[27] J.J. Allaire, François Chollet, Keras: R Interface to 'Keras'. R Package Version 2.2.5.0, 2020. HYPERLINK "https://keras.rstudio.com, https://keras.rstudio.com/, https://keras.rstudio.com.
[28] K. He, X. Zhang, S. Ren, J. Sun, Deep Residual Learning for Image Recognition, 2015 arXiv:1512.03385v1.
[29] Zeiler, M.D. ADADELTA, An Adaptive Learning Rate Method, 2012. ArXiv: 1212.5701vol. 1.
[30] L. Smith, Cyclical Learning Rates for Training Neural Networks, 2017. ArXiv: 1506.01186vol. 6.
[31] J.J. Allaire, Yuan Tang, Tensorflow: R Interface to 'TensorFlow'. R Package Version 2.2.0, 2020. HYPERLINK "https://CRAN.R-project.org/package=tensorflow, https://cran.r-project.org/package=tensorflow, https://CRAN.R-project.org/package=tensorflow.
[32] Winston Chang, Joe Cheng, J.J. Allaire, Yihui Xie, Jonathan McPherson, Shiny: Web Application Framework for R. R Package Version 1.4.0.2, 2020. HYPERLINK "https://CRAN.R-project.org/package=shiny, https://cran.r-project.org/package=shiny, https://CRAN.R-project.org/package=shiny.
[33] Y. Wu, F. Yang, Y. Liu, X. Zha, S. Yuan, A Compariosn of 1.D and 2-D Deep Convolutional Neural Networks in ECG Classification, 2018 arXiv: 1810.07088vol. 1.
[34] L.A. Micio, G.A. Schwartz, From chemical structure to quantitative polymer properties prediction through convolutional neural networks, Polymer 193 (2020) 122341.
[35] V.I. Babushok, P.J. Linstrom, I.G. Zenkevich, Retention indices for frequently reported compounds of plant essential oils, J. Phys. Chem. Ref. Data 40 (2011), 043101-1-47.
[36] M.B. Wilson, B.B. Barnes, P.G. Boswell, What experimental factors influence the accuracy of retention projections in gas chromatography-mass spectrometry? J. Chromatogr. A 1373 (2014) 179–189.
[37] J. Zhang, I. Koo, B. Wang, Q.-W. Gao, C.-H. Zheng, X. Zhang, A large scale test dataset to determine optimal retention index threshold based on three mass spectral similarity measures, J. Chromatogr. A 1251 (2012) 188–193.

Appendix 2

Table 1. List of NCD-positive and false-positive compounds.

Group	Compound	Relative NCD response*	Note	Reference
N-nitroso	NPIP	1.17	c	3
N-nitroso	*N*-nitrosodiphenylamine	1.11	c	3
N-nitroso	*N*-nitrosodipropylamine	1.09	c	3
N-nitroso	NDEA	1.07	c	3
N-nitroso	*N*-nitroso-*N*-methyl urethane	1.04	c	3
N-nitroso	*N*-nitroso-*N*-ethyl aniline	1.03	c	3
N-nitroso	9-nitrosocarbazole	1.03	c	3
N-nitroso	*N*-methyl-*N*-nitroso-*N*-nitro guadinine	1.02	c	3
N-nitroso	*N*-nitrosodibutylamine	1.01	b	2
N-nitroso	Ethyl-*N*-nitrososarcosinate	0.97	c	3
N-nitroso	NMOR	0.96	b	2
N-nitroso	*N*-nitroso-*N*-phenylbenzyl amine	0.92	c	3
N-nitroso	*N*-nitrosodiphenylamine	0.90	b	2
N-nitroso	Dinitrosopiperazine	0.87	c	3
N-nitroso	*N*-nitrodiethanolamine	0.75	b	2
N-nitroso	*N*-methyl-*N*-nitroso toluenesulphonamide	0.17	a	1
N-nitroso	*N*-ethyl-*N*-nitrosourea	<0.05	a	1
C-nitroso	4-nitrosophenol	<0.05	b	2
C-nitroso	4-nitrosodiphenylamine	<< 0.01	c	3
C-nitroso	Dimethylglyoxime	<< 0.01	c	3
C-nitroso	2-nitroso-1-naphthol	<< 0.01	c	3
Oxime	cyclohexanone oxime	<< 0.01	a	1
S-nitroso	nitrosogluthathione	0.82	b	2
S-nitroso	*S*-nitrosotriphenylmethanethiol	0.53	a	1
N-nitro	*N*-nitrodipropylamine	0.50	a	4
N-nitro	*N*-nitrodimethylamine	<0.05	a	1
C-nitro	2,2',4,4',6,6'-hexanitrodiphenylamine	1.40	c	3
C-nitro	2-nitropropane	0.41	a	1
C-nitro	5-nitrouracil	<0.05	c	3
C-nitro	nitrobenzene	<0.05	a	1
C-nitro	chloropicrin	<0.05	b	2
C-nitro	4-nitrophenol	<0.05	b	2
C-nitro	3-nitrophthalidimide	<< 0.01	c	3
C-nitro	Nitromethane	<< 0.01	c	3
Other	Nitrite	1.20	b	2
Other	ethyl nitrate	1.10	a	1
Other	Isopentyl nitrite	1.00	c	3
Other	pentyl nitrite	1.00	c	3
Other	cyclohexylamine nitrite	1.00	c	3
Other	sodium nitrite (in H_2O)	1.00	c	3
Other	sodium nitrate (in H_2O)	1.00	c	3
Other	nitric acid	1.00	c	3
Other	ethyl nitrite	0.70	a	1
Other	dimethylsulfoxide	<0.05	c	3
Other	hydrazine	<0.05	c	3
Other	azobisisobutyronitrile	<< 0.01	a	1
Other	imidazole	<< 0.01	a	1
Other	pyrrole	<< 0.01	a	1
Other	azoxyanisole	<< 0.01	a	1
Other	furan	<< 0.01	a	1
Other	thiophene	<< 0.01	a	1
Other	linoleic acid	<< 0.01	a	1
Other	crotonaldehyde	<< 0.01	a	1
Other	methylvinylketone	<< 0.01	a	1
Other	nitrate	<< 0.01	b	2
Other	ammonium hydroxide	<< 0.01	c	3
Other	dimethylamine hydrochloride	<< 0.01	c	3
Other	diphenyl carbazone	<< 0.01	c	3
Other	aniline	<< 0.01	c	3

* Standardized numeric response within listed compounds. Note that estimations of response vary, depending on the reference: *a* - Molar response relative to NDMA

b - Recovery calculated as the ratio of the slope of the NDMA standard curve

c - Relative response, nitrosyl mole basis

References: 1 [23], 2 [116], 3 [110], 4 [117].

Appendix 3

Supporting Information
for publication

Characterization of nitrite related reaction products in beer

Michaela Malečková[1,2], Tomáš Vrzal[1,*], Jana Olšovská[1], Jana Sobotníková[2]

[1] Research Institute of Brewing and Malting, Lípová 511/15, 120 00, Prague, Czech Republic

[2] Charles University, Faculty of Science, Department of Analytical Chemistry, Albertov 6, 128 43, Prague, Czech Republic

*Corresponding author: tomas.vrzal@beerresearch.cz

Table of content:

1. Retention indices prediction by DeepRel tool

To compare predicted retention indices (RI) with the experimental ones, 100 RI predictions by the DeepRel model (through enabling the dropout during the prediction phase) were carried out for each SMILES string. Obtained predicted RI values were processed by Bayesian analysis (10000 Markov Chain Monte Carlo iteration; uniform distribution from 0 to 4400, and 0 – 100 was set as prior distribution for mean and standard deviation, respectively). The mean, the 95% highest density interval of the mean, and 95% highest density interval of prediction were calculated according to posterior distribution and are listed in **Table S1**. The R packages *rjags* and *HDInterval* were used.


```
Martyn Plummer (2019). rjags: Bayesian Graphical Models
  using MCMC. R package version 4-10.
  https://CRAN.R-project.org/package=rjags

Mike Meredith and John Kruschke (2020). HDInterval: Highest
  (Posterior) Density Intervals. R package version 0.2.2.
  https://CRAN.R-project.org/package=HDInterval
```

Table S1: Results of predicted RI by DeepRel according to proposed structures of studied compounds

RT [min]	Name	SMILES	mean RI	HDI^{95} (mean)	HDI^{95} (prediction)
8.6	cyclohex-2-en-1-oxime, TMS	C[Si](C)(C)O\N=C1/C=CCCC1	1284	1280 - 1288	1241 - 1327
8.6	cyclopent-2-en-1-oxime, TMS	O=C1C=C/C(=N\O[Si](C)(C)C)C1	1331	1326 - 1451	1272 - 1391
8.6	pyrrole-2-carboxylic acid, TMS	C[Si](C)(C)OC(=O)c1cccn1	1446	1440 - 1451	1392 - 1499
8.6	pyrrole-3-carboxylic acid, TMS	C[Si](C)(C)OC(=O)c1ccnc1	1398	1394 - 1403	1355 - 1442
8.9	pyruvic acid oxime, 2TMS	C[Si](C)(C)O\N=C(\C)C(=O)O[Si](C)(C)C	1211	1206 - 1215	1167 - 1254
13.3	4-cyanophenol, TMS	C[Si](C)(C)Oc1ccc(cc1)C#N	1384	1380 - 1388	1343 - 1426
13.7	N-nitrosoproline ethylester	O=NN1CCCC1C(=O)OCC	1418	1414 - 1422	1379 - 1456
14.7	N-nitrosoproline, TMS	O=NN1CCCC1C(=O)O[Si](C)(C)C	1446	1443 - 1449	1415 - 1477
15.0	2-ethyl-3-nitrosophenol, TMS	C[Si](C)(C)Oc1cccc(N=O)c1CC	1564	1559 - 1568	1518 - 1609
15.0	2-ethyl-4-nitrosophenol, TMS	C[Si](C)(C)Oc1ccc(cc1CC)N=O	1665	1660 - 1670	1616 - 1714
15.0	2-ethyl-5-nitrosophenol, TMS	C[Si](C)(C)Oc1cc(ccc1CC)N=O	1542	1538 - 1546	1499 - 1584
15.0	2-ethyl-6-nitrosophenol, TMS	C[Si](C)(C)Oc1c(cccc1N=O)CC	1481	1477 - 1484	1445 - 1517
15.6	1-nitroso-5-oxoproline, TMS	O=NN1C(=O)CCC1C(=O)O[Si](C)(C)C	1529	1526 - 1533	1494 - 1564
15.6	1-nitroso-4-oxoproline, TMS	O=C1CC(C(=O)O[Si](C)(C)C)N(N=O)C1	1586	1581 - 1590	1542 - 1630
15.6	1-nitroso-3-oxoproline, TMS	O=C1CCN(N=O)C1C(=O)O[Si](C)(C)C	1646	1641 - 1651	1598 - 1694
15.6	1-nitrosopiperidine-2-carboxylic acid, TMS	O=NN1CCCCC1C(=O)O[Si](C)(C)C	1530	1526 - 1533	1491 - 1568
15.6	1-nitrosopiperidine-3-carboxylic acid, TMS	O=NN1CCCC(C1)C(=O)O[Si](C)(C)C	1615	1610 - 1621	1564 - 1667
15.6	1-nitrosopiperidine-4-carboxylic acid, TMS	O=NN1CCC(CC1)C(=O)O[Si](C)(C)C	1620	1615 - 1626	1567 - 1675
16.8	2-methoxy-3-nitrosophenol, TMS	COc1c(cccc1O[Si](C)(C)C)N=O	1611	1606 - 1615	1566 - 1656
16.8	2-methoxy-4-nitrosophenol, TMS	C[Si](C)(C)Oc1ccc(cc1OC)N=O	1700	1695 - 1704	1654 - 1746
16.8	2-methoxy-5-nitrosophenol, TMS	C[Si](C)(C)Oc1cc(ccc1OC)N=O	1580	1576 - 1584	1540 - 1620
16.8	2-methoxy-6-nitrosophenol, TMS	C[Si](C)(C)Oc1c(cccc1OC)N=O	1520	1517 - 1524	1484 - 1557
17.4	4-nitrobenzoic acid, TMS	O=[N+]([O-])c1ccc(cc1)C(=O)O[Si](C)(C)C	1672	1668 - 1676	1632 - 1712
17.4	3-nitrobenzoic acid, TMS	O=[N+]([O-])c1cc(ccc1)C(=O)O[Si](C)(C)C	1646	1642 - 1650	1606 - 1685
17.4	2-nitrobenzoic acid, TMS	O=[N+]([O-])c1ccccc1C(=O)O[Si](C)(C)C	1633	1630 - 1636	1604 - 1662
18.2	2-methoxy-5-nitrophenol, TMS	C[Si](C)(C)Oc1cc(ccc1OC)[N+]([O-])=O	1706	1702 - 1710	1667 - 1745
23.2	4-hydroxy-5-methoxy-2-nitrosobenzoic acid, TMS	C[Si](C)(C)Oc1cc(N=O)c(cc1OC)C(=O)O[Si](C)(C)C	2067	2062 - 2072	2021 - 2114
23.2	4-hydroxy-5-methoxy-3-nitrosobenzoic acid, TMS	C[Si](C)(C)Oc1c(cc(cc1OC)C(=O)O[Si](C)(C)C)N=O	1910	1905 - 1916	1859 - 1962
23.2	4-hydroxy-3-methoxy-2-nitrosobenzoic acid, TMS	COc1c(N=O)c(ccc1O[Si](C)(C)C)C(=O)O[Si](C)(C)C	1941	1936 - 1946	1893 - 1989
26.4	4-hydroxyphenyllactic acid, 3TMS	C[Si](C)(C)Oc1ccc(cc1[N+]([O])=O)CC(O[Si](C)(C)C)C(=O)O[Si](C)(C)C	2182	2178 - 2186	2142 - 2222

2. Structure elucidation of nitrite reaction products

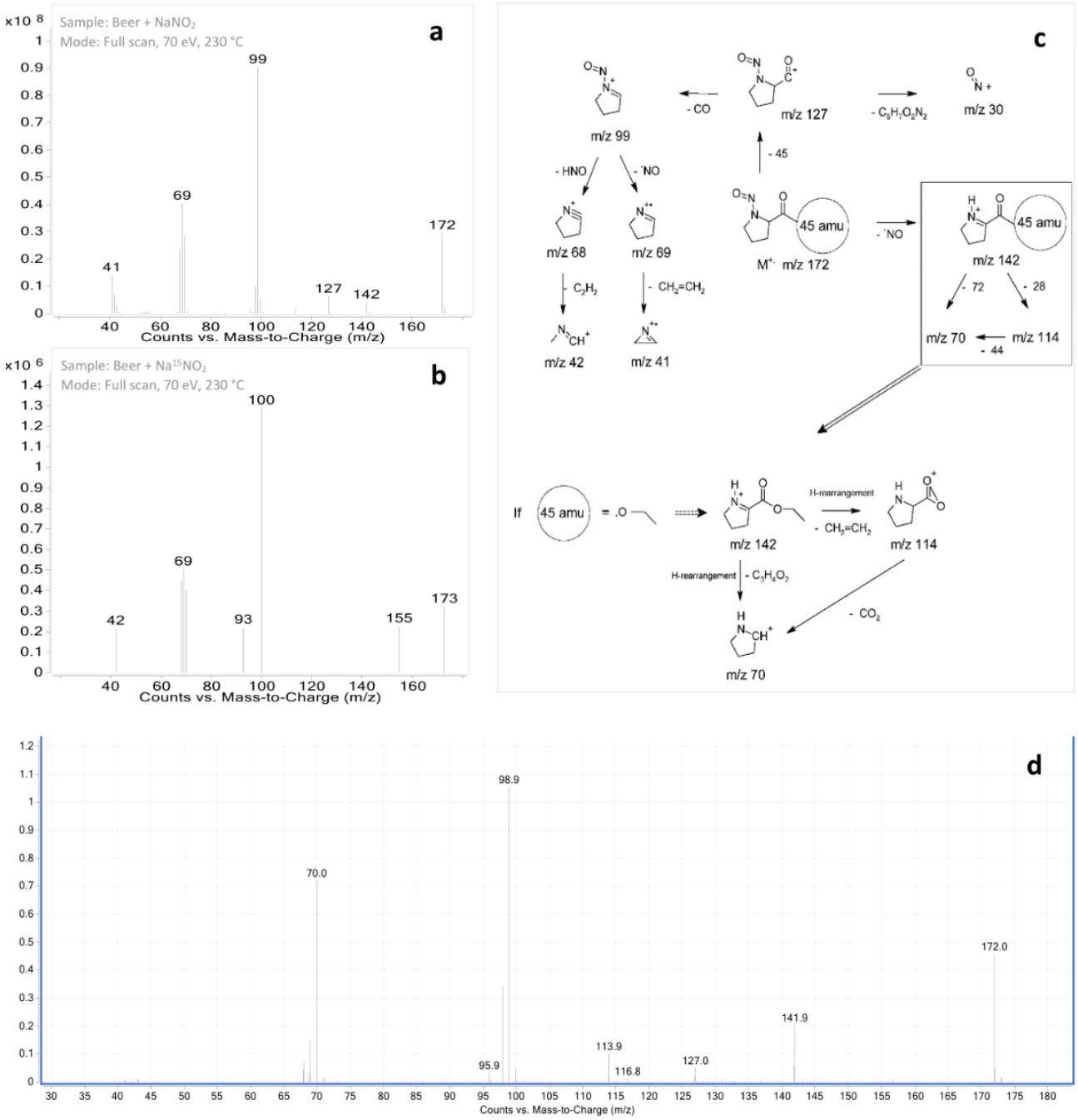

Figure S1: MS spectra of the peak **5** (**a**) and the same peak in the isotopic experiment (**b**) found in beer samples. Proposed fragmentation (**c**) and MS spectrum of the peak identified as NPRO-Et (**d**) copied from previous publication. [1]

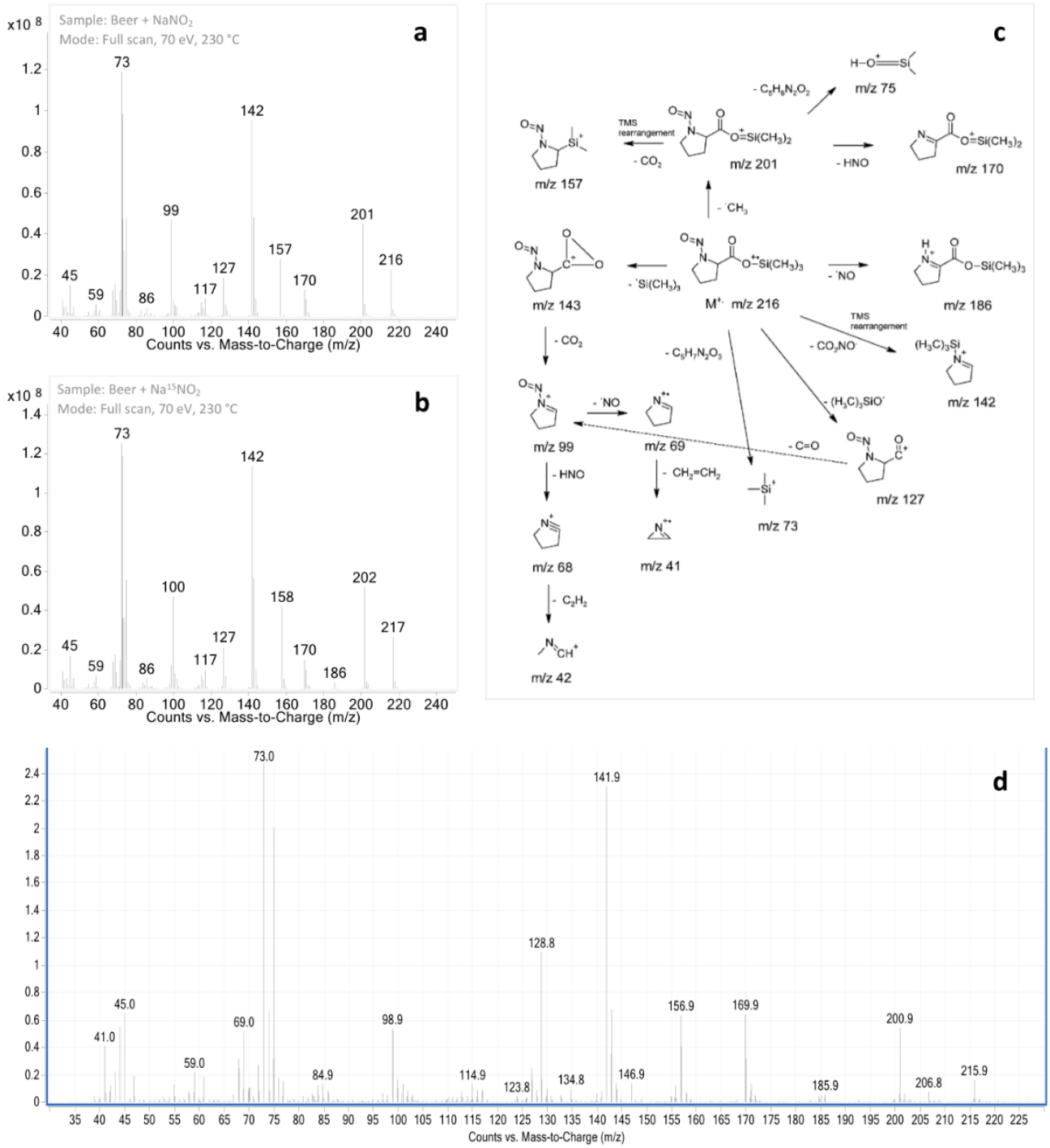

Figure S2: MS spectra of the peak **6** (**a**) and the same peak in the isotopic experiment (**b**) found in beer samples. Proposed fragmentation (**c**) and MS spectrum of the peak identified as NPRO-TMS (**d**) copied from previous publication. [1]

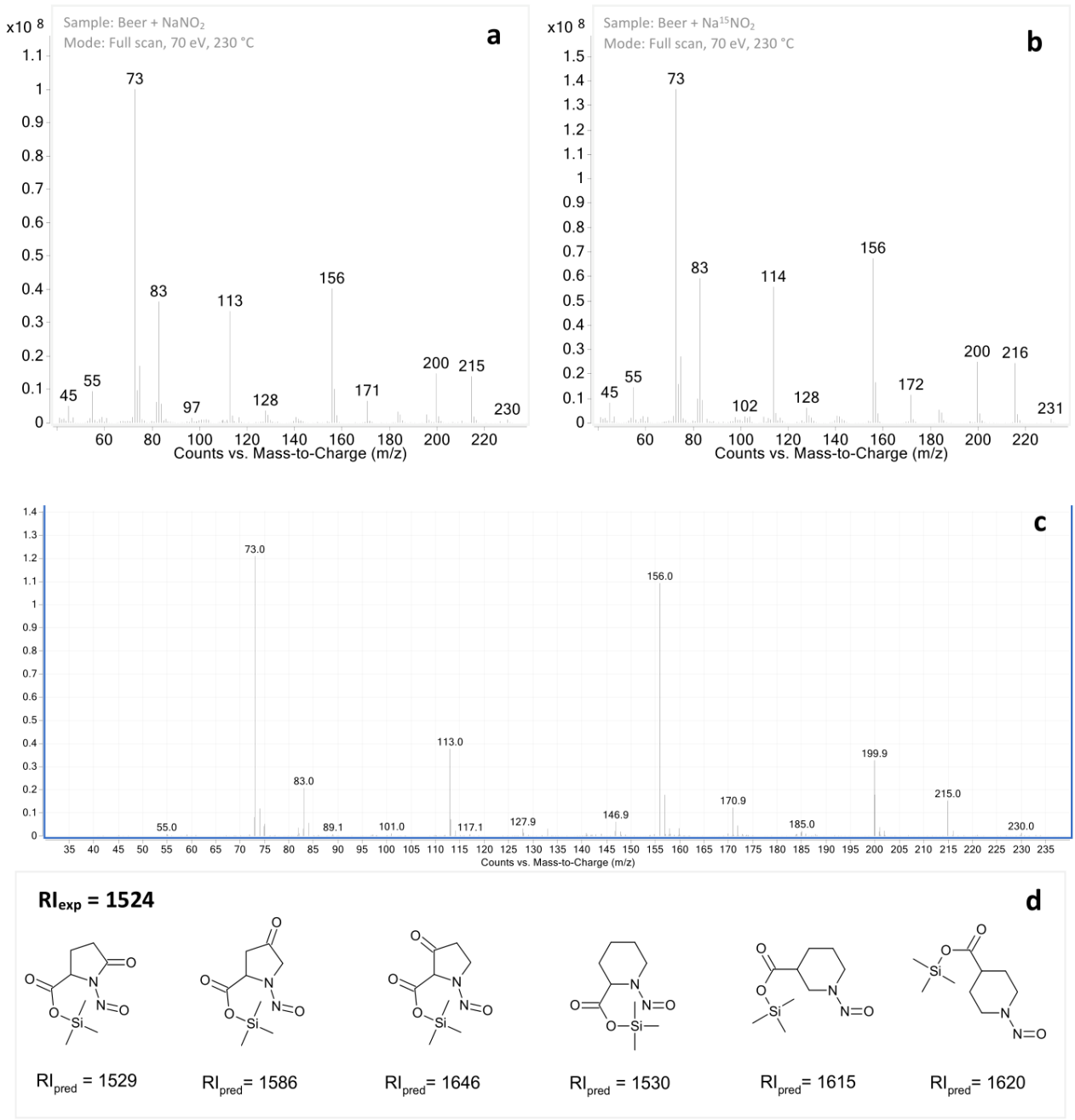

Figure S3: MS spectra of the peak **7** (**a**) and the same peak in the isotopic experiment (**b**) found in beer samples. MS spectrum of the peak found in artificially nitrosated beer at 14.7 min (**c**) copied from the previous publication. [1] Comparison of peak's experimental RI and predicted RIs of NPIC-TMS (first 3 isomers) and NPGA-TMS (second 3 isomers) (**d**).

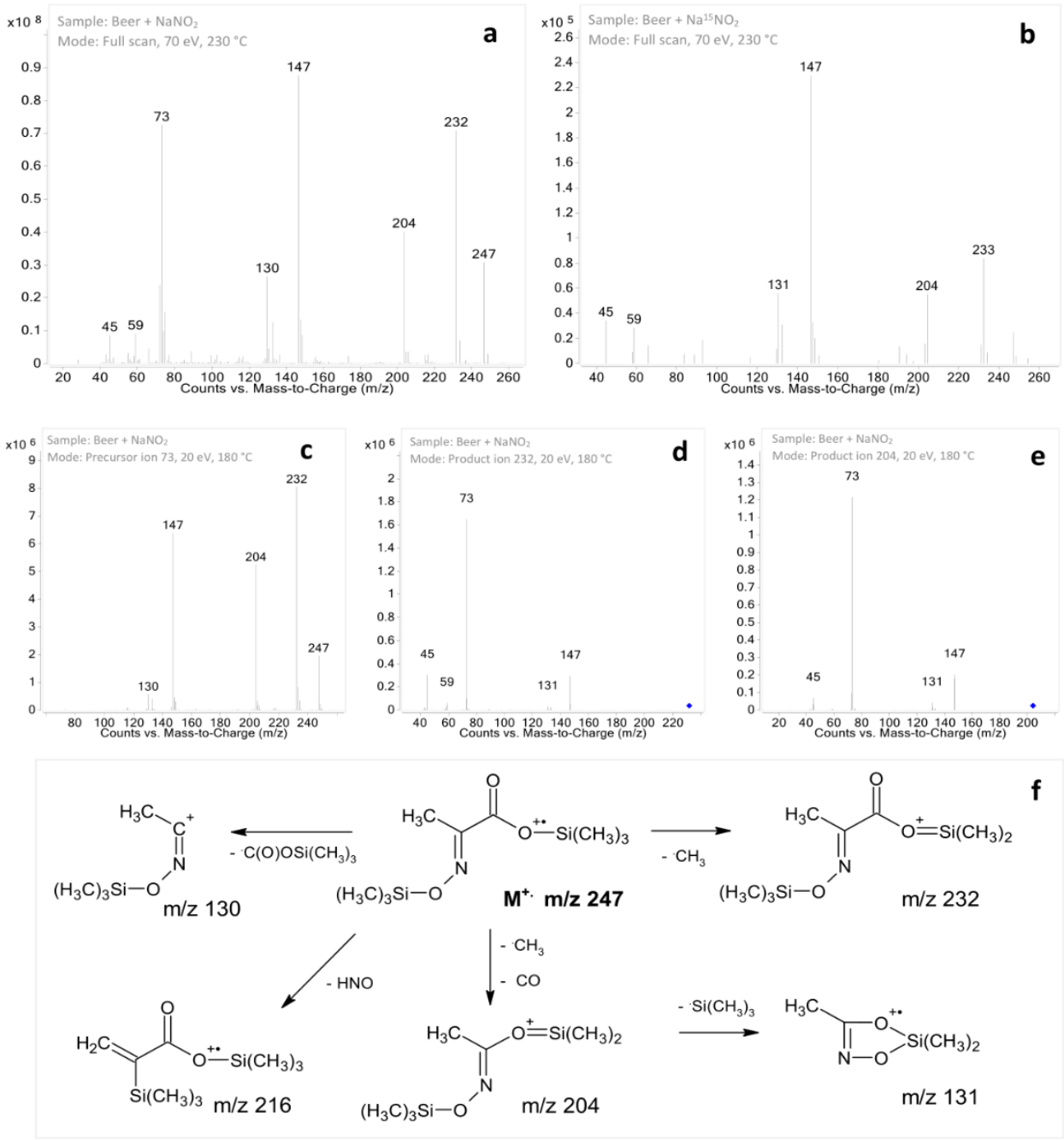

Figure S4: MS spectra of the peak **2** (**a**) and the same peak in the isotopic experiment (**b**) found in beer samples. Precursor ion spectrum of *m/z* 73 (**c**), and product ion spectra of *m/z* 232 (**d**), and *m/z* 204 (**e**) of the same peak. Suggested fragmentation of pyruvic acid oxime-2TMS (**f**).

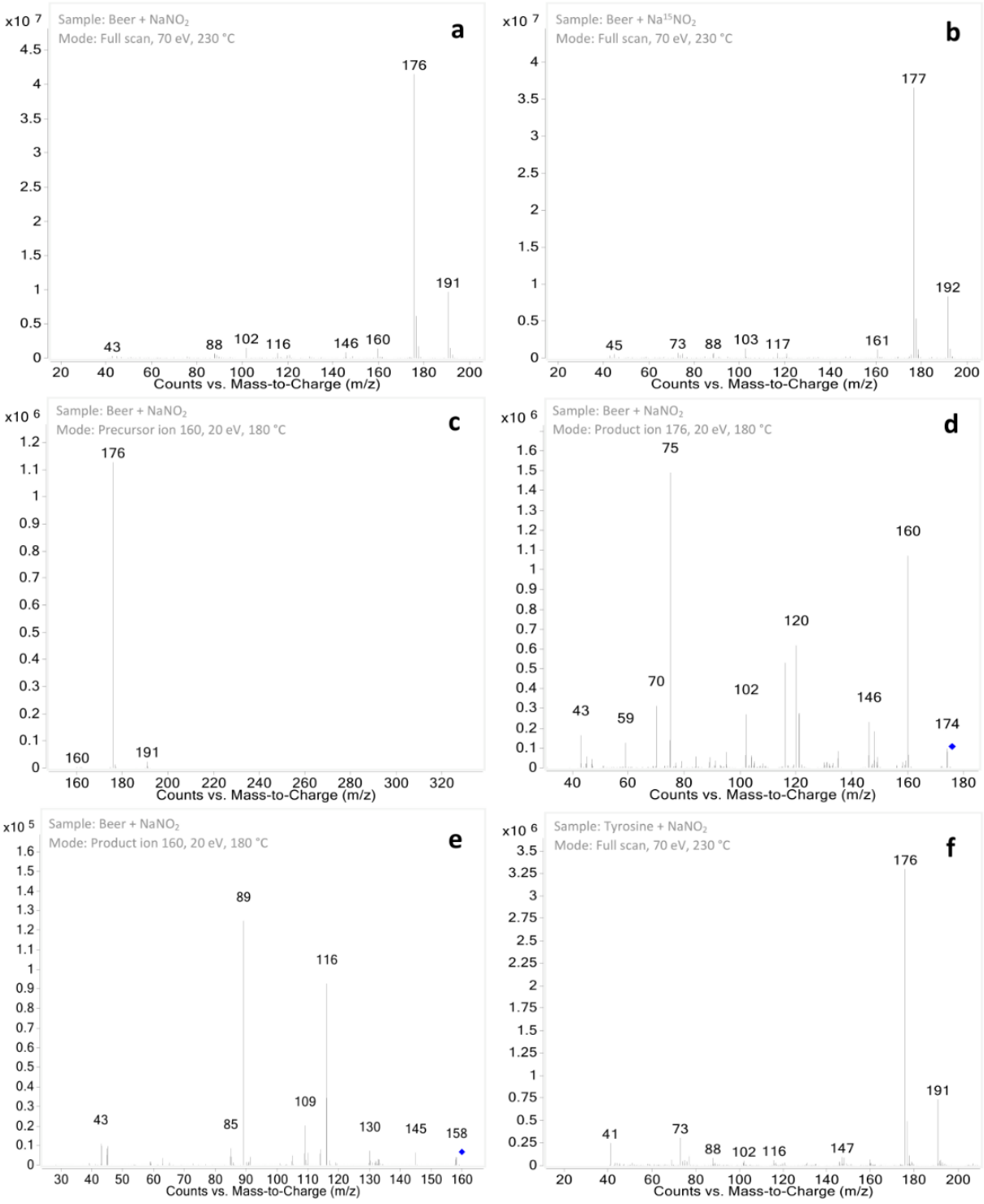

Figure S5: MS spectra of the peak **3** (**a**) and the same peak in the isotopic experiment (**b**). The precursor ion spectrum of *m/z* 160 (**c**), product ion spectra of *m/z* 176 (**d**), and *m/z* 160 (**e**) of the same peak. MS spectrum of the product from tyrosine with the nitrite reaction (**f**).

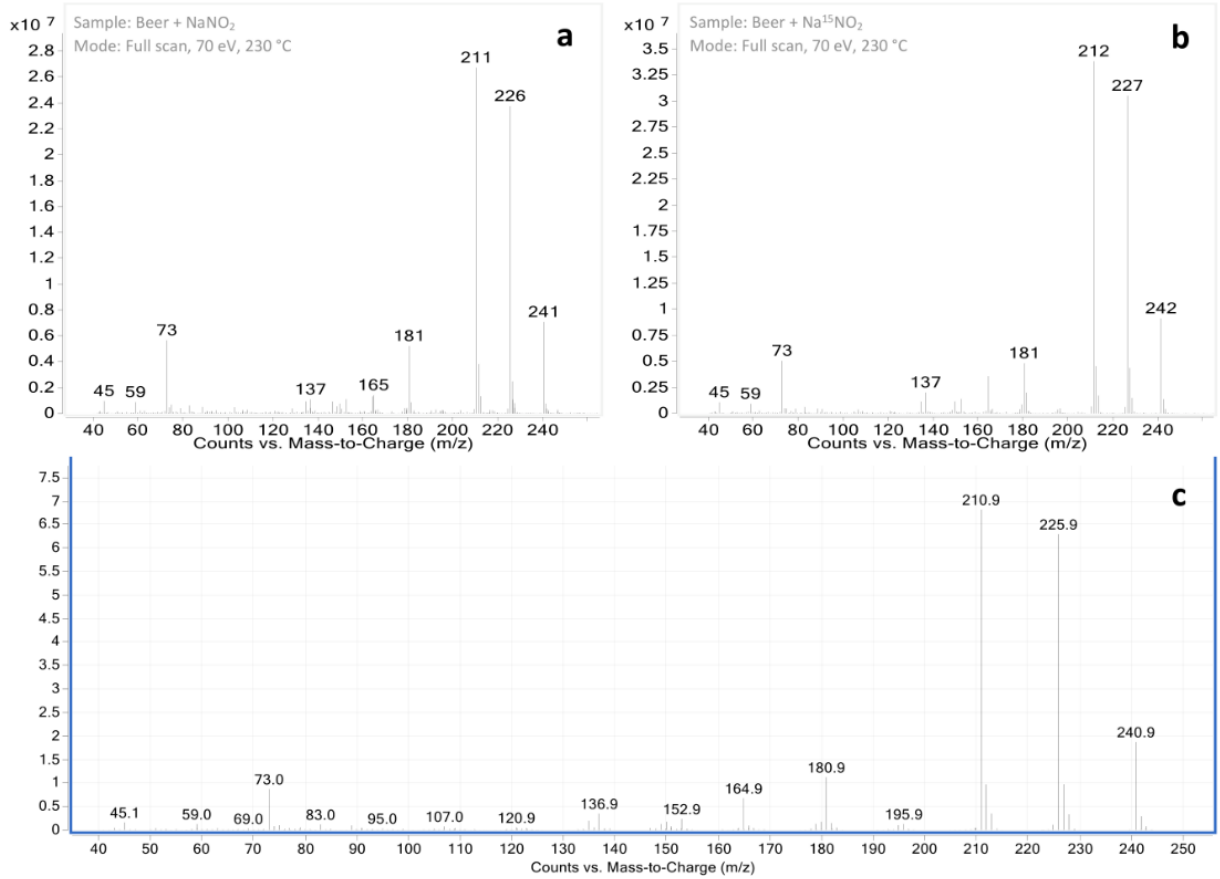

Figure S6: MS spectra of the peak **10** (**a**) and the same peak in the isotopic experiment (**b**). MS spectrum of the product from the vanillic acid with the nitrite reaction (**c**), copied from the previous study. [2]

Table S2: Remaining unidentified peaks and their best match results of MS spectra comparison with the reference library

No.	RT [min]	MW [g/mol]	RI_{exp}	Best match compound in NIST 14 MS Library	Match Factor (%)	CAS	MW [g/mol]	RI_{lib} [b]	RI_{predl} [a]
1	8.6	183	1116	1,2-butanediol, 2x TMS	69.6	1000099-91-9	234	-	1084
4	13.5	212	1408	5-nitroisophthaloyl dichloride	56.4	13438-30-7	247	-	1828
8	17.4	239	1627	4-nitrobenzoic acid, 1x TMS	76.6	1000373-27-8	239	1617	1679
9	17.7	218	1655	5H-oxazolo[3,2-a]pyridine-8-carbonitrile, 6-ethyl-2,3-dihydro-2,7-dimethyl-5-oxo-	78.8	1000337-58-3	218	-	1874
11	20.5	306	1821	4-[[4-[(4-methoxyphenyl)amino]phenyl]amino]phenol	51.5	1000397-62-8	306	-	3209
12	21.3	269	1866	benzoic acid, 2-[(2,3-dimethylphenyl)amino]-, methyl ester	60.5	1222-42-0	255	-	2272
13	22.1	327	1912	methyl 3,5-dihydroxybenzoate, 2TMS derivative	66.3	27798-59-0	312	-	1687
14	23.0	286	1972	4-[2-(4-methoxyphenyl)ethenyl]-2-nitrophenol	71.2	1000396-99-6	271	-	2566
15	23.2	341	1981	benzoic acid, 4,4'-(1,2-ethanediyl)biS, diethyl ester	57.8	1000402-36-8	326	-	2594
16	24.6	357	2082	9,10-anthracenedione, 1-(methylamino)-4-[(4-methylphenyl)amino]-	67.3	128-85-8	342	-	3287
17	25.9	443	2189	1,6-dihydroxy-8-methoxy-3-methylanthraquinone, 2x TMS	75.2	91701-23-4	428	-	2908
18	26.2	389	2209	2,3-bis(2-ethoxyethoxy)-5,8-quinoxalinediyl diacetate	44.6	2452-34-8	422	-	2987
19	26.4	443	2230	3-[Tris(hydroxymethyl)methylamino]-1-propanesulfonic acid, 4x TMS	49.3	1000366-67-9	531	-	2330

a – predicted by the DeepRel (Vrzal, 2021); b – obtained from NIST 14 Library (semi-standard non-polar)

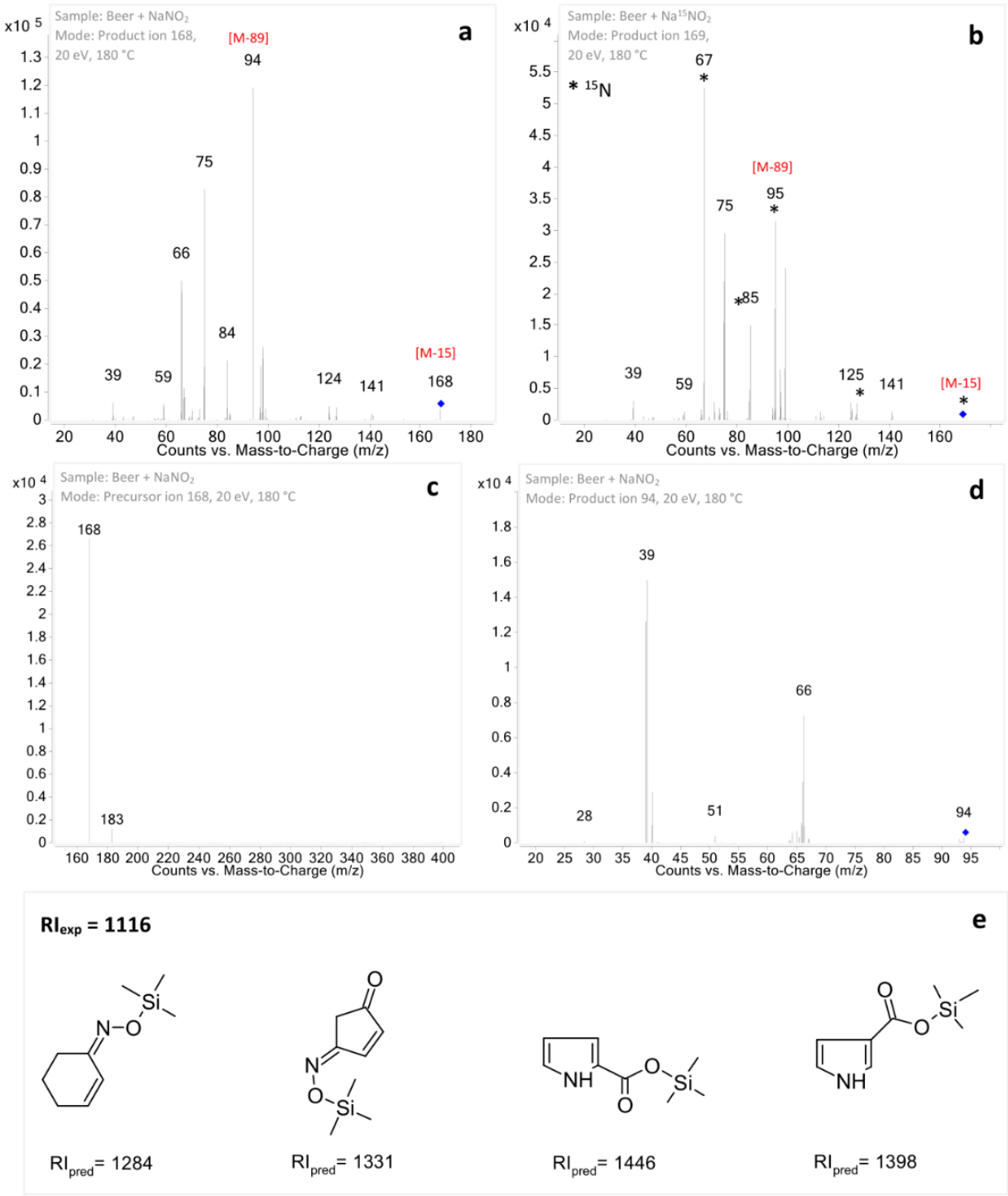

Figure S7: Product ion spectra of *m/z* 168 (**a**) and *m/z* 169 in the isotopic experiment (**b**) of the peak **1**; fragments bearing ^{15}N are highlighted by asterisk. The precursor ion spectrum of *m/z* 168 (**c**) and product ion spectrum of *m/z* 94 (**d**). Comparison of peak's experimental RI and predicted RIs of proposed structures (**e**).

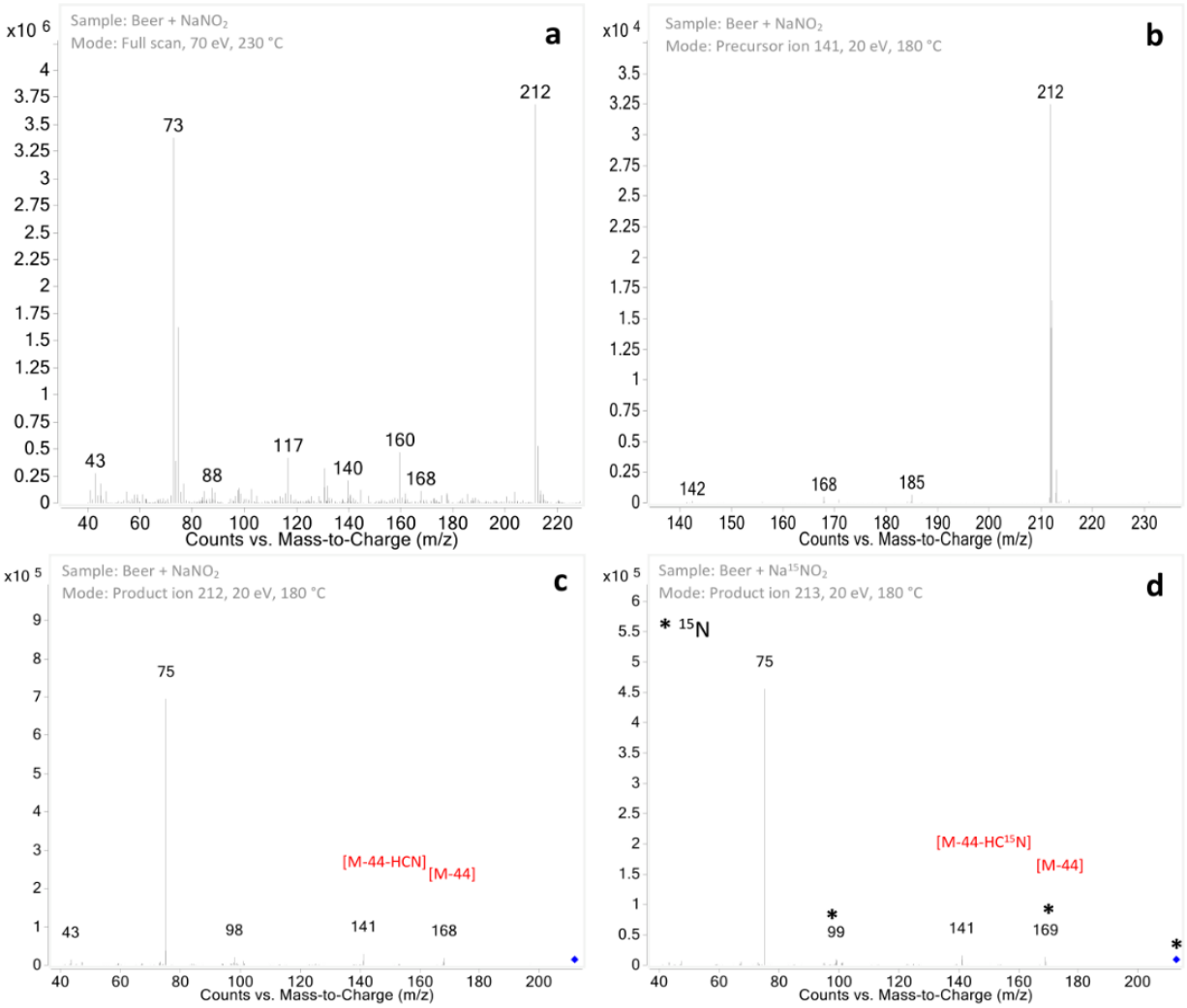

Figure S8: MS spectrum of the peak **4** (**a**) and precursor ion spectrum of *m/z* 212 (**b**). The product ion spectra of *m/z* 212(**c**) and *m/z* 213 in the isotopic experiment (**d**) of the same peak. Fragments bearing ^{15}N are highlighted by asterisk.

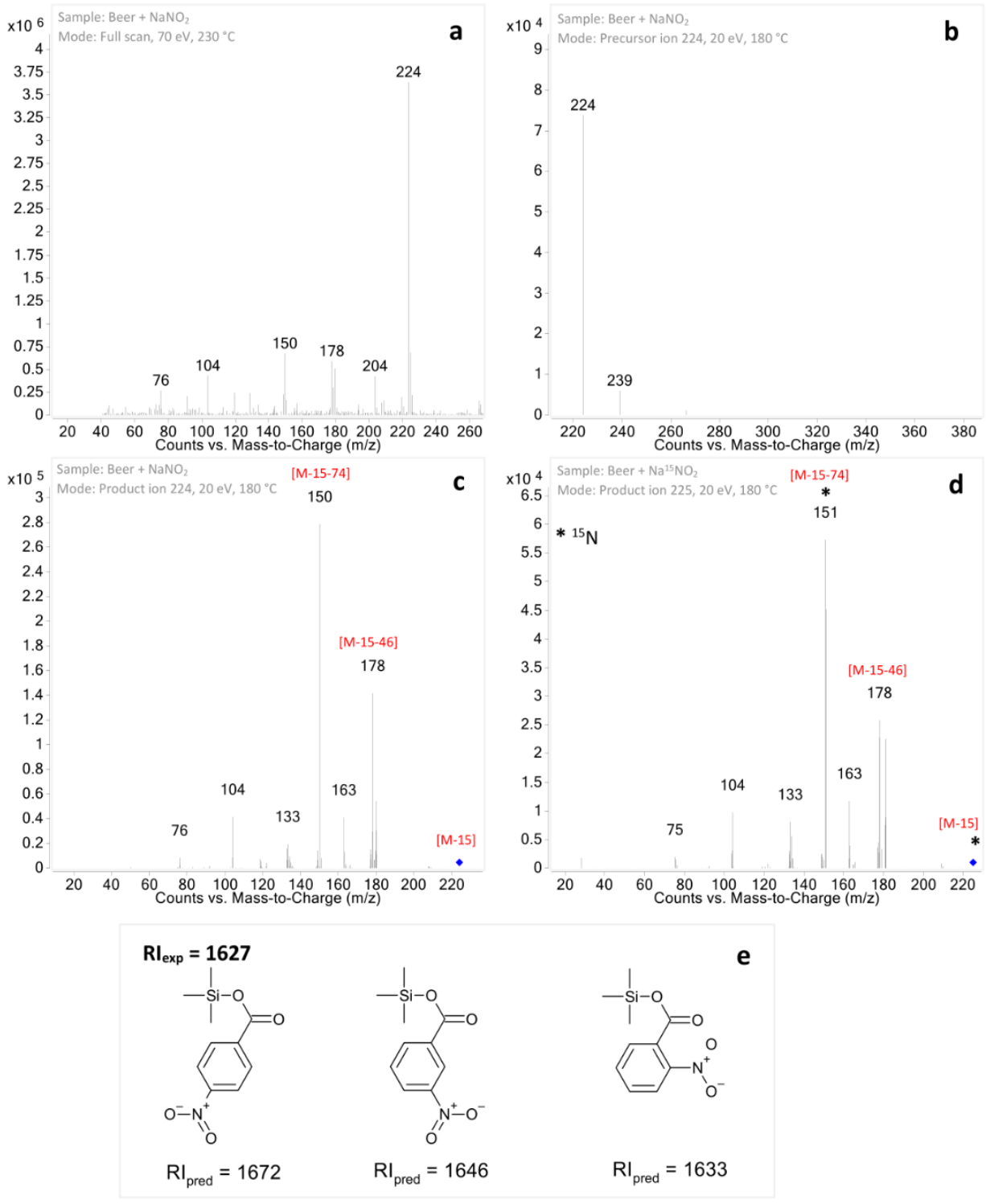

Figure S9: MS spectrum of the peak **8** (**a**) and precursor ion spectrum of *m/z* 224 (**b**). Product ion spectra of *m/z* 224 (**c**) and *m/z* 225 in the isotopic experiment (**d**) of the same peak. Comparison of peak's experimental RI and predicted RIs of proposed structures (**e**). Fragments bearing ^{15}N are highlighted by asterisk.

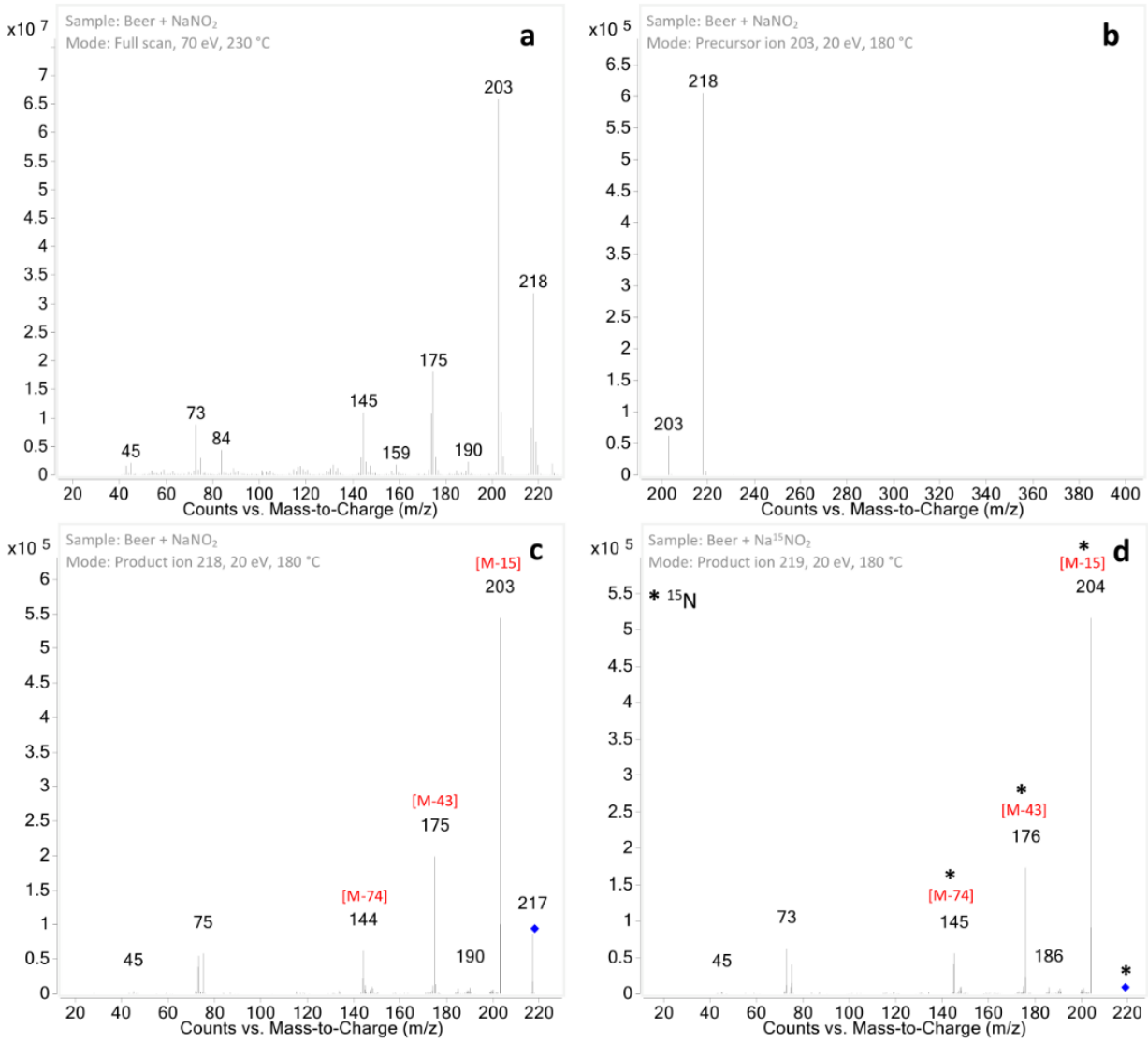

Figure S10: MS spectrum of the peak **9** (**a**) and precursor ion spectrum of *m/z* 203 (**b**). Product ion spectra of *m/z* 218 (**c**) and *m/z* 219 in the isotopic experiment (**d**) of the same peak. Fragments bearing ^{15}N are highlighted by asterisk.

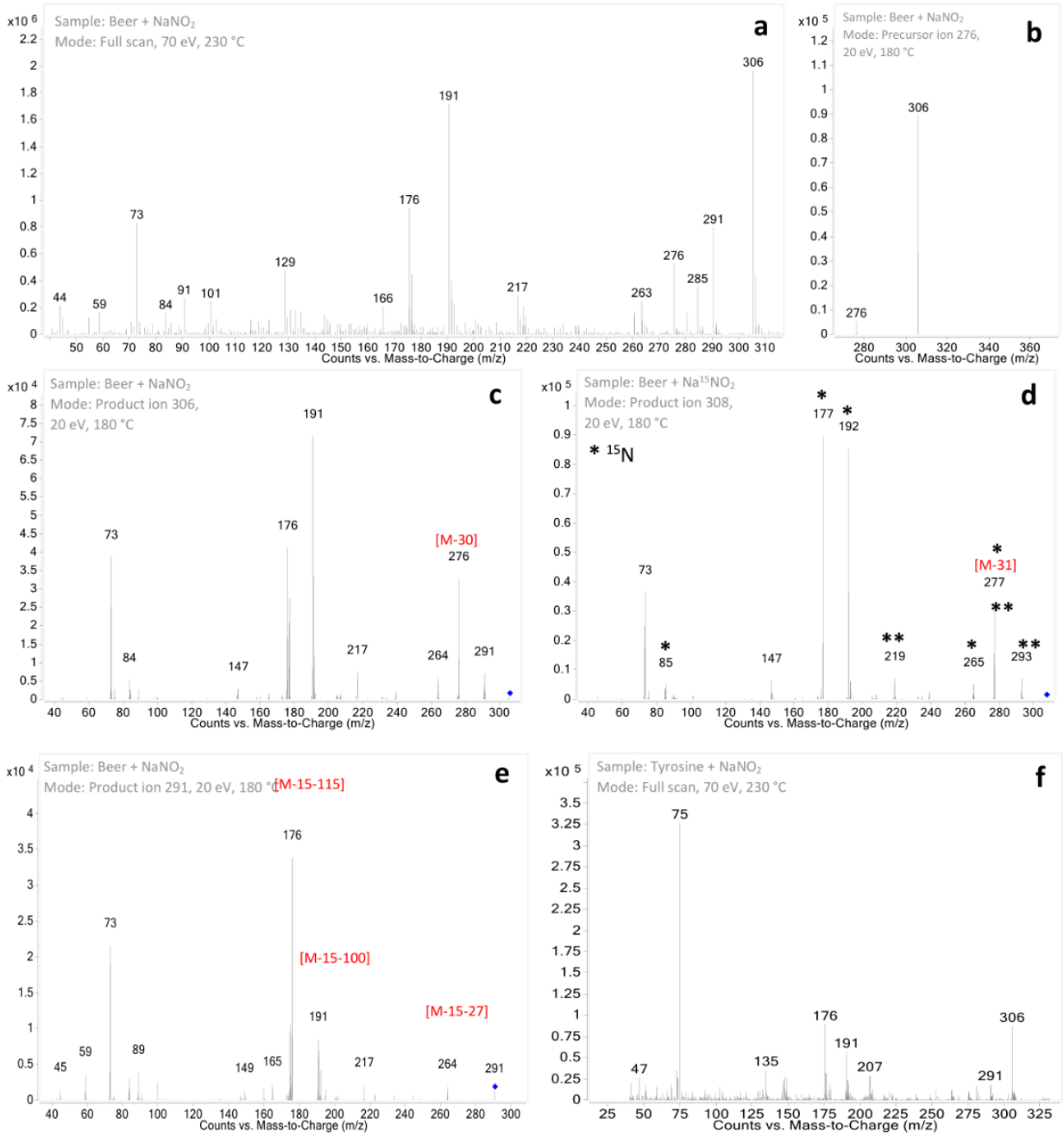

Figure S11: MS spectrum of the peak **11** (**a**) and precursor ion spectrum of *m/z* 276 (**b**). Product ion spectra of *m/z* 306 (**c**), *m/z* 308 in the isotopic experiment (**d**), and *m/z* 291 (**e**) of the same peak. MS spectrum of the product from tyrosine with the nitrite reaction (**f**). Fragments bearing ^{15}N are highlighted by asterisk.

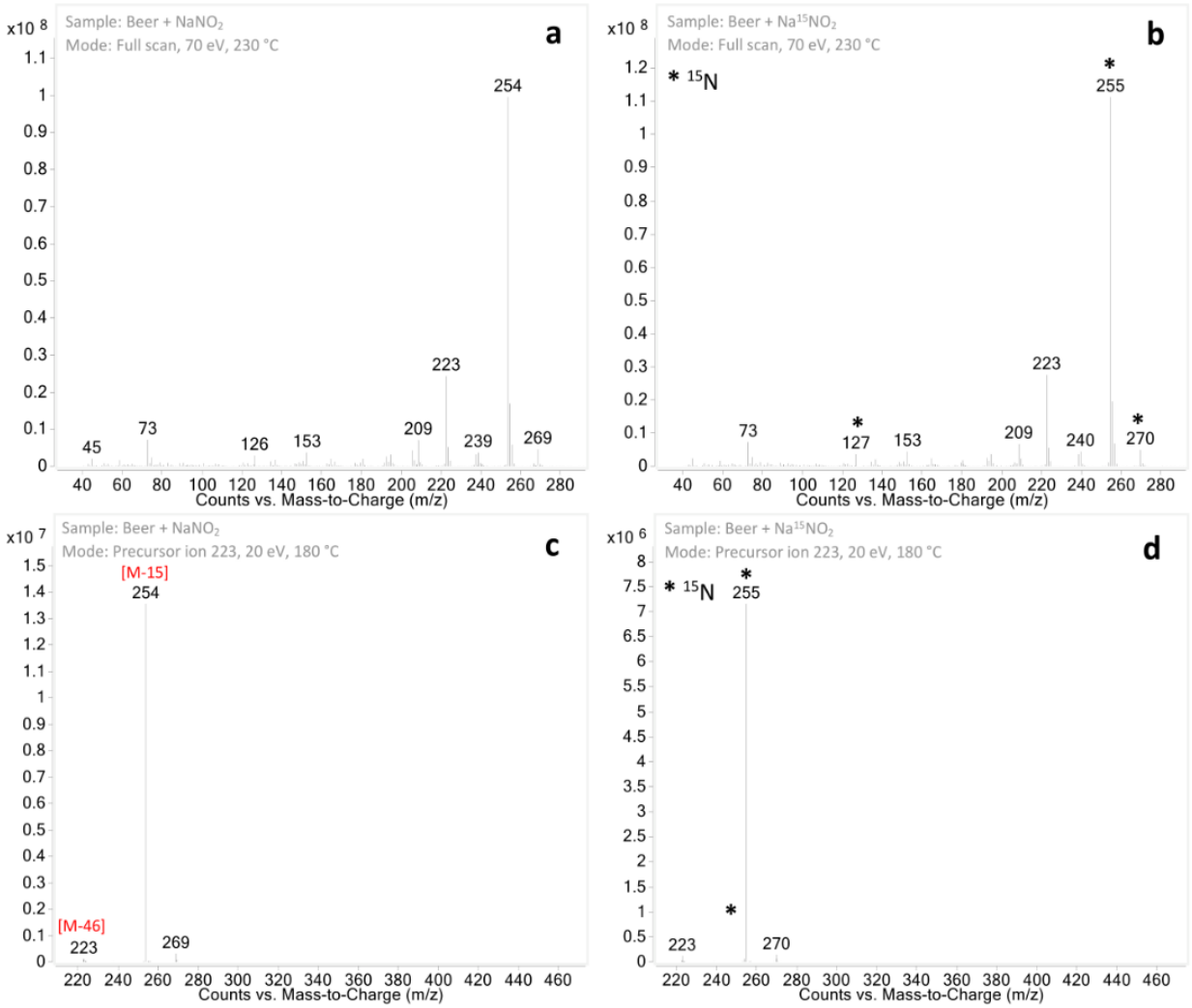

Figure S12: MS spectra of the peak **12** (**a**) and the same peak in the isotopic experiment (**b**). Precursor ion spectra of *m/z* 223 (**c**) and *m/z* 223 in the isotopic experiment (**d**) of the same peak. Fragments bearing ^{15}N are highlighted by asterisk.

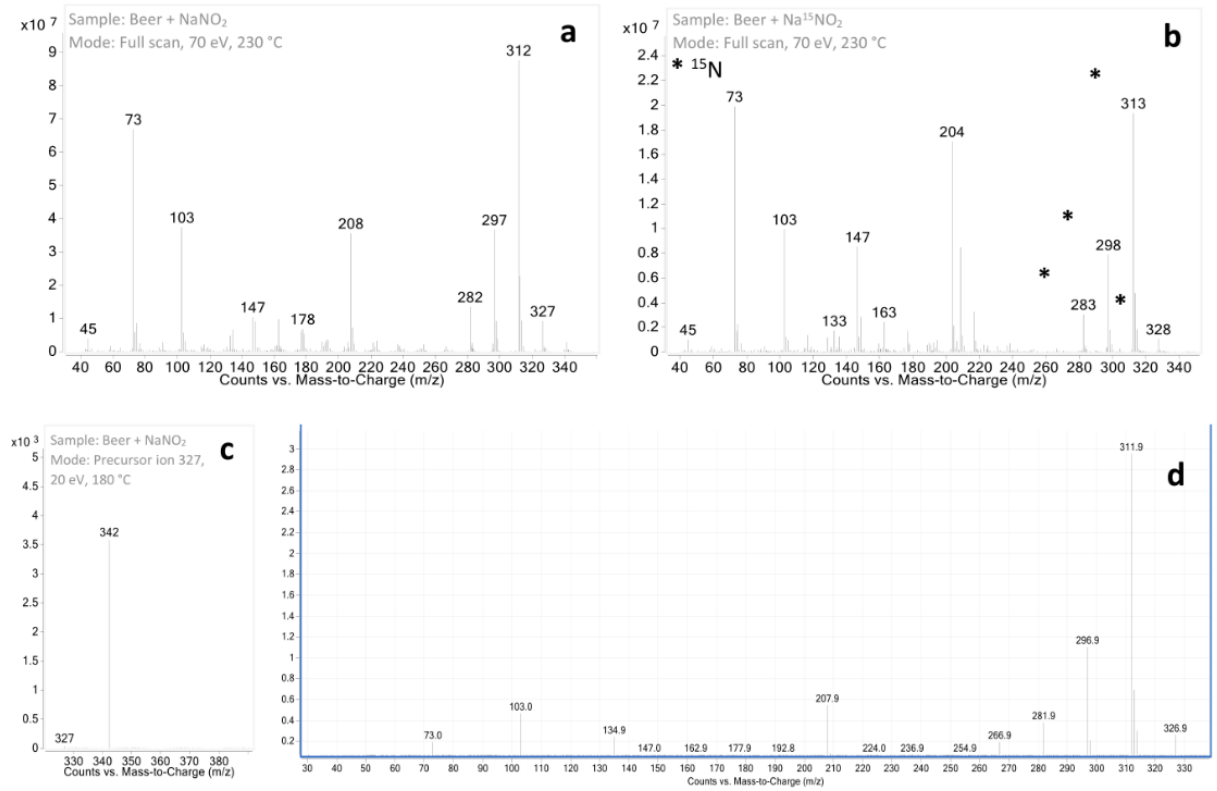

Figure S13: MS spectra of the peak **13** (**a**) and the same peak in the isotopic experiment (**b**). Precursor ion spectrum of *m/z* 223 (**c**) and MS spectrum of the peak at 18.3 min found in artificially nitrosated beer (**d**). [1] Fragments bearing ^{15}N are highlighted by asterisk.

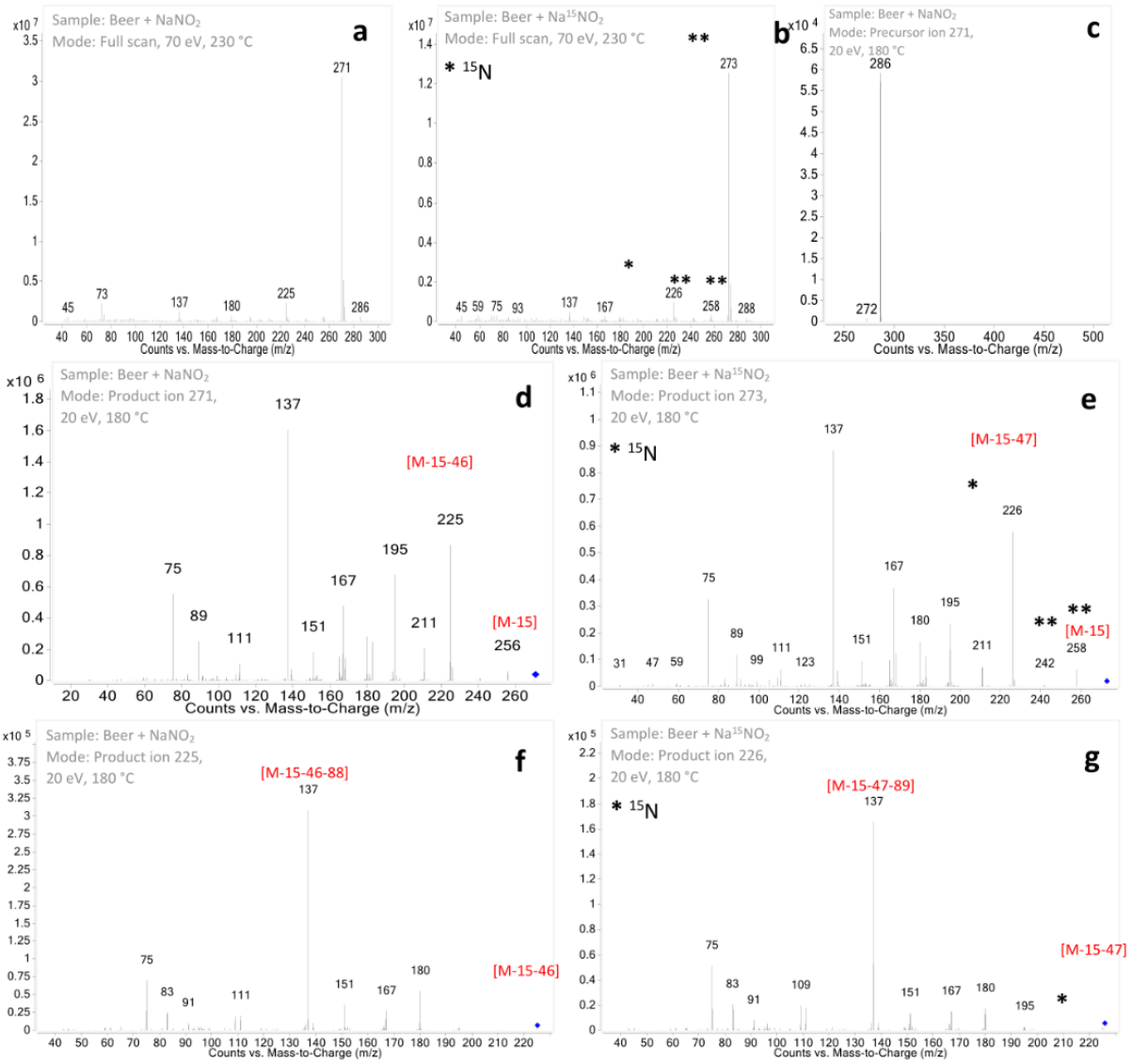

Figure S14: MS spectra of the peak **14** (**a**) and the same peak in the isotopic experiment (**b**). Precursor ion spectrum of *m/z* 271 (**c**), product ion spectra of *m/z* 271 (**d**), *m/z* 273 in the isotopic experiment (**e**), *m/z* 225 (**f**), and *m/z* 226 in the isotopic experiment (**g**). Fragments bearing ^{15}N are highlighted by asterisk.

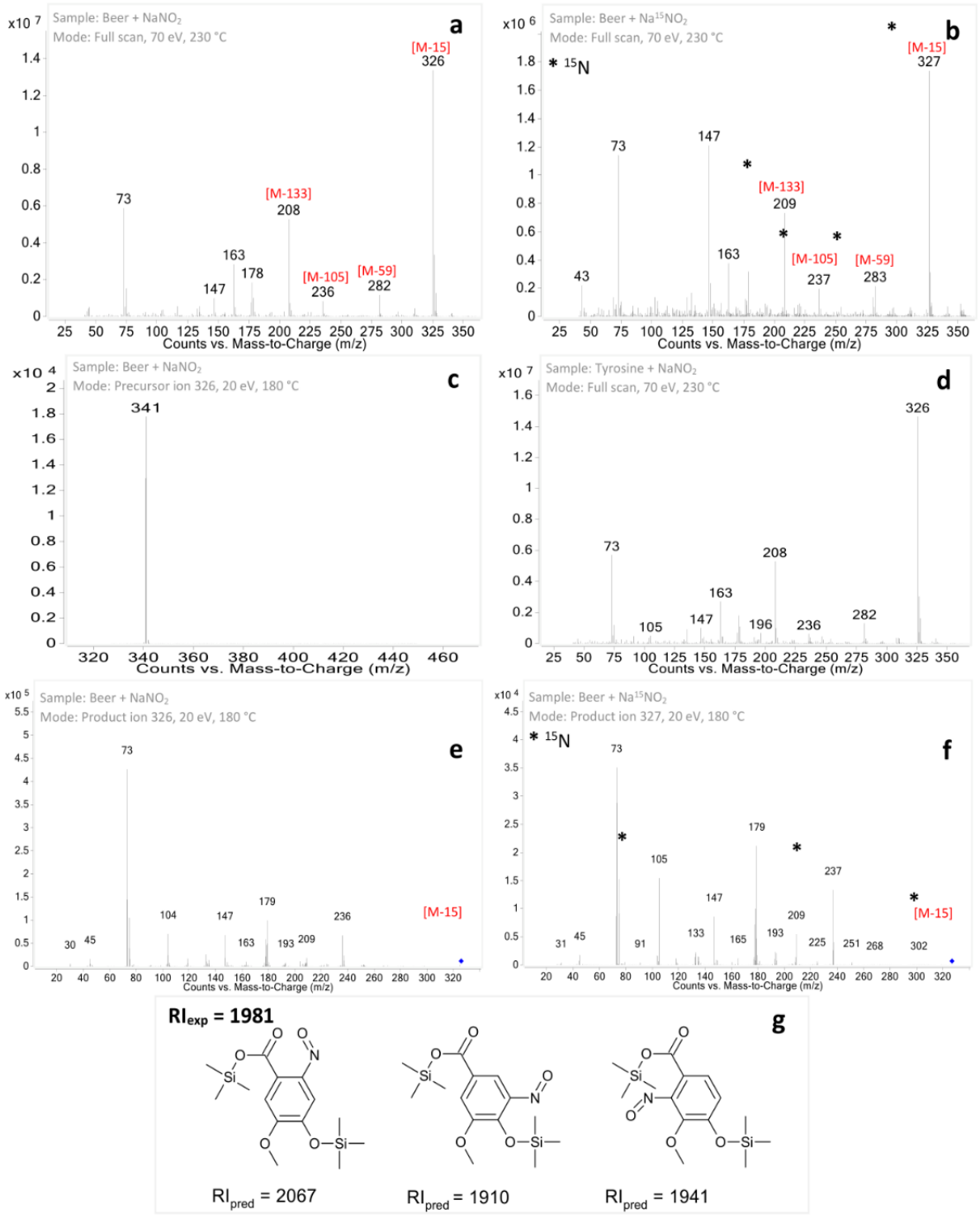

Figure S15: MS spectra of the peak **15** (**a**) and the same peak in the isotopic experiment (**b**). Precursor ion spectrum of *m/z* 326 (**c**), and MS spectrum of the product from tyrosine with the nitrite reaction (**d**). Product ion spectra of *m/z* 326 (**e**) and *m/z* 327 in the isotopic experiment (**f**). Comparison of peak's experimental RI and predicted RIs of proposed structures (**g**). Fragments bearing ^{15}N are highlighted by asterisk.

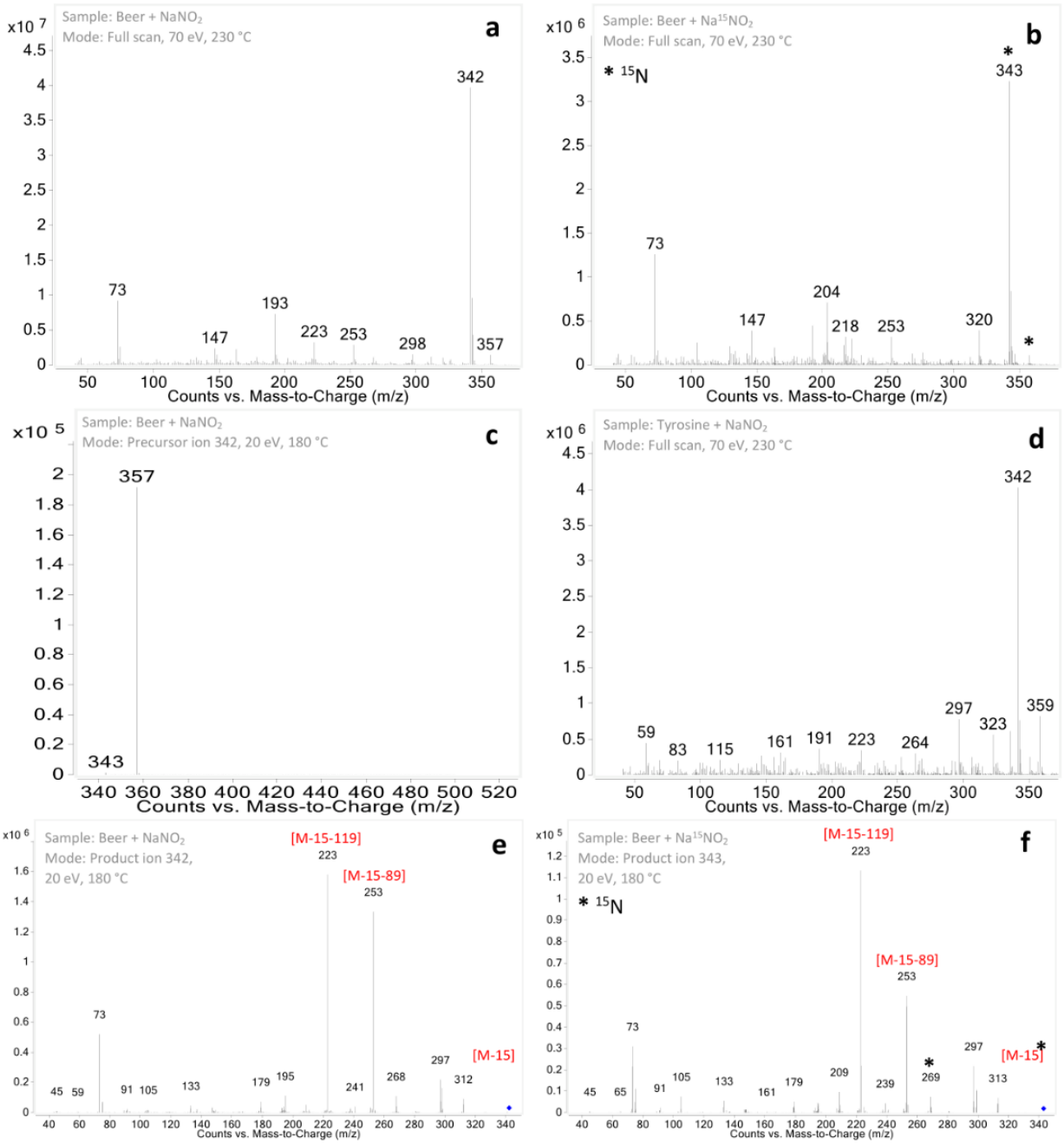

Figure S16: MS spectra of the peak **16** (**a**) and the same peak in the isotopic experiment (**b**). The precursor ion spectrum of *m/z* 342 (**c**), and MS full scan spectrum of the product from tyrosine with the nitrite reaction (**d**) of the same peak. Product ion spectra of *m/z* 342 (**e**) and *m/z* 343 in the isotopic experiment (**f**). Fragments bearing ^{15}N are highlighted by asterisk.

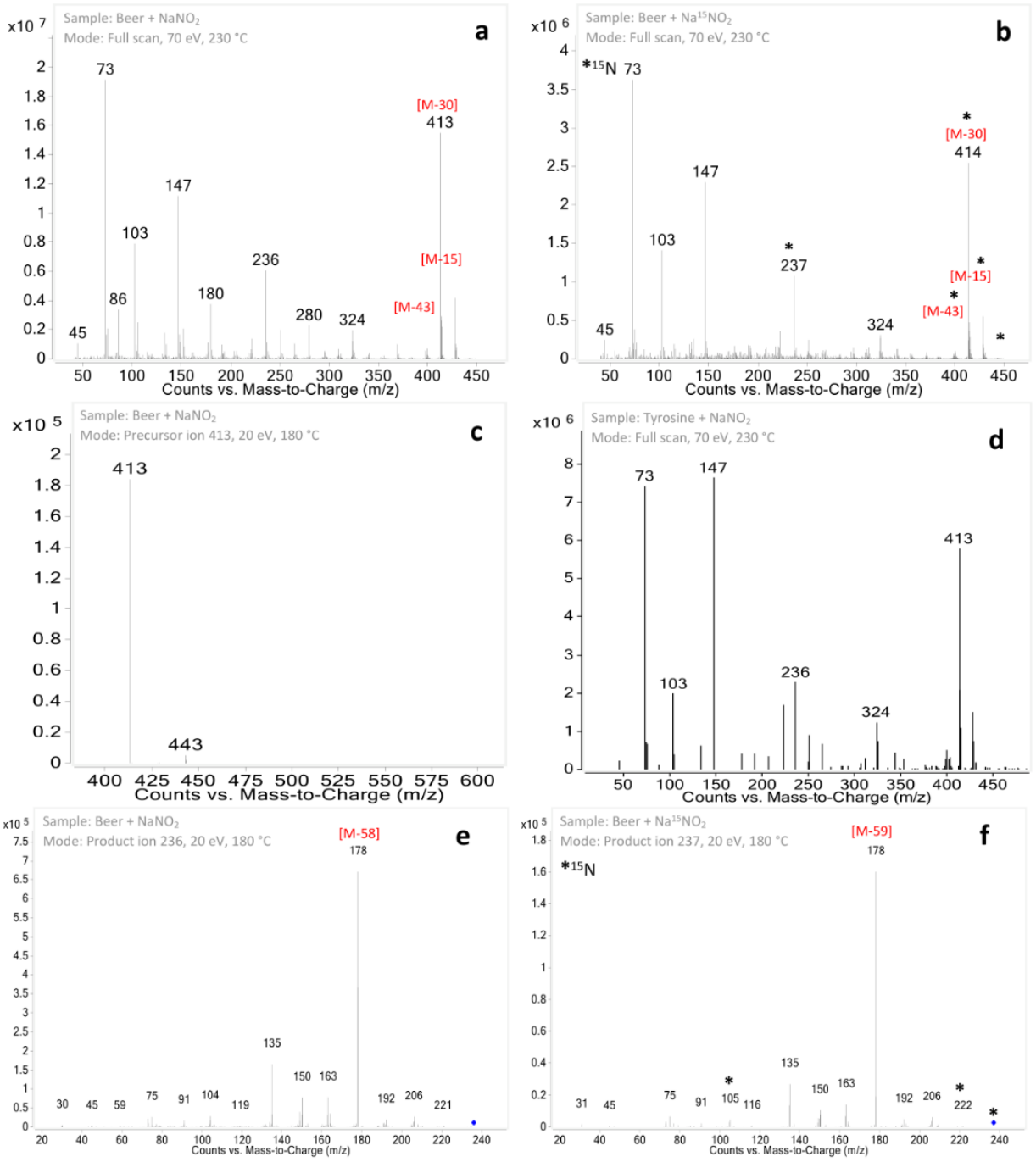

Figure S17: MS spectra of the peak **17** (**a**) and the same peak in the isotopic experiment (**b**). The precursor ion spectrum of *m/z* 413 (**c**), and MS spectrum of the product from tyrosine with the nitrite reaction (**d**) of the same peak. Product ion spectra of *m/z* 236 (**e**) and *m/z* 237 in the isotopic experiment (**f**). Fragments bearing ^{15}N are highlighted by asterisk.

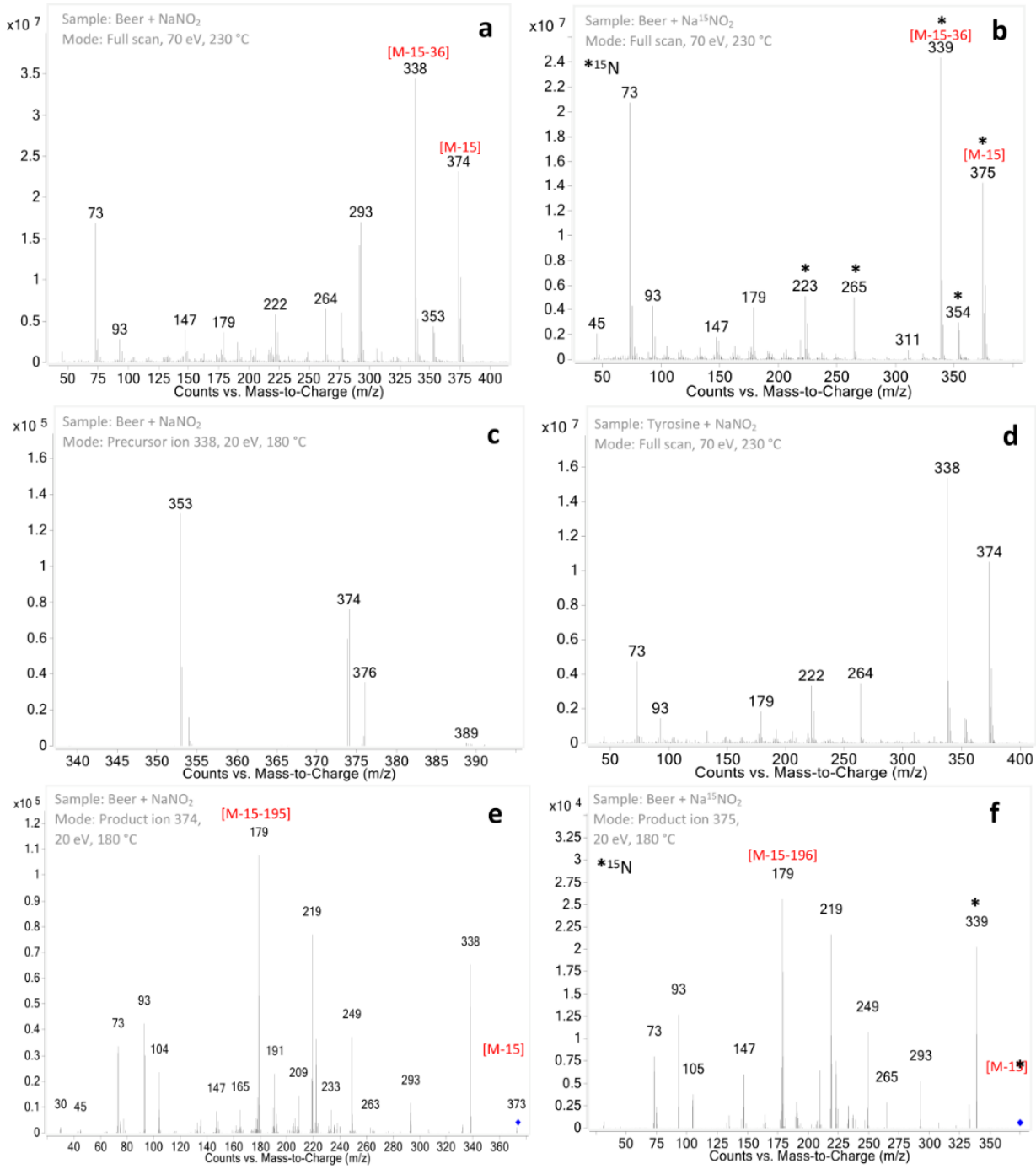

Figure S18: MS spectra of the peak **18** (**a**) and the same peak in the isotopic experiment (**b**). Precursor ion spectrum of *m/z* 338 (**c**), and MS spectrum of the product from tyrosine with the nitrite reaction (**d**). Product ion spectra of *m/z* 374 (**e**), and *m/z* 375 in the isotopic experiment (**f**) of the same peak. Fragments bearing ^{15}N are highlighted by asterisk.

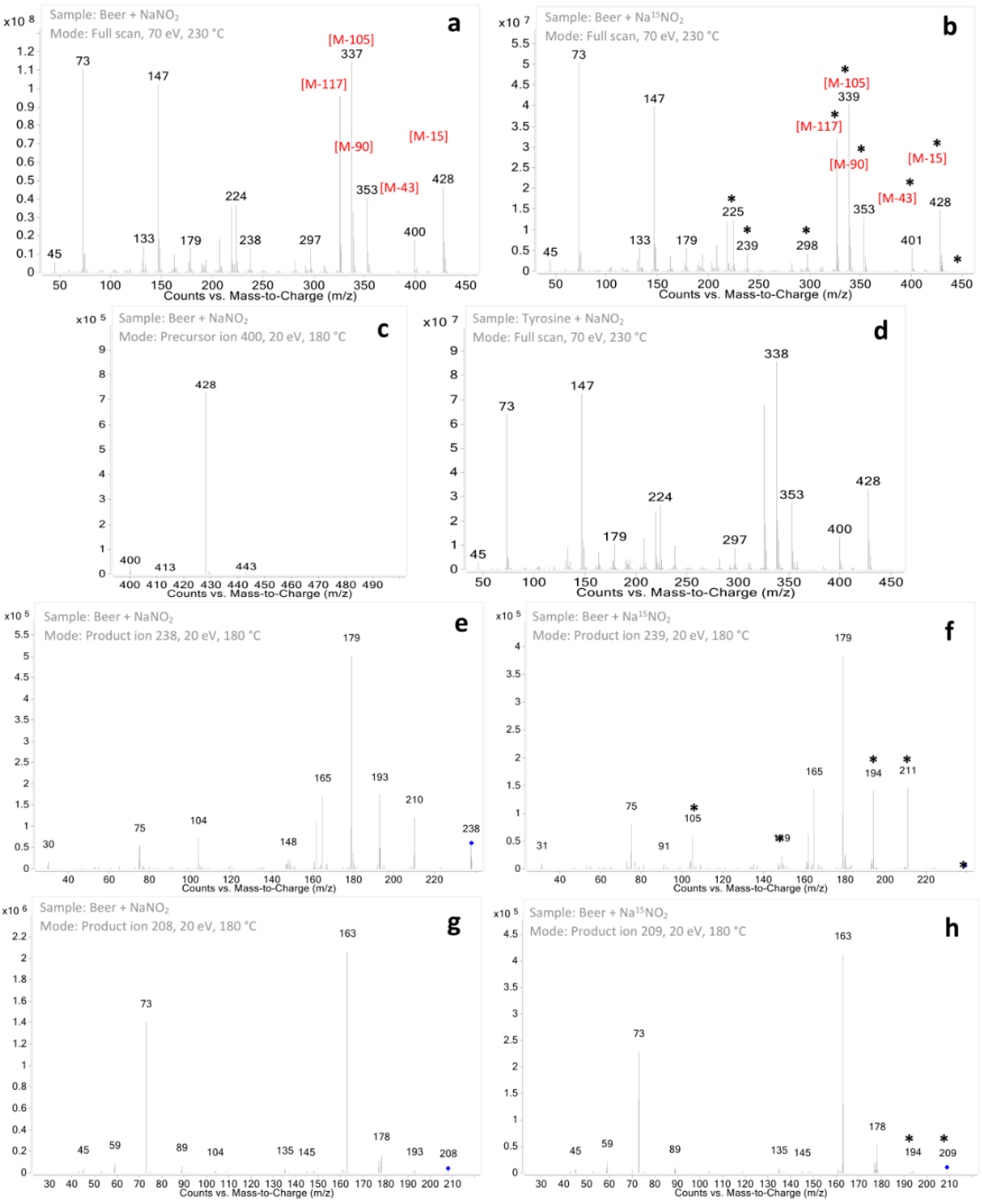

Figure S19: MS spectra of the peak **19** (**a**) and the same peak in the isotopic experiment (**b**). Precursor ion spectrum of *m/z* 400 (**c**), and MS spectrum of the product from tyrosine with the nitrite reaction (**d**). Product ion spectra of *m/z* 238 (**e**), *m/z* 239 in the isotopic experiment (**f**), *m/z* 208 (**g**), and *m/z* 209 in the isotopic experiment (**h**) of the same peak. Fragments bearing ^{15}N are highlighted by asterisk.

3. Reaction products of nitrite with standard compounds

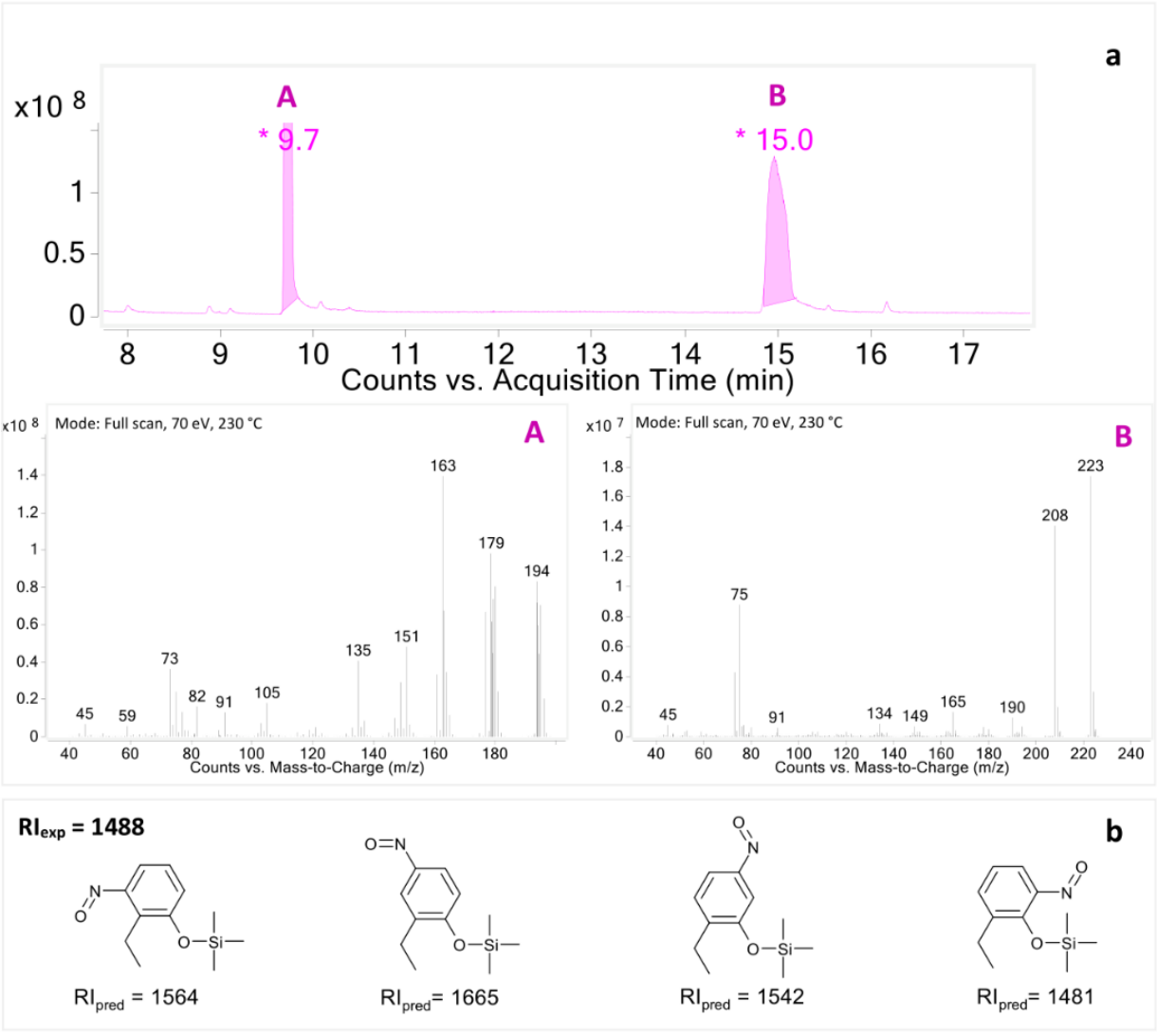

Figure S20: Chromatogram of the 2-ethyl phenol after the reaction with sodium nitrite and MS spectra of the reaction products. Comparison of peak's experimental RI and predicted RIs of proposed structures.

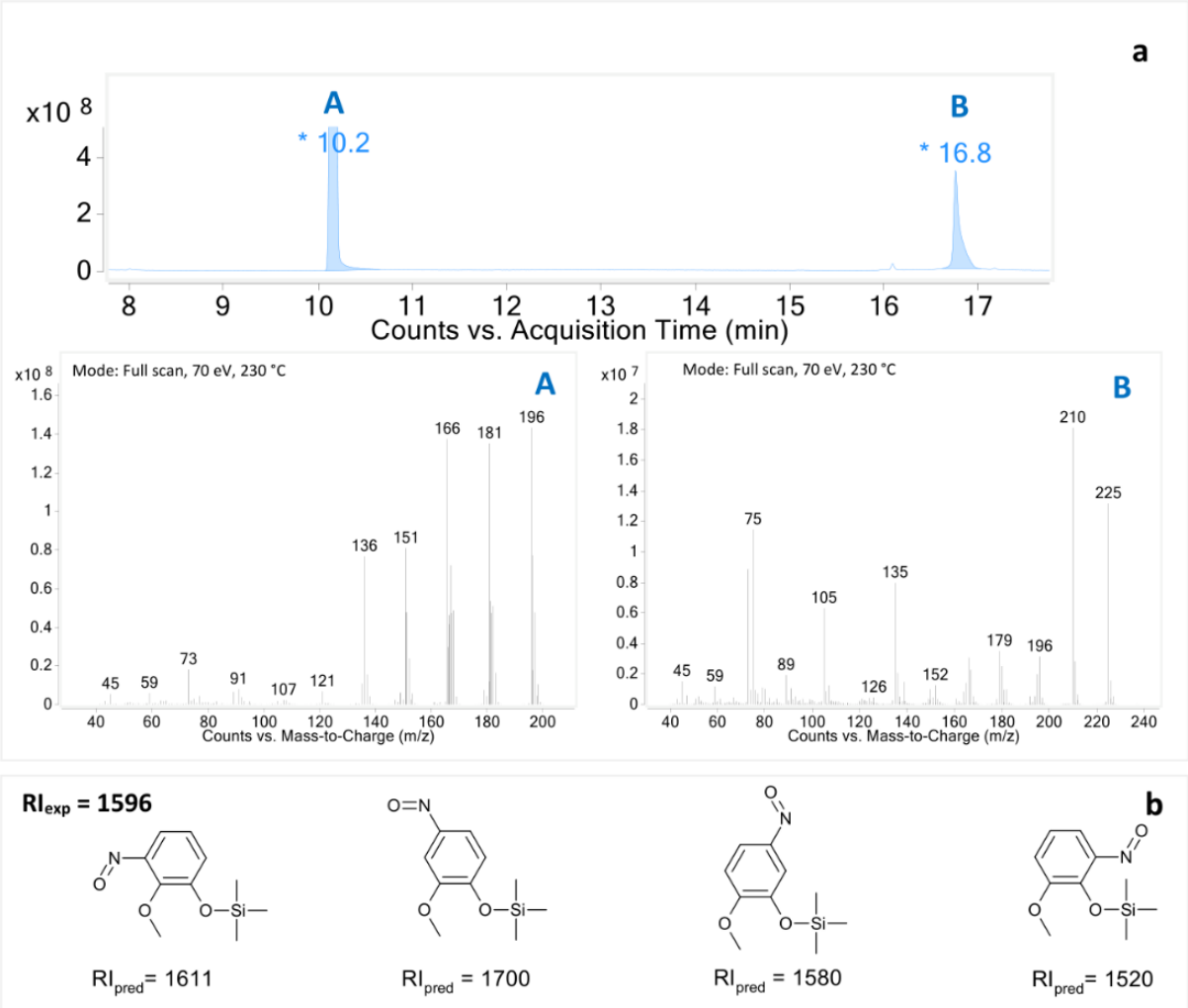

Figure S21: Chromatogram of the guaiacol after the reaction with sodium nitrite and MS spectra of the reaction products. Comparison of peak's experimental RI and predicted RIs of proposed structures.

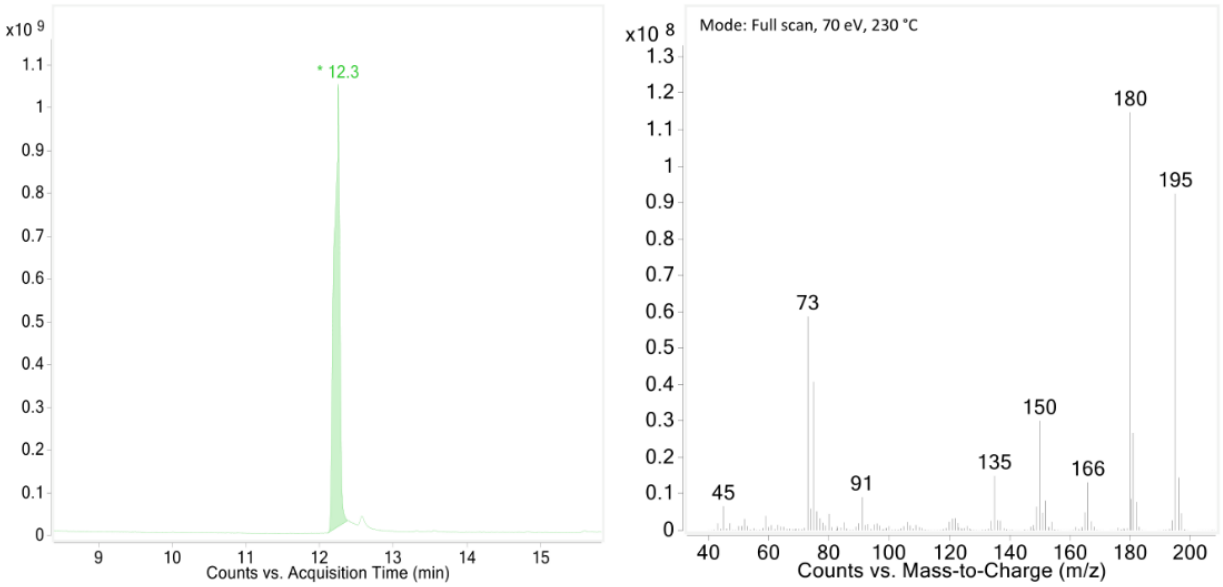

Figure S22: Chromatogram of 4-nitroso phenol tri(methyl)silyl ether and its MS spectrum.

4. Semi-quantitative determination of the products in commercial beers

Table S3: List of beers used for primary monitoring of the identified products

No.	Origin	Type of beer	Brewery type
A	Czech	Lager beer	Industrial brewery
B	Czech	Lager beer	Industrial brewery
C	Czech	Premium lager	Industrial brewery
D	Czech	Special beer 14°	Industrial brewery
E	Czech	Mid-dark lager	Microbrewery
F	Czech	Lager beer	Microbrewery
G	Czech	Lager beer	Industrial brewery
H	Czech	Lager beer	Industrial brewery
I	USA	IPA	Industrial brewery
J	GB	Lager beer	Microbrewery
K	Belgium	Red ALE	Industrial brewery
L	Czech	Mosaic ALE	Homebrewer
M	Mexico	Amber ALE	Microbrewery
N	Czech	White IPA	Homebrewers
0	Czech	Lager beer	Microbrewery
P	Czech	Lager beer	Microbrewery

Table S4: List of monitored compounds, supplemented by MRM transitions at optimal collision energies.

RT [min]	MW [g/mol]	Identity name	Precursor Ion *m/z*	Product Ion *m/z*	CE [eV]
8.6	183	unknown	168	94	15
12.5	195	4-nitrosophenol	195	180	5
13.3	191	4-cyanophenol. TMS	191	176	10
13.5	212	unknown	212	168	5
13.7	172	N-nitrosoproline ethylester	172	99	10
14.7	216	N-nitrosoproline . TMS	201	157	5
15.6	230	unknown	200	156	5
17.0	225	nitrosoguaiacol. TMS	225	210	10
17.4	239	unknown	224	150	15
17.7	310	phenylalanin-1-^{13}C (IS). TMS	295	205	15
17.7	218	unknown	218	203	10
18.2	241	2-methoxy-5-nitrophenol. TMS	226	211	10
20.5	306	unknown	306	191	15
21.3	269	unknown	254	223	15
22.1	327	unknown	312	179	30
23.0	286	unknown	271	137	25
23.2	341	unknown	326	236	10
24.6	357	unknown	342	223	25
25.9	443	unknown	413	236	15
26.2	389	unknown	338	219	25
26.4	443	unknown	338	219	25

Table S5: Semi-quantitation results of the products in beer samples

	Cpd No.	1	-	3	4	5	6	7	-	8	9	10	11	12	13	14	15	16	17	18	19
	RT [min]	8.6	12.3	13.3	13.5	13.7	14.7	15.6	16.8	17.4	17.7	18.2	20.5	21.3	22.1	23.0	23.2	24.6	25.9	26.2	26.4
Beer sample	A	51.77	0.04	5.32	0.29	0.03	0.18	0.32	0.20	0.02	0.14	1.70	-	0.25	91.63	0.02	2.96	0.36	-	-	-
	B	21.04	-	12.63	0.35	0.13	0.63	0.40	0.37	-	0.21	1.39	0.01	0.23	-	0.03	2.87	0.56	-	-	0.33
	C	-	-	18.46	0.45	0.07	0.29	0.43	0.32	-	0.16	1.31	0.01	0.44	-	-	5.18	0.47	0.01	-	0.54
	D	23.73	-	5.10	0.36	-	0.18	0.19	0.39	-	0.44	1.43	-	0.45	-	-	1.84	0.62	-	-	0.13
	E	16.26	0.38	8.37	0.78	0.05	0.32	1.35	1.53	0.26	0.66	4.46	-	1.14	-	0.06	3.33	0.73	-	-	0.51
	F	12.16	-	2.57	0.33	0.05	0.10	0.27	0.91	0.09	0.26	3.12	-	0.57	82.38	-	1.87	0.37	-	-	0.43
	G	21.77	-	10.72	0.71	0.05	0.38	0.33	0.43	0.07	0.93	3.58	-	0.63	-	-	3.17	1.25	-	-	0.17
	H	13.80	-	24.85	0.42	-	0.20	0.60	0.81	0.10	0.62	3.40	-	0.65	-	-	4.29	0.41	-	-	0.31
	I	20.27	0.14	8.38	0.23	0.03	1.96	0.23	0.25	-	0.12	6.29	0.01	0.40	68.17	-	2.17	0.46	-	0.18	0.16
	J	11.87	0.04	3.10	0.30	-	0.10	0.11	0.13	0.04	0.06	2.01	-	0.50	88.46	-	3.13	0.18	-	-	-
	K	21.00	-	2.09	1.38	-	0.06	0.27	0.06	0.04	0.21	1.11	-	0.15	61.76	-	1.26	0.19	-	-	0.45
	L	12.62	0.07	3.93	0.36	0.04	0.16	0.16	0.53	-	0.35	6.65	-	1.80	-	0.03	1.23	2.09	-	-	0.32
	M	-	0.41	8.14	0.64	0.03	0.25	0.85	0.88	0.09	0.35	3.70	-	1.23	95.74	-	2.66	0.27	-	-	0.26
	N	22.74	0.09	3.96	0.32	0.04	0.23	0.21	0.71	-	0.22	6.25	-	0.90	-	0.04	1.88	1.37	-	-	0.70
	O	27.53	-	15.16	0.78	0.07	0.24	0.62	0.39	-	0.20	3.50	-	1.57	-	0.08	12.19	0.49	0.02	0.32	1.06
	P	24.80	-	6.82	0.88	0.07	0.69	0.47	0.40	0.03	0.15	3.84	-	0.85	-	-	4.31	0.61	0.04	-	0.95

Levels are represented by relative units (RU), where values corresponding to the peaks with responses lower than the internal standard response are non-colored. Peaks with higher responses than the internal standard response are colored as follows: 1 -10 RU (yellow), 10 - 50 RU (blue), and ≥ 50 RU (red).

References

(1) Vrzal, T.; Olšovská, J. Pyrolytic profiling nitrosamine specific chemiluminescence detection combined with multivariate chemometric discrimination for non-targeted detection and classification of nitroso compounds in complex samples. *Anal. Chim. Acta* **2019**, *1059* (1), 136-145

(2) Vrzal, T.; Malečková, M.; Olšovská, J. DeepReI: Deep learning-based gas chromatographic retention index predictor. *Anal. Chim. Acta* **2021**, *1147*, 64-71

Appendix 4

Supporting Information

for publication

Natural Occurrence of Nitrite-Related Compounds in Malt and Beer

Michaela Malečková[1,2], Tomáš Vrzal[1,*], Tomáš Vaško[3], Jana Olšovská[1], Jana Sobotníková[2]

[1] Research Institute of Brewing and Malting, Lípová 511/15, 120 00, Prague, Czech Republic

[2] Charles University, Faculty of Science, Department of Analytical Chemistry, Albertov 6, 128 43, Prague, Czech Republic

[3] Czech University of Life Sciences Prague, Faculty of Agrobiology, Food and Natural Resources, Department of Chemistry, Kamýcká 129, 165 00, Prague, Czech Republic

[*]Corresponding author: tomas.vrzal@beerresearch.cz

Table of content:

1. Materials and Methods – Additional Information

1.1 Nitrosation of Malt

Malt nitrosation by gaseous nitrogen oxides followed the previously published procedure:[1]

Approximately 50 g of whole malt grains were soaked in 10 ml water in a glass vessel. Nitrogen dioxide was generated in a separated flask filled with 50 ml of concentrated nitric acid. By slowly adding zinc plates, nitrogen dioxide was generated according to the following equation:

$$Zn + 4\,HNO_3 \rightarrow Zn(NO_3) + 2\,H_2O + 2\,NO_2$$

Generated gaseous nitrogen dioxide was driven towards a moisture malt, and the flask was closed. Schemes of apparatus for nitrosation at higher (**Scheme A**) and at room temperature (**Scheme B**) are shown below.[1] Samples were then treated as follows:

a) The closed flask was heated for 2 hours at approximately 40 °C to prepare malt treated at the higher temperature. Moist nitrosated malt was dried in an electric dryer at 80 °C for 2 hours. The drying temperature was chosen according to a typical kilning temperature of the most common Pilsen malt (80-90 °C).[2]

b) During the preparation of malt nitrosated at a lower temperature, the closed flask was left overnight at room temperature without light exposure. Then, the malt was dried in the electric dryer at 40 °C for 2 hours. The drying temperature was chosen according to a typical drying temperature of the barley or malt when used to decrease moisture content (40-50 °C).[2]

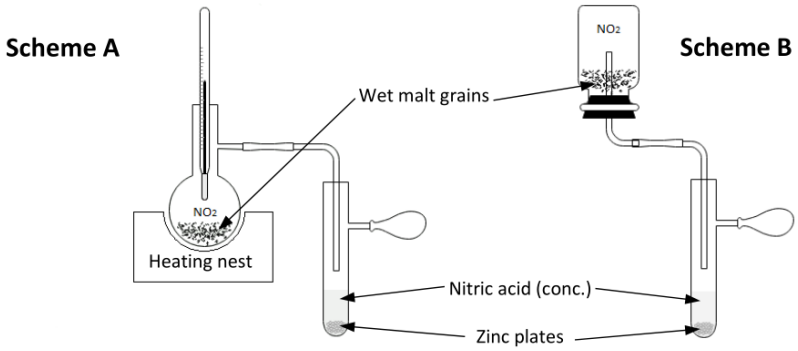

1.2 Preparation of congress wort

Nitrosated malt grains (10 g) were finely ground in an electric mixer. Homogenized malt powder (2 g) and 8 g of deionized water (45°C) were mixed and heated at 45°C for 30 min with occasional stirring. The heating temperature increased (1°C/min) to 70 °C, and 4 g of warm deionized water (70 °C) was added to the mash. The mash was kept at 70 °C for one hour with occasional stirring. The mash was cooled down for 10-15 min to reach laboratory temperature (20 °C), and freshwater was added to reach 18 g of the whole mixture. The mash was filtrated through a filtration paper with a yield of approximately 15 ml of congress wort.

Table S1. Conditions of multiple-reaction monitoring for N-products determination by GC-MS/MS.[3]

Sample ID	RT [min]	MW [g/mol]	Name of the product	Precursor Ion m/z	Product Ion m/z	CE [eV]
N-01	8.6	183	-	168	94	15
N-02	8.9	247	Pyruvic acid oxime, 2xTMS, isomer 1	204	131	25
N-03	9.1	247	Pyruvic acid oxime, 2xTMS, isomer 2	204	131	25
N-04	12.3	195	4-nitrosophenol, TMS	195	180	5
N-05	13.3	191	4-cyanophenol, TMS	191	176	10
N-06	13.5	212	-	212	168	5
N-07	13.7	172	N-nitrosoproline ethylester	172	99	10
N-08	14.7	216	N-nitrosoproline, TMS	201	157	5
N-09	15.6	230	N-nitrosopipecolic / N-nitrosopyroglutamic acid, TMS	200	156	5
N-10	16.8	225	nitrosoguaiacol, TMS	225	210	10
N-11	17.4	239	-	224	150	15
ISTD	17.7	310	Phenylalanine-1-^{13}C, TMS	295	205	15
N-12	17.7	218	-	218	203	10
N-13	18.2	241	2-methoxy-5-nitrophenol, TMS	226	211	10
N-14	20.5	306	-	306	191	15
N-15	21.3	269	-	254	223	15
N-16	22.1	327	-	312	179	30
N-17	23.0	286	-	271	137	25
N-18	23.2	341	-	326	236	10
N-19	24.6	357	-	342	223	25
N-20	25.9	443	-	413	236	15
N-21	26.2	389	-	338	219	25
N-22	26.4	443	-	338	219	25

1.3 R packages

RStudio: R Core Team (2020). R: A language and environment for statistical computing. R Foundation for Statistical Computing, Viena, Austria. URL. https://www.R-project.org/

Raivo Kolde (2019). **pheatmap**: Pretty Heatmaps. R package version 1.0.12. https://CRAN.R-project.org/package=pheatmap

Sebastien Le, Julie Josse, Francois Husson (2008). **FactoMineR**: An R Package for Multivariate Analysis. Journal of Statistical Software, 25(1), 1-18. 10.18637/jss.v025.i01

Alboukadel Kassambara and Fabian Mundt (2020). **factoextra**: Extract and Visualize the Results of Multivariate Data Analyses. R package version 1.0.7. https://CRAN.R-project .org/package =factoextra

Frank E Harrell Jr and Charles Dupont (2022). **Hmisc:** Harrell Miscellaneous. R package version 4.7-2. https://CRAN.R-project.org/package=Hmisc

Taiyun Wei, Viliam Simko, Michael Levy, Yihui Xie, et al. (2021). **corrplot:** Visualization of a Correlation Matrix. R package version 0.92. https://CRAN.R-project.org/package=corrplot

2. Results and Discussion – Additional information

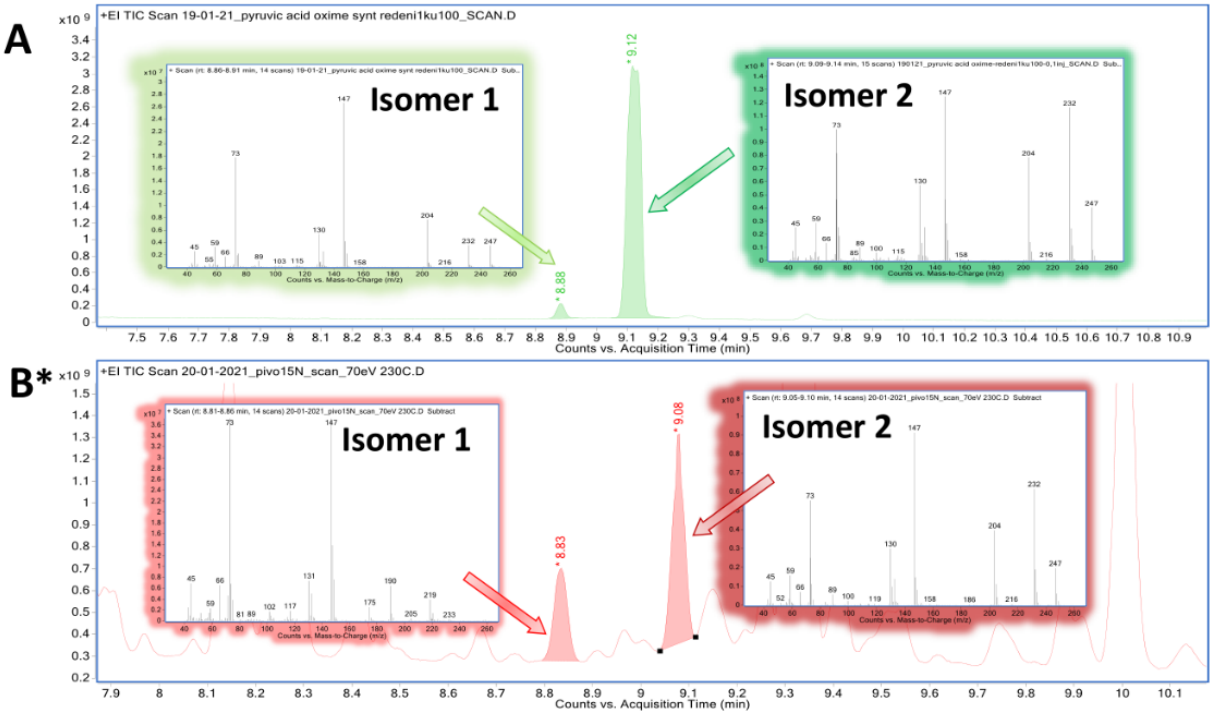

Figure S1. Chromatograms and mass spectra of laboratory-prepared pyruvic acid oxime (**A**) and of a beer sample treated by isotopically labeled nitrite-^{15}N(**B**).

*Spectra of nitrosated beer by ^{15}N did not show isotopically different spectra, probably due to a high natural occurrence of pyruvic acid oxime in used beer. Pyruvic acid oxime is probably formed by more complex mechanisms than other N-products, as was previously confirmed by a laboratory preparation of standard pyruvic acid oxime.[2]

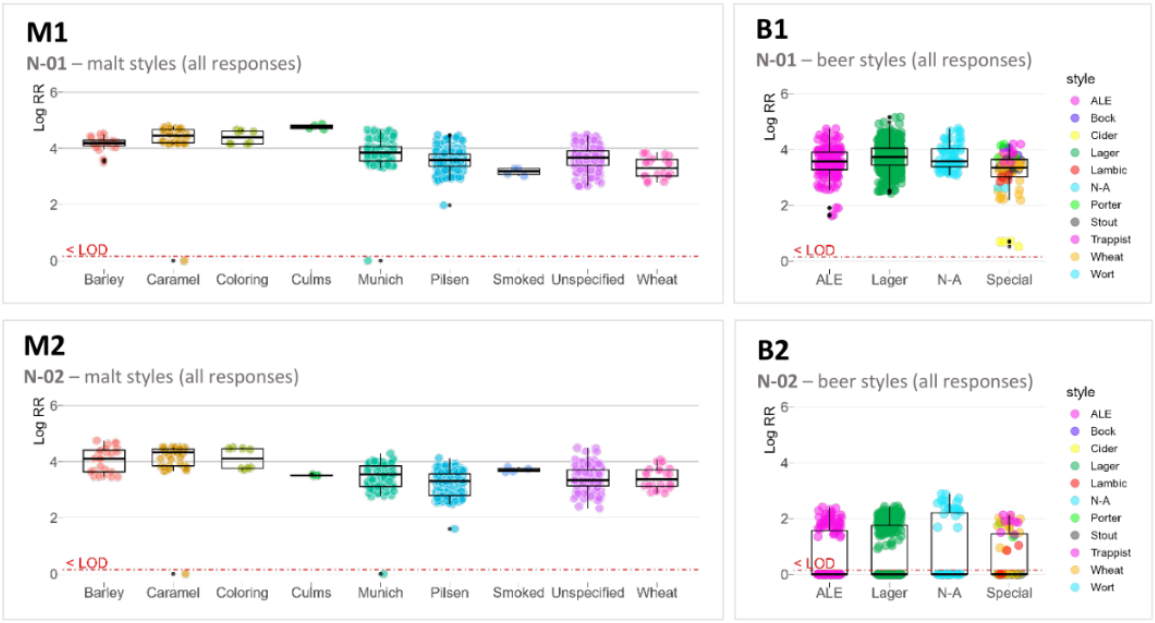

Figure S2 Distributions of detected N-products within malt and beer styles.

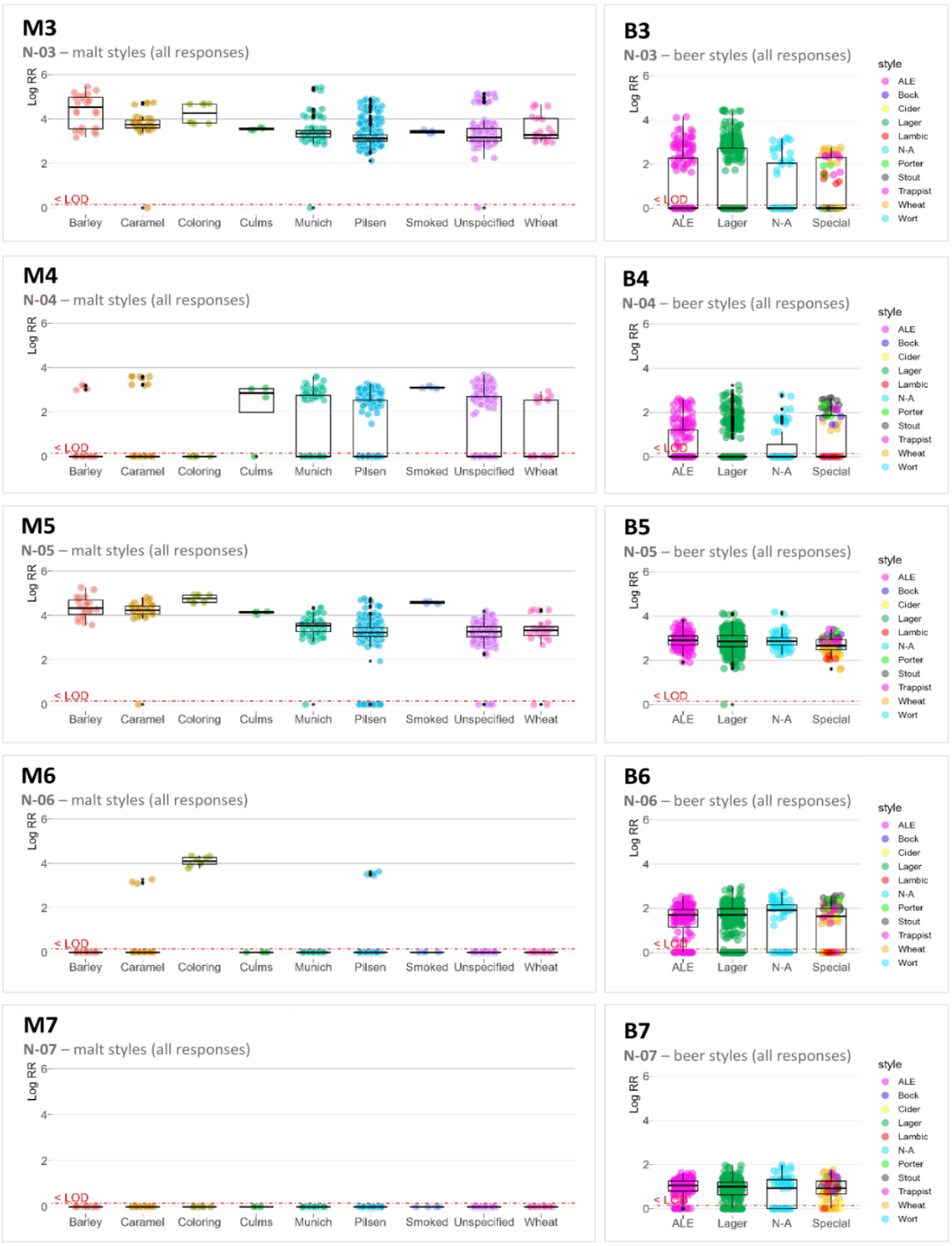

Figure S2 (continue). Distributions of detected N-products within malt and beer styles.

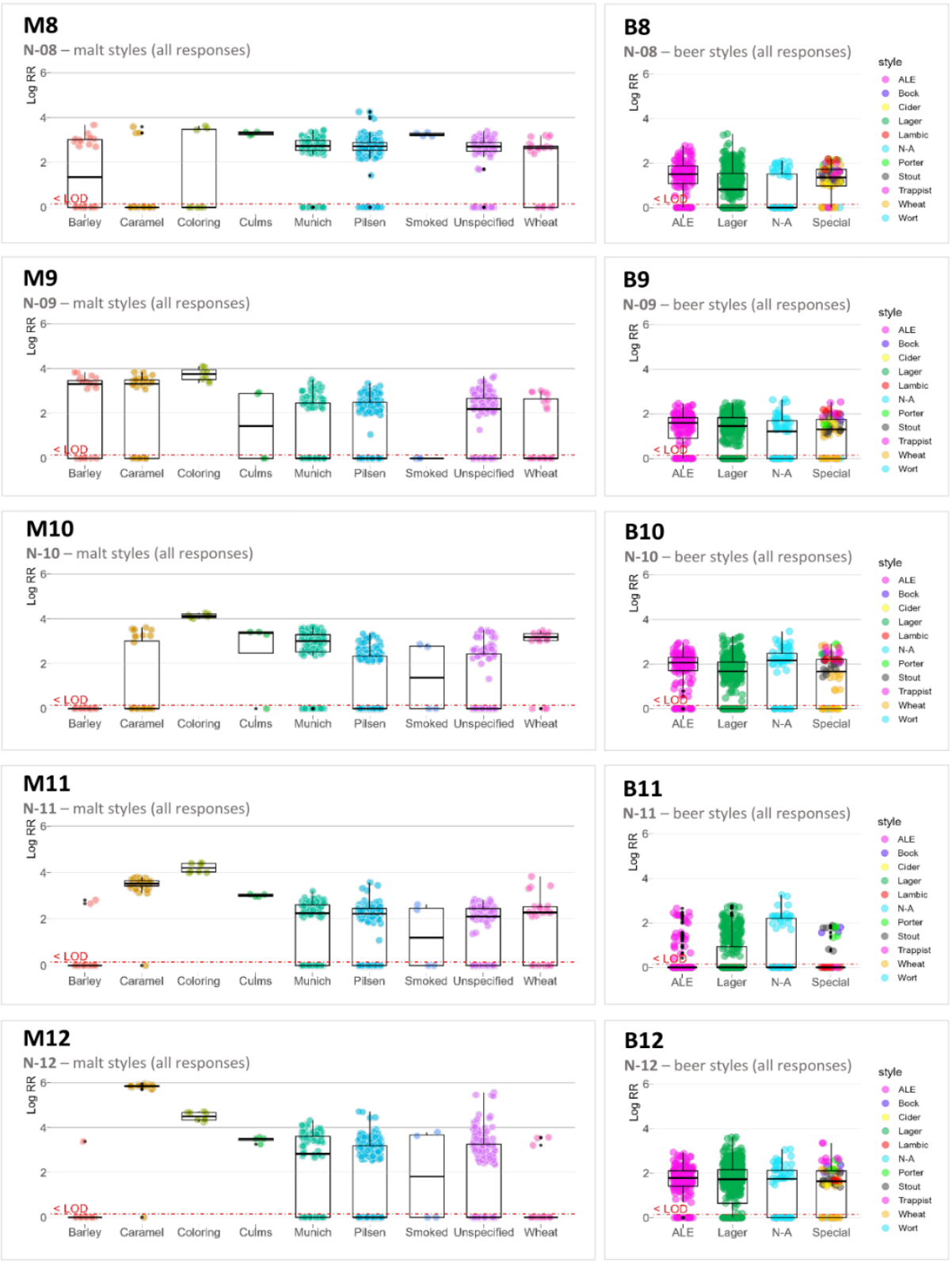

Figure S2 (continue). Distributions of detected N-products within malt and beer styles.

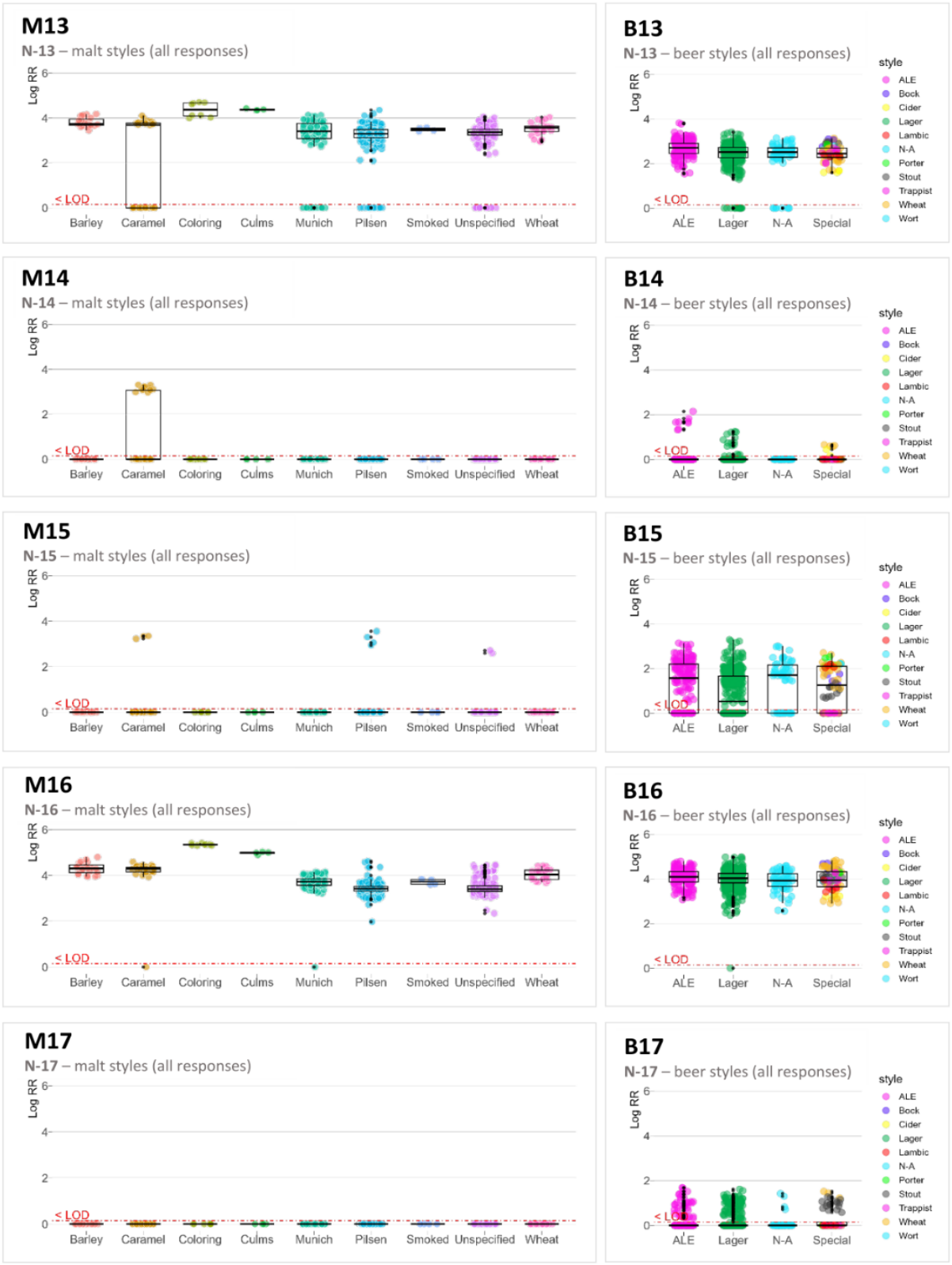

Figure S2 (continue). Distributions of detected N-products within malt and beer styles.

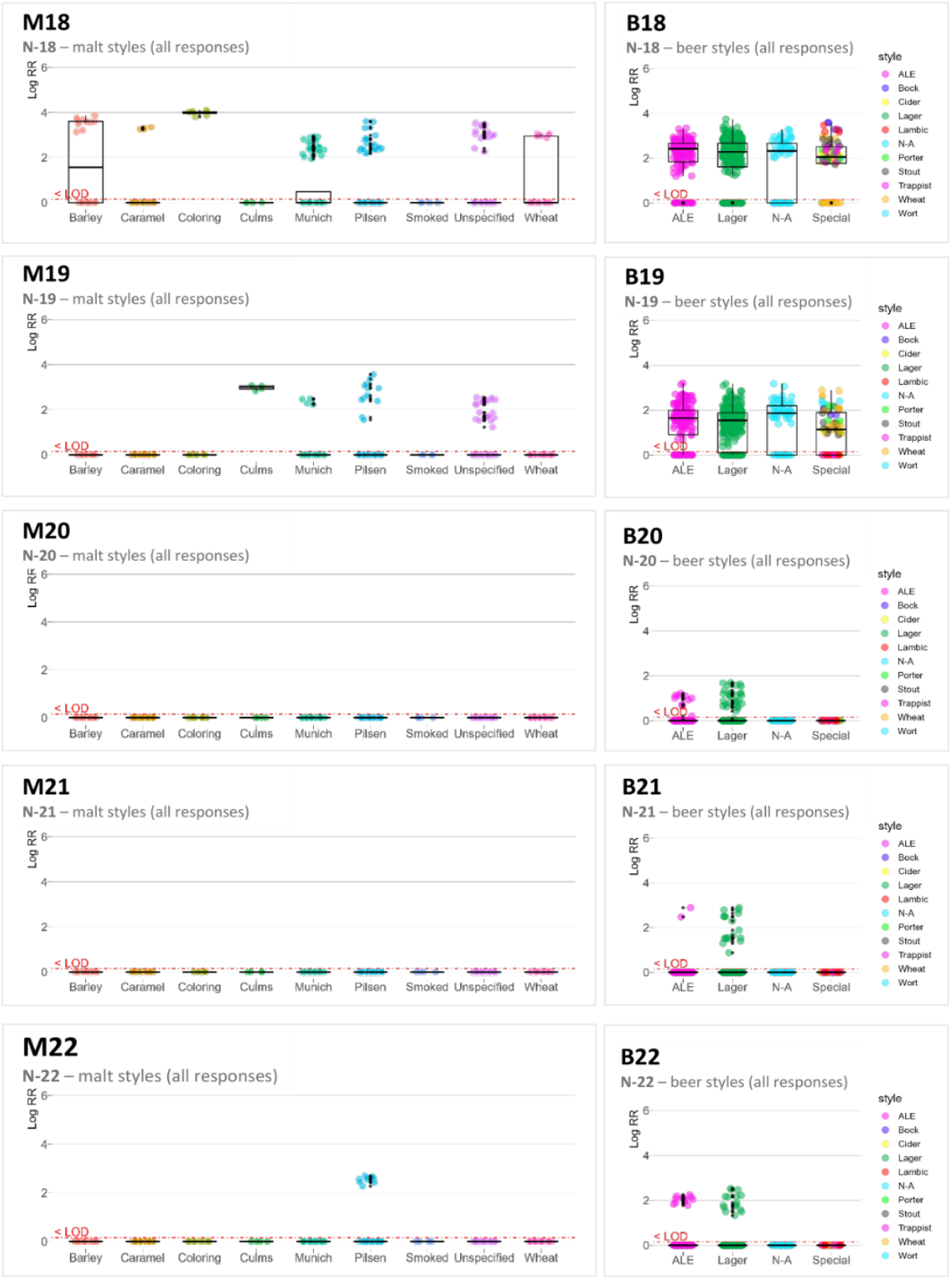

Figure S2 (continue). Distributions of detected N-products within malt and beer styles. The red dashed line shows the limit of detection. Boxplots of all responses for N-01 within malt styles (**M1**), and beer styles (**B1**); for N-02 within malt styles (**M2**), and beer styles (**B2**); for N-03 within malt styles (**M3**), and beer styles (**B3**); for N-04 within malt styles (**M4**), and beer styles (**B4**); for N-05 within malt styles (**M5**), and beer styles (**B5**); for N-06 within malt styles (**M6**), and beer styles (**B6**); for N-07 within malt styles (**M7**), and beer styles (**B7**); for N-08 within malt styles (**M8**), and beer styles (**B8**); for N-09 within malt styles (**M9**), and beer styles (**B9**); for N-10 within malt styles (**M10**),

and beer styles (**B10**); for N-11 within malt styles (**M11**), and beer styles (**B11**); for N-12 within malt styles (**M12**), and beer styles (**B12**); for N-13 within malt styles (**M13**), and beer styles (**B13**); for N-14 within malt styles (**M14**), and beer styles (**B14**); for N-15 within malt styles (**M15**), and beer styles (**B15**); for N-16 within malt styles (**M16**), and beer styles (**B16**); for N-17 within malt styles (**M17**), and beer styles (**B17**); for N-18 within malt styles (**M18**), and beer styles (**B18**); for N-19 within malt styles (**M19**), and beer styles (**B19**); for N-20 within malt styles (**M20**), and beer styles (**B20**); for N-21 within malt styles (**M21**), and beer styles (**B21**); for N-22 within malt styles (**M22**), and beer styles (**B22**).

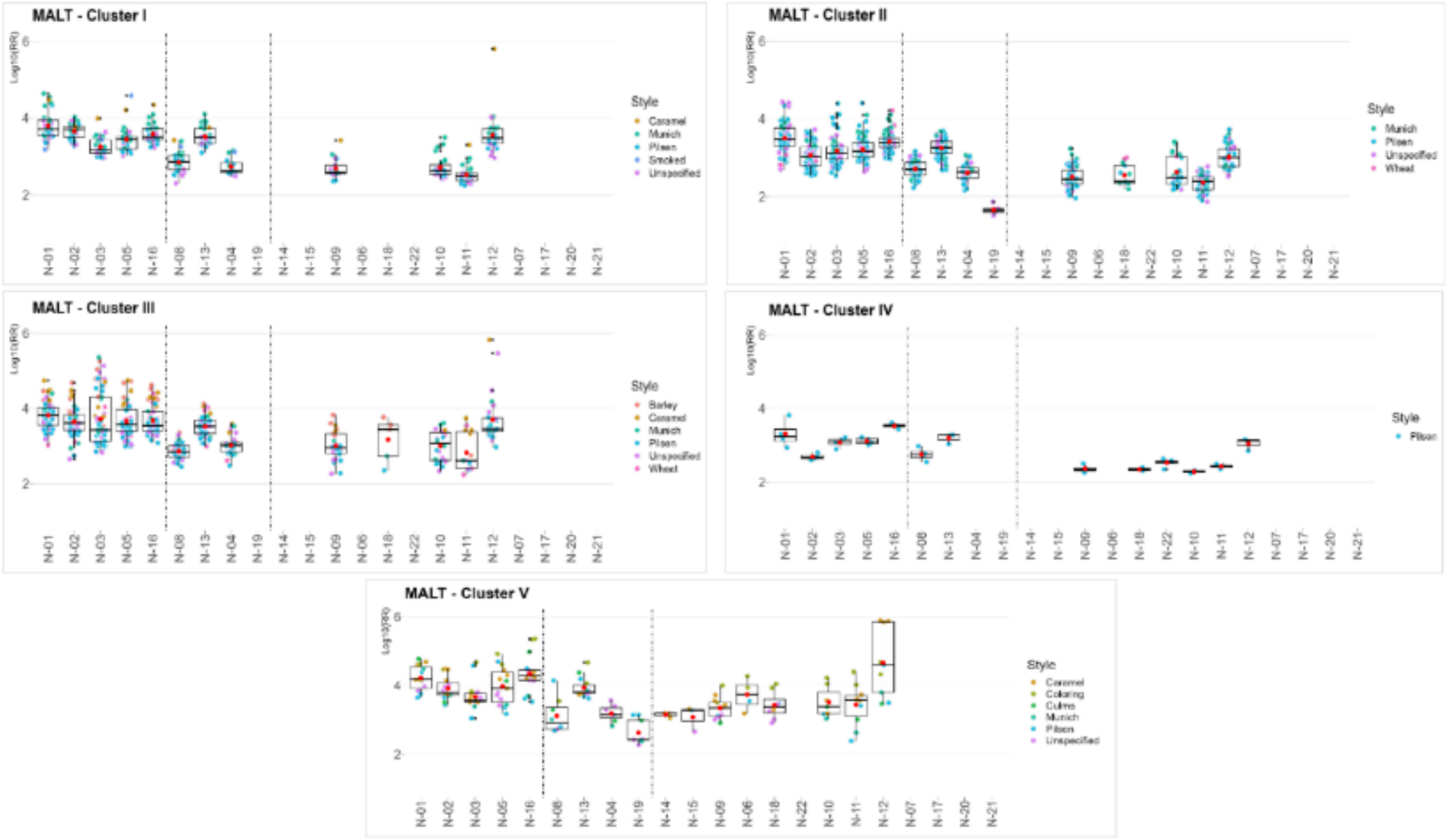

Figure S3. Distributions of N-product responses within individual clusters, which were distinguished according to a hierarchically clustered heatmap of malt samples (**MALT – Cluster I** to **Cluster V**). Individual malt styles are in boxplots of N-product responses distinguished by different colors.

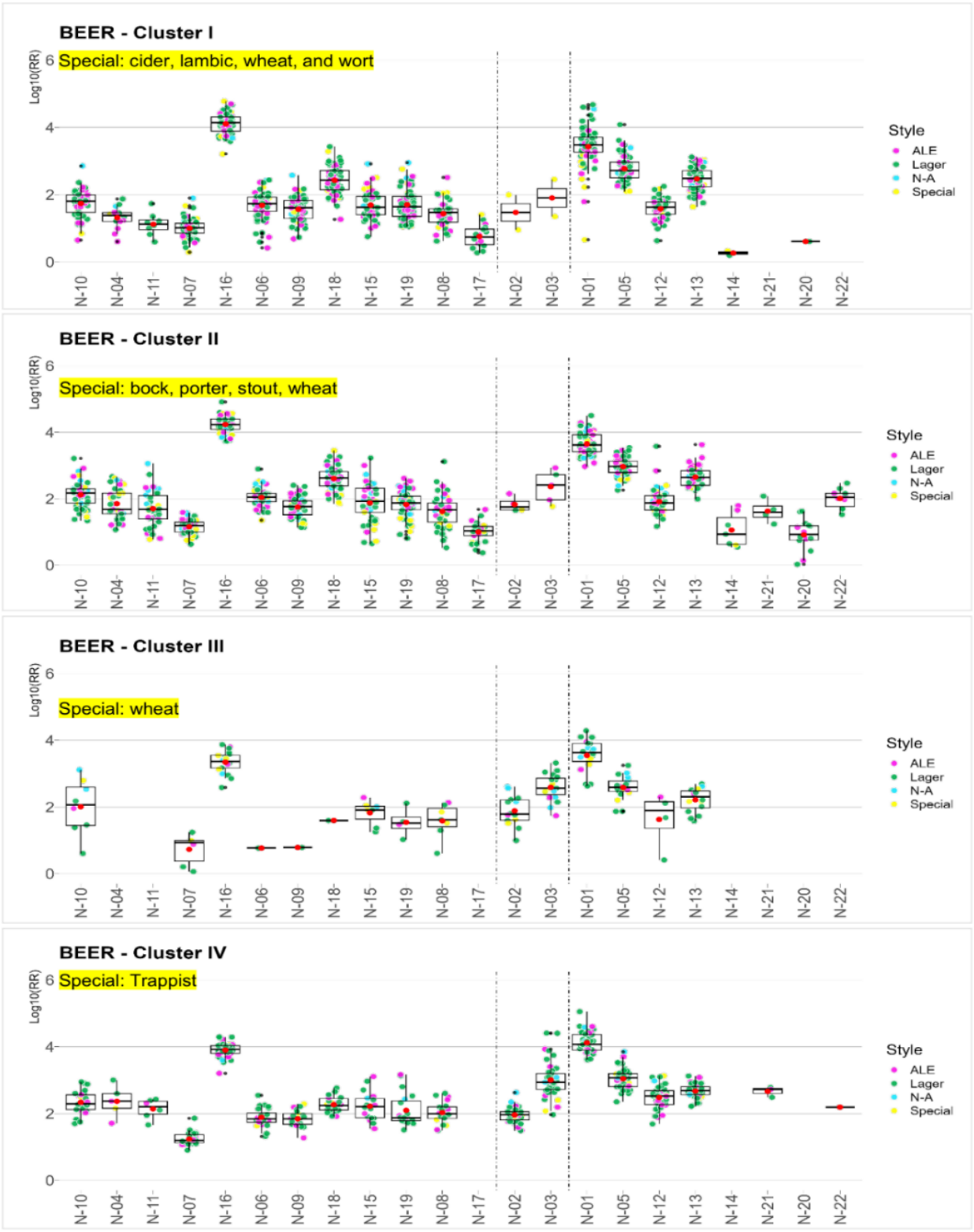

Figure S4. Distributions of N-product responses within individual clusters, which were distinguished according to a hierarchically clustered heatmap of beer samples (**BEER – Cluster I** to **Cluster IV**). Individual beer styles are in boxplots of N-product responses distinguished by different colors. All special beers were labeled by yellow for clarity, and are specified individually in each graph.

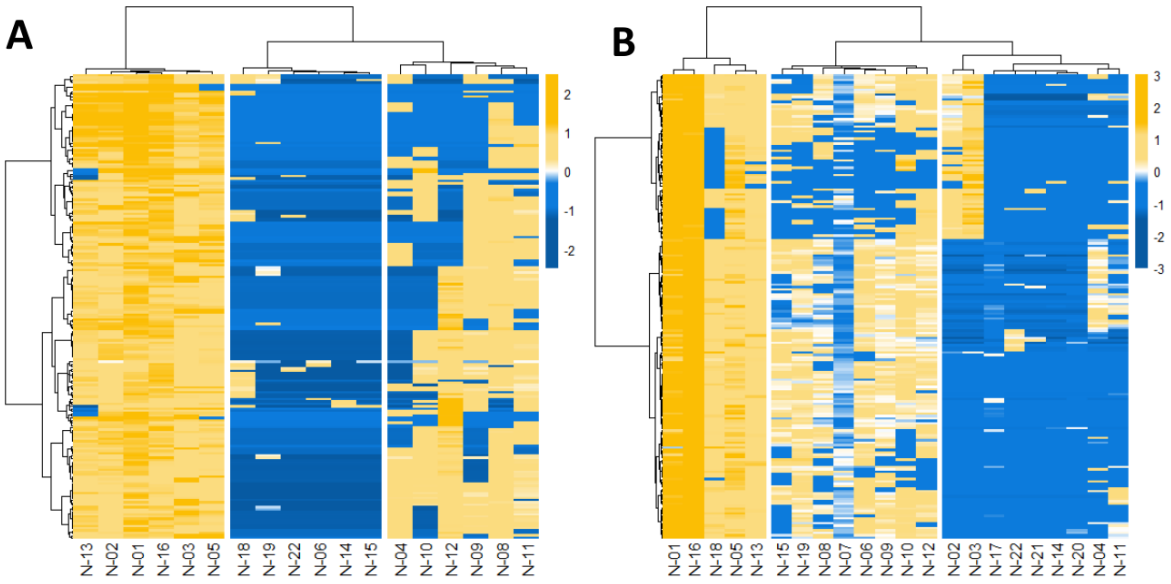

Figure S5. 2D hierarchical clustered heatmap of malt (**A**) and beer (**B**) standardized by rows (N-products). Color intensity corresponds to z-scored responses of N-products within individual samples.

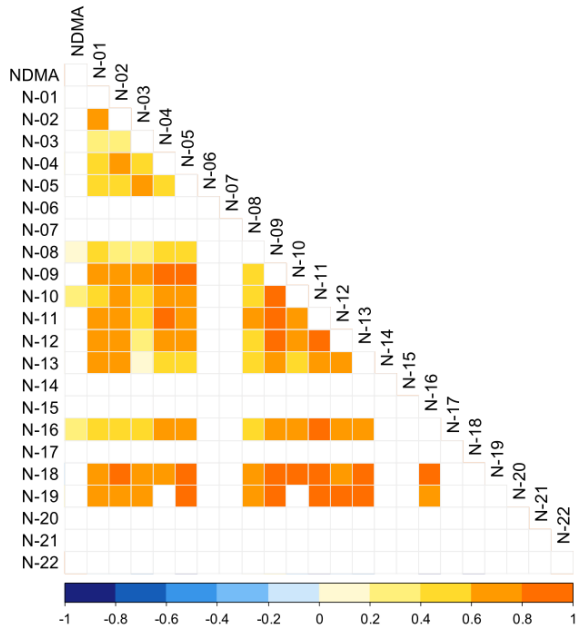

Figure S6. Correlogram of NDMA and N-products in malts. Color intensity corresponds to r- value. Only significant r-values ($p<0.05$) are shown.

Table S2. Correlation coefficients (r), p-values (p), and number of counts (n) for NDMA and N-products Pearson analysis in malt samples.

Var1	Var 2	r	p	n
NDMA	N-08	0.190	3.40E-02	125
NDMA	N-10	0.336	5.78E-03	66
NDMA	N-16	0.300	4.03E-04	135
N-01	N-02	0.660	<0.0001	198
N-01	N-03	0.316	5.80E-06	198
N-01	N-04	0.575	3.78E-08	78
N-01	N-05	0.522	6.22E-15	194
N-01	N-08	0.413	2.49E-08	169
N-01	N-09	0.689	<0.0001	124
N-01	N-10	0.487	7.28E-07	93
N-01	N-11	0.698	<0.0001	146
N-01	N-12	0.710	<0.0001	118
N-01	N-13	0.699	<0.0001	188
N-01	N-16	0.566	<0.0001	198
N-01	N-18	0.759	2.84E-06	28
N-01	N-19	0.794	4.03E-04	15
N-02	N-03	0.354	3.02E-07	198
N-02	N-04	0.770	2.22E-16	78
N-02	N-05	0.569	<0.0001	194
N-02	N-08	0.381	3.12E-07	169
N-02	N-09	0.767	<0.0001	124
N-02	N-10	0.621	3.15E-11	93
N-02	N-11	0.705	<0.0001	146
N-02	N-12	0.751	<0.0001	118
N-02	N-13	0.709	<0.0001	188
N-02	N-16	0.561	<0.0001	198
N-02	N-18	0.844	1.62E-08	28
N-02	N-19	0.719	2.52E-03	15
N-03	N-04	0.550	1.78E-07	78
N-03	N-05	0.705	<0.0001	194
N-03	N-08	0.380	3.35E-07	169
N-03	N-09	0.610	5.77E-14	124
N-03	N-10	0.476	1.45E-06	93
N-03	N-11	0.440	2.85E-08	146
N-03	N-12	0.393	1.10E-05	118
N-03	N-13	0.163	2.58E-02	188
N-03	N-16	0.471	2.54E-12	198
N-03	N-18	0.763	2.40E-06	28
N-03	N-19	0.672	6.12E-03	15
N-04	N-05	0.557	1.15E-07	78
N-04	N-08	0.500	1.06E-05	70
N-04	N-09	0.836	4.17E-14	50
N-04	N-10	0.674	1.33E-06	41
N-04	N-11	0.807	1.66E-13	54
N-04	N-12	0.756	5.16E-10	48
N-04	N-13	0.556	2.27E-07	75
N-04	N-16	0.618	1.71E-09	78
N-04	N-18	0.750	1.24E-02	10
N-05	N-08	0.458	3.73E-10	169
N-05	N-09	0.806	<0.0001	124
N-05	N-10	0.715	8.88E-16	93
N-05	N-11	0.788	<0.0001	146
N-05	N-12	0.727	<0.0001	117
N-05	N-13	0.452	1.17E-10	184
N-05	N-16	0.703	<0.0001	194
N-05	N-18	0.867	2.48E-09	28
N-05	N-19	0.861	3.83E-05	15
N-08	N-09	0.566	9.51E-11	111
N-08	N-10	0.487	3.09E-06	83
N-08	N-11	0.655	<0.0001	134
N-08	N-12	0.591	6.05E-11	102
N-08	N-13	0.514	1.49E-12	166
N-08	N-16	0.508	1.82E-12	169
N-08	N-18	0.618	2.16E-03	22
N-08	N-19	0.700	7.70E-03	13
N-09	N-10	0.869	<0.0001	58
N-09	N-11	0.826	<0.0001	102
N-09	N-12	0.817	<0.0001	81
N-09	N-13	0.611	1.97E-13	118
N-09	N-16	0.750	<0.0001	124
N-09	N-18	0.900	9.09E-10	25
N-09	N-19	0.847	5.12E-04	12
N-10	N-11	0.726	2.55E-14	80
N-10	N-12	0.667	1.32E-09	65
N-10	N-13	0.590	2.81E-09	85
N-10	N-16	0.773	<0.0001	93
N-10	N-18	0.908	1.96E-07	18
N-11	N-12	0.863	<0.0001	98
N-11	N-13	0.730	<0.0001	140
N-11	N-16	0.816	<0.0001	146
N-11	N-18	0.894	2.11E-08	22
N-11	N-19	0.830	2.95E-03	10
N-12	N-13	0.629	1.45E-13	111
N-12	N-16	0.676	<0.0001	118
N-12	N-18	0.741	1.02E-03	16
N-12	N-19	0.912	2.38E-04	10
N-13	N-16	0.652	<0.0001	188
N-13	N-18	0.847	5.00E-08	26
N-13	N-19	0.848	6.58E-05	15
N-16	N-18	0.940	1.14E-13	28
N-16	N-19	0.750	1.28E-03	15

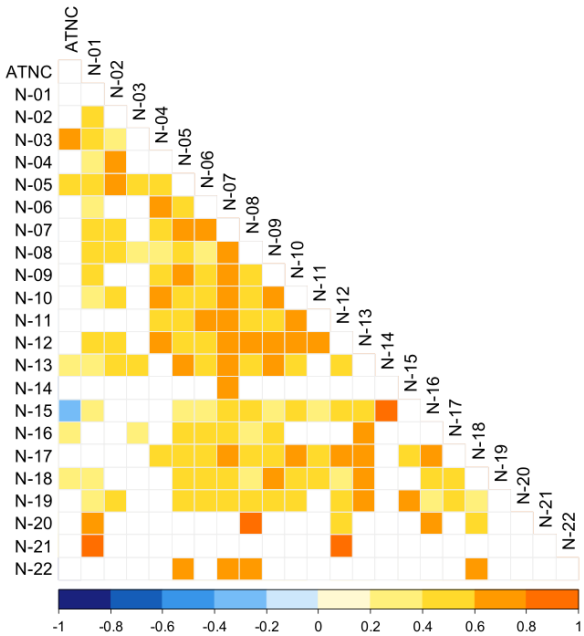

Figure S7. Correlogram of ATNC and N-products in beers. Color intensity corresponds to r- value. Only significant r-values (p<0.05) are shown.

Table S3. Correlation coefficients (r), p-values (p), and number of counts (n) for NDMA and N-products Pearson analysis in beer samples.

Var1	Var 2	r	p	n
ATNC	N-03	0.610	4.83E-05	38
ATNC	N-05	0.544	1.27E-11	133
ATNC	N-13	0.277	1.32E-03	132
ATNC	N-15	-0.244	2.15E-02	89
ATNC	N-16	0.224	9.63E-03	133
ATNC	N-18	0.294	1.59E-03	113
N-01	N-02	0.480	6.95E-05	63
N-01	N-03	0.458	7.72E-05	69
N-01	N-04	0.390	2.98E-03	56
N-01	N-05	0.469	7.86E-12	191
N-01	N-06	0.380	2.66E-06	144
N-01	N-07	0.545	5.11E-14	163
N-01	N-08	0.406	1.81E-06	129
N-01	N-09	0.408	6.08E-07	139
N-01	N-10	0.384	2.03E-06	144
N-01	N-12	0.587	6.66E-16	157
N-01	N-13	0.387	4.50E-08	187
N-01	N-15	0.205	2.40E-02	121
N-01	N-18	0.271	7.22E-04	152
N-01	N-19	0.281	5.34E-04	148
N-01	N-20	0.680	3.74E-03	16
N-01	N-21	0.902	5.53E-03	7
N-02	N-03	0.356	4.24E-03	63
N-02	N-04	0.733	3.86E-02	8
N-02	N-05	0.618	6.71E-08	63
N-02	N-07	0.579	4.78E-05	43
N-02	N-08	0.453	1.36E-02	29
N-02	N-10	0.575	1.03E-04	40
N-02	N-12	0.494	2.69E-04	50
N-02	N-13	0.509	2.82E-05	61
N-02	N-19	0.535	4.87E-03	26
N-03	N-05	0.468	4.99E-05	69
N-03	N-08	0.374	3.80E-02	31
N-03	N-13	0.460	1.16E-04	65
N-03	N-16	0.257	3.33E-02	69
N-04	N-05	0.556	8.47E-06	56
N-04	N-06	0.727	3.41E-10	55
N-04	N-07	0.547	1.91E-05	54
N-04	N-08	0.366	9.67E-03	49
N-04	N-09	0.443	9.01E-04	53
N-04	N-10	0.613	1.08E-06	53
N-04	N-11	0.546	1.50E-03	31
N-04	N-12	0.611	1.15E-06	53
N-04	N-17	0.564	1.16E-03	30
N-05	N-06	0.480	1.17E-09	144
N-05	N-07	0.646	<0.0001	163
N-05	N-08	0.500	1.63E-09	129
N-05	N-09	0.612	1.33E-15	139
N-05	N-10	0.550	9.14E-13	144
N-05	N-11	0.490	2.29E-04	52
N-05	N-12	0.529	1.11E-12	157
N-05	N-13	0.648	<0.0001	187
N-05	N-15	0.265	3.29E-03	121
N-05	N-16	0.436	2.81E-10	191
N-05	N-17	0.531	1.22E-04	47
N-05	N-18	0.515	1.09E-11	152
N-05	N-19	0.410	2.29E-07	148
N-05	N-22	0.764	6.16E-03	11
N-06	N-07	0.672	<0.0001	140
N-06	N-08	0.328	4.35E-04	111
N-06	N-09	0.596	1.22E-13	128
N-06	N-10	0.517	1.04E-09	122
N-06	N-11	0.624	1.68E-06	49
N-06	N-12	0.562	2.85E-12	131
N-06	N-13	0.472	2.36E-09	144
N-06	N-15	0.340	4.41E-04	103
N-06	N-16	0.410	3.40E-07	144
N-06	N-17	0.454	1.97E-03	44
N-06	N-18	0.529	4.13E-11	135
N-06	N-19	0.466	1.97E-08	131
N-07	N-08	0.603	1.97E-13	122
N-07	N-09	0.732	<0.0001	136
N-07	N-10	0.734	<0.0001	134
N-07	N-11	0.740	1.91E-09	48
N-07	N-12	0.685	<0.0001	142
N-07	N-13	0.697	<0.0001	163
N-07	N-14	0.760	2.87E-02	8
N-07	N-15	0.450	6.23E-07	112
N-07	N-16	0.575	8.88E-16	163
N-07	N-17	0.697	5.12E-08	47
N-07	N-18	0.544	7.55E-13	149
N-07	N-19	0.594	5.33E-15	143
N-07	N-22	0.669	2.43E-02	11
N-08	N-09	0.512	8.10E-09	112
N-08	N-10	0.562	1.10E-10	112
N-08	N-11	0.427	4.77E-03	42
N-08	N-12	0.608	2.25E-13	119
N-08	N-13	0.560	5.39E-12	129
N-08	N-15	0.523	4.51E-08	96
N-08	N-16	0.264	2.46E-03	129
N-08	N-17	0.592	1.47E-05	46
N-08	N-18	0.373	3.24E-05	118
N-08	N-19	0.486	7.38E-08	110
N-08	N-20	0.800	1.97E-04	16
N-08	N-22	0.754	1.17E-02	10
N-09	N-10	0.663	<0.0001	121
N-09	N-11	0.577	4.16E-05	44
N-09	N-12	0.617	9.33E-15	128
N-09	N-13	0.617	4.44E-16	139
N-09	N-15	0.366	1.96E-04	99
N-09	N-16	0.476	3.05E-09	139
N-09	N-17	0.589	1.34E-05	47
N-09	N-18	0.670	<0.0001	134
N-09	N-19	0.426	7.33E-07	125
N-10	N-11	0.694	1.63E-08	51
N-10	N-12	0.774	<0.0001	130
N-10	N-13	0.580	3.24E-14	143
N-10	N-15	0.461	9.41E-07	103
N-10	N-17	0.689	1.68E-07	45
N-10	N-18	0.430	4.00E-07	128
N-10	N-19	0.462	1.07E-07	120
N-11	N-12	0.691	7.65E-08	47
N-11	N-15	0.383	1.62E-02	39
N-11	N-17	0.595	3.52E-03	22
N-11	N-18	0.482	6.00E-04	47
N-12	N-13	0.486	1.14E-10	157
N-12	N-15	0.550	1.46E-09	104
N-12	N-17	0.668	5.24E-07	45
N-12	N-18	0.240	4.77E-03	137
N-12	N-19	0.438	2.33E-07	128
N-12	N-20	0.557	3.10E-02	15
N-12	N-21	0.839	1.83E-02	7
N-13	N-15	0.510	2.28E-09	121
N-13	N-16	0.603	<0.0001	187
N-13	N-17	0.631	1.95E-06	47
N-13	N-18	0.629	<0.0001	152
N-13	N-19	0.663	<0.0001	148
N-14	N-15	0.841	3.57E-02	6
N-15	N-17	0.521	3.39E-04	43
N-15	N-19	0.653	8.44E-15	111
N-16	N-17	0.689	8.54E-08	47
N-16	N-18	0.597	4.44E-16	152
N-16	N-19	0.318	8.06E-05	148
N-16	N-20	0.698	2.62E-03	16
N-17	N-18	0.551	5.99E-05	47
N-17	N-19	0.548	6.58E-05	47
N-18	N-19	0.357	1.67E-05	138
N-18	N-20	0.526	3.64E-02	16
N-18	N-22	0.681	3.01E-02	10

References

(1) Malečková, M.; Sobotníková, J.; Olšovská, J. Development of Miniaturized extraction method used for GC-NCD screening of non-volatile nitroso compounds in malt. *Diploma Thesis*, **2018**, Prague (https://dspace.cuni.cz/handle/20.500.11956/98172)

(2) Wolfgang Kunze. Technology Brewing and Malting, Chapter 2 – Malt production, *3rd international edition, VLB Berlin*, **2004**, 97-188. (ISBN 3-921690-49-8)

(3) Malečková, M.; Vrzal, T.; Olšovská, J. Characterization of Nitrite-Related Reaction Products in Beer. *J. Agric. Food Chem.* **2021**, *69*, 11687−11695.